SCUOLA DI DOTTORATO
UNIVERSITÀ DEGLI STUDI DI MILANO-BICOCCA

School of Medicine and Surgery

PhD program in Neuroscience Cycle XXX

Curriculum in Experimental Neurosciences

Evaluation of pain components in an animal model of chronic inflammatory pain: a study towards new therapeutics

Surname: Milia Name: Chiara

Registration number: 798326

Tutor: Dr. Caselli Gianfranco

Coordinator: Prof. Cavaletti Guido Angelo

ACADEMIC YEAR 2016/2017

Table of Contents

List of Abbreviations

2-BFI	2-(2-benzofuranyl)-4,5-dihydro-1H-imidazole hydrochloride
ACLT	Anterior cruciate ligament transection
Akt	Protein Kinase B
AMPAR	AMPA receptor
ANOVA	Analysis of Variance
ATP	Adenosine Triphosphate
AUC	Area Under the Curve
BK	Bradykinin
BL	Baseline
BORTZ	Bortezomib
CAIA	Collagen Antibody-Induced Arthitis
CaMKII	Calmodulin-dependent protein kinase II
cAMP	Cyclic adenosine monophosphate
CCI	Chronic Constriction Injury
CCR3	C-C chemokine receptor 3
CD11b	Cluster of differentiation molecule 11 b
CFA	Complete Freund's Adjuvant
CGRP	Calcitonin Gene Related Peptide
CI	Confidence Interval
CIPN	Chemotherapy-induced peripheral neuropathy
CL	Contralateral

COX	Cyclo-oxigenase
CX3CL1	Chemokine (C-X3-C motif) ligand 1
DAG	Diacylglycerol
DMEM	Dulbecco's Modified Eagle's Medium
DRG	Dorsal Root Ganglion
DWB	Dynamic Weight Bearing
ED50	Median Effective Dose
EFIC	European Pain Federation
EPAC	Exchange Protein directly Activated by cAMP
ERK	Extracellular signal–Regulated Kinase
GBP	Gabapentin
GFAP	Glial fibrillary acidic protein
GPCR	G protein-coupled receptor
HEK293	Human embryonic kidney cells 293
HSP	Heat Shock Protein
HPMC	Hydroxyl-Propyl-carboxyMethyl Cellulose
I1R/I2R	Imidazoline 1/2 receptor
IASP	International Association for the Study of Pain
IB4	Isolectin B4
IBA1	Ionized calcium-binding adapter molecule 1
ICD	International Classification of Diseases
IL	Ipsilateral
IL-1β	Interleukin-1β

IL-6	Interleukin-6
iNOS	Inducible Nitric Oxide Synthase
IP	Intraperitoneal administration
IP3	Inositol Triphosphate
IV	Intravenous
Kir3	Potassium channel Inwardly Rectifying 3
K.O.	Knock Out
L4/5	Lumbar 4/5
LPS	Lipopolysaccharide
MAO A/B	Monoamine Oxidase A/B
MAPK	Mitogen-Activated Protein Kinase
MC	Methylcellulose
MIA	Monosodium Iodo Acetate
MMT	Medial Meniscus Tear
MOR	μ Opioid Receptor
MPE	Maximum Possible Effect
NA/NE	Noradrenaline/Norepinephrine
NaN3	Sodium Azide
NGF	Nerve Growth Factor
NO	Nitric Oxide
NSAID	Non-Steroidal Anti-Inflammatory Drug
OS	Per os administration
PBS	Phosphate Buffered Saline

PBST	0.3% Triton X-100 PBS
PGE2	Prostaglandin E2
PKA	Protein Kinase A
PKC	Protein Kinase C
pPKCε	Phosphorylated PKCε
PLC	Phospholipase C
PMA	Phorbol 12-Myristate 13-Acetate
PTX	Pertussis Toxin
P2X3R	P2X Purinoceptor 3
RA	Rheumatoid Arthritis
RACK	Receptor for activated C-kinase
RM	Repeated Measures
RT	Room Temperature
SC	Subcutaneous administration
SEM	Standard Error of the Mean
SIN	Sciatic Inflammatory Neuritis
SNI	Spared Nerve Injury
SNL	Spinal Nerve Ligation
SNT	Spinal Nerve Transection
TB	True Blue
TENS	Transcutaneous Electrical Nerve Stimulation
TGF-β1	Transforming Growth Factor-β1
Th1	T helper 1

THR	Thrombin
TLR	Toll-Like Receptor
TNF-α	Tumor Necrosis Factor-α
TRAM	Trif-Related Adapter Molecule
TRP channels	Transient Receptor Potential
TRPV1 (VR1)	Transient Receptor Potential channel V1 (Vanilloid Receptor 1)
WHO	World Health Organization

1. Abstract

Chronic pain is a disabling and long-lasting cross-pathology condition that affects up to 25% of global population. Major pharmacological treatment for chronic pain is represented by opioid drugs, which are currently being dangerously over-prescribed, leading to a severe epidemic of side-effects such as constipation, respiratory depression, addiction and tolerance. New effective drugs or combinations of drugs are therefore eagerly needed to effectively and safely control pain conditions.

Recently, imidazoline receptor 2 (I2R) ligands have been shown to have analgesic effects and to contrast opioid tolerance development when administered in combination with these drugs. CR4056, a novel I2R-agonist drug, has been proposed as analgesic drug and its efficacy has been proved in several animal models of chronic pain, being the first I2R ligand entering clinical phase 1 and 2 studies.

In preclinical studies on several animal models of pain, a strong synergistic effect between morphine and CR4056 has been observed, ED50 of both drugs being 4-fold reduced in combined administration, compared to single drug administration.

The aim of my study was therefore to deepen our knowledge on the interaction between morphine and CR4056, especially regarding the effect of the latter on opioid tolerance, and trying to understand the mechanistic basis of this pharmacological interaction.

To this scope, I selected an animal model of chronic inflammatory pain, induced by a single injection of Complete Freund's Adjuvant (CFA) in the right hind limb of male adult rats. In this model, behavioral effects of morphine-induced analgesic tolerance and synergistic effect of CR4056 on tolerance development and expression were assessed in the short and in the long period. Putative CR4056 action on opioid-induced side effects and spinal microgliosis were also assessed. It is known, in fact, that spinal microglia has an important role in chronic pain and opioid-induced tolerance, since, in these conditions, a sustained microglia activation (evaluated by IBA-1 expression and conformational change) has been observed. This activation is related to release of pro-inflammatory factors, suggesting that microglia could have a pivotal role in the development and maintenance of analgesic tolerance.

Lastly, we aimed to better understand CR4056-morphine synergy at molecular level, which has recently been discovered in vitro rat dorsal root ganglia (DRG) primary cultures. In fact, it has been shown that DRG neurons of animal models of chronic pain display higher activation of TRPV1 receptor, depending on PKCε phosphorylation and translocation to cell membrane. Moreover, there is evidence that several analgesics such as paracetamol, gabapentin or

nimesulide are able to inhibit PKCε phosphorylation in cultured sensory neurons. Interestingly, in preliminary data obtained in our laboratory in collaboration with University of Modena (unpublished data), we observed that morphine and CR4056 can contrast PKCε translocation induced by inflammatory factors in primary rat DRG cultures. Therefore, in this work we aimed to elucidate the effects of acute administrations of morphine or CR4056 in ex vivo DRG from CFA-treated rats, by quantification of PKCε phosphorylation and TRPV1 expression, and in the spinal cord, by evaluation of microgliosis.

My results demonstrated that CFA-induced inflammation triggered mechanical hyperalgesia and the acute administration of morphine produced a robust time-dependent alleviation of mechanical hyperalgesia. After 4 days of morphine treatment, the analgesic effect of the drug was significantly reduced; combined administration of morphine with CR4056 or 2-BFI, a standard I2R ligand, caused a dose-dependent prevention of morphine tolerance. After 14 days of morphine treatment the analgesic effect of the drug was negligible; combined CR4056 administration produced a reduction of morphine analgesic tolerance and a partial recovery of morphine analgesic effect. Moreover, when CR4056 was co-administered with morphine in already tolerant rats, it was able to improve morphine analgesic activity. In the same animals, spinal microglia activation was augmented in CFA-injected rats, either vehicle- or morphine-treated, but not in the group with CR4056-morphine combined administration.

Besides, the association of CR4056 with morphine or codeine did not show a synergistic or additive modulation of opioid-induced constipation, therefore demonstrating that I2R ligands are able to selectively synergize with the analgesic effect of opiate, but not with their known side effects, probably linked to a different intracellular pathway.

In the search for the mechanism of action, in L4-L5 DRG of CFA-injected rats I found a significant increase in the phosphorylation of PKCε, compared to the control group. Percentage of VR1 expressing cells was not influenced, while colocalization between PKCε and VR1 expressing cells was significantly higher in non-treated CFA rats compared to sham and treated animals. In the same animals, activated microglial cells were significantly increased in CFA vehicle-treated animals compared to control and CR4056-treated animals, but not to morphine-treated rats.

In conclusion, concurrent sub-chronic and chronic administration of morphine and different not-analgesic doses of I2R ligands, such as CR4056 and 2-BFI, prevented or attenuated the development of opioid tolerance. Moreover, combined administration of morphine and

CR4056 to already tolerant subjects restored morphine analgesic power. Nevertheless, CR4056 did not worsen opioid-induced constipation. These data suggest that CR4056 seems to be a valid drug to prevent and rescue opioid tolerance without exacerbate collateral aspects of such treatment. Moreover, in vitro data on CR4056 and morphine synergistic mechanism on PKCε were also validated in ex vivo DRG from an animal model of CFA-induced inflammation. In fact, my data confirmed that inflammation triggers PKCε activation, and that acute treatment with either CR4056 or morphine is able to inhibit it; moreover, this phenomenon is associated with changes in TRPV1 activity in cells receiving from the injured limb. Lastly, it was found that CFA-induced inflammation and morphine tolerance are associated with spinal microglia activation, and that CR4056 single administration or CR4056-morphine combined treatment are able to reduce it to control level. Morphine single administration does not cause any significant change in spinal microgliosis.

Further studies will be needed to elucidate effects of combined treatment on DRG and spinal cord in order to understand the mechanism of CR4056 and opioids synergy.

2. Introduction

2.1. Chronic pain

2.1.1 Chronic pain: a clinical chronic issue

"Pain is a major healthcare problem in Europe. Although acute pain may reasonably be considered a symptom of disease or injury, chronic and recurrent pain is a specific healthcare problem, a disease in its own right." *(European Pain Federation EFIC, Declaration on Pain).*

Chronic pain is a cross-pathology symptom that affects 20% of European population, and 12 to 25% of U.S.A. citizens *(Goldberg & McGee, 2011)*. Estimated world incidence of chronic pain is about 1 out of 10 adults with new chronic pain diagnosis every year *(Fact Sheet, IASP & EFIC)* and its sanitary costs per year are currently about €200 billion in Europe and $150 billion in the U.S.A. *(van Hecke et al., 2013)*.

Pain is considered chronic when it persists or relapses for more than 3 months. Three major clinical areas contribute to the issue of chronic pain: osteo and rheumatoid arthritis (40%), surgeries and injuries (25%) and spine problems (20%) *(Fact Sheet, IASP & EFIC)*.

The difficulty of dealing with this life-interfering disease is its high co-morbidity with a wide variety of diseases and its long-lasting persistence (7 years in average). Moreover, mental and physical stress at work, socioeconomic conditions and education are considered influencing variables. In fact, lower socio-economic status, adverse socio-economic circumstances and history of abuse are considered important risk-factors for pain incidence and severity; in turn, the presence of these factors can sharpen pain perception and delay recovery in people suffering from chronic pain, in a biopsychosocial pain model *(Priest & Hoggart, 2002)*

Due to the variable epidemiology (regardless of age, sex, race) and the lack of a proper coding in the current International Classification of Diseases (ICD), it is hard to characterize and quantify frequency of pain in the population (not always followed by medical examination) *(Treede et al., 2015)*. For these reasons, the International Association for the Study of Pain (IASP) under the supervision of the World Health Organization (WHO) is currently developing a new classification of chronic pain, which will consider this condition as a disease per se, and which will be included in the new ICD version, upcoming in 2018.

This classification will assess pain severity based on intensity, pain-related distress and functional impairment; it will include: chronic primary pain (all those forms with unknown etiology); chronic cancer pain (caused by cancer itself or by its treatment); chronic postsurgical and post-traumatic pain; chronic neuropathic pain (caused by a lesion or disease of the somatosensory nervous system); chronic headache and orofacial pain; chronic visceral pain; chronic musculoskeletal pain.

Finding a better way to diagnose and treat chronic pain it's becoming necessary to limit dependence of ill people from medical care, thus to reduce costs of healthcare services.

Besides, such chronic condition is often associated with low efficacy or inability to work, impaired everyday life and social relationships, major depression and suicidal attempts, burdening on family, society, employers. Therefore, a deeper understanding of chronic pain is needed, while simplifying the diagnostic framework, to explain the key pathologic mechanisms that lead to chronic pain, which has to be considered a continuum, ranging from predominantly peripheral nociceptive, to predominantly centralized pain conditions *(Arnold et al., 2016)* (**Figure 1**).

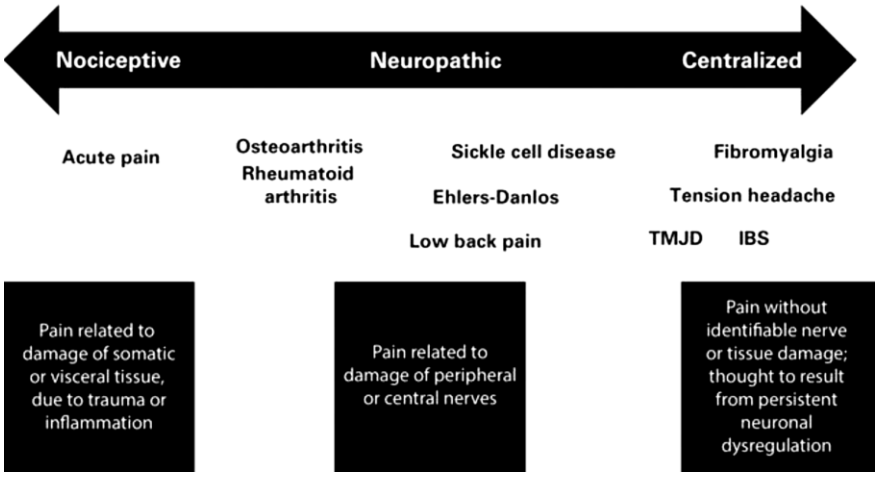

Figure 1 The pain continuum *(Arnold et al., 2016).*

2.1.2 Main therapeutic strategies for diagnosis and treatment of chronic pain

Clinical phases 2 for novel analgesics are complicated by several problems: first of all, which modalities to measure pain, since it is a subjective experience influenced by many psychological and social variables, which it is not easy to control over subjects. Second, the high risk of placebo or nocebo effects has to be controlled. These variables are new entries in the passage from preclinical to clinical trials, which need to be addressed. Therefore, clinical diagnosis still remains a difficult procedure, although preclinical pain research is succeeding in the classification of different types of pain basing on different underlying mechanisms *(Yekkirala et al., 2017)*.

For these reasons, the most important method of assessment is to ask the patient a verbal description of the pain, usually using a written questionnaire. X-ray, electromyography and evoked-potential recording can later on confirm nerve damage, but may be no more sensitive than clinical history and examination.

With regard to pharmaceutical treatment, paracetamol and non-steroidal anti-inflammatory drugs (NSAIDs) are the most used drugs. NSAIDs' chronic use, though, is associated with significant side-effects such as damage to the stomach mucosa and peptic ulceration, caused by non-selective inhibition of cyclooxygenase (COX)-1 and COX-2, resulting in reduction of proinflammatory prostaglandins also in the gastric mucosa, where they are protective. Selective inhibition of COX-2 over COX-1 would improve the side-effect profile. Muscle-relaxants, benzodiazepines, antidepressants, α2-adrenoceptor agonists, and anticonvulsants also have analgesic properties. Indeed, most commonly used analgesic drugs are opioids, which are often the most effective, but produce analgesic tolerance, addiction and unwanted side-effects such as constipation and respiratory depression.

Other therapeutic strategies include, for example, the injection of local anesthetics into the lumbar epidural space, which temporarily relieves pain, and transcutaneous electrical nerve stimulation (TENS), whose mode of action is based on the "gate theory" (**Figure 2**) of pain modulation: stimulation of non-nociceptive fibers (tactile fibers) can temporarily relieve pain perception through a spinal cross-inhibition of nociceptive fibers *(Priest & Hoggart, 2002)*.

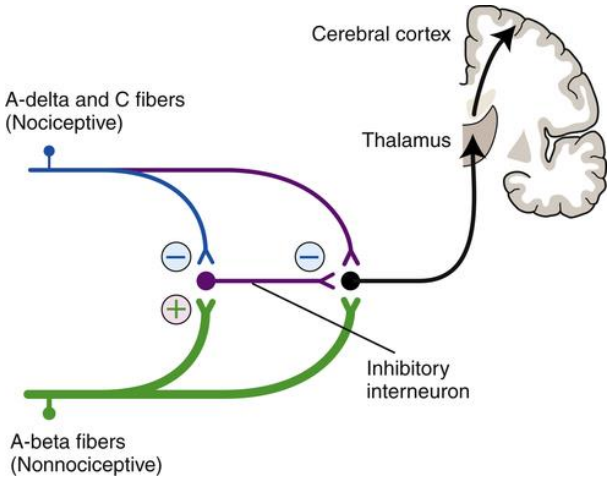

Figure 2 The "gate control theory of pain" *(Melzack & Wall, 1965)* states that stimulation of non-nociceptive fibers (tactile fibers) can temporarily relieve pain perception through a spinal cross-inhibition of nociceptive fibers *(Priest & Hoggart, 2002).*

2.2. Modeling chronic pain

2.2.1 From clinics to preclinics: behavioral outcomes and tests

In clinical patients, two major symptoms of chronic pain are **allodynia** (i.e., pain elicited by a stimulus that normally does not cause pain) and **hyperalgesia** (i.e., an increased pain response produced by a stimulus that normally causes pain). In theory, allodynia can be defined as a painful response to a non-painful stimulus (i.e., not encoded by nociceptors) but in the clinical setting it is difficult to draw the line between nociceptors-activating and non-activating stimuli in the individual patient. Therefore, in clinics the terms allodynia and hyperalgesia are used comparing the reaction to the stimulus observed in a non-affected body part of the same patient, usually the contralateral part (**Figure 3**).

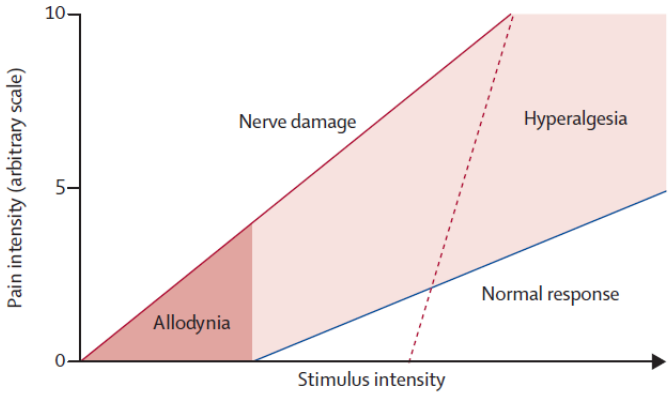

Figure 3 Stimulus-response function illustrating allodynia and hyperalgesia. In the case of hypoalgesia, the stimulus-response function can be shifted to the right (red dashed line) *(Jensen & Finnerup, 2014)*.

In the evaluation of nociceptive sensitivity, trigger points, mapping of the area of abnormality and intensity of hypersensitivity, are taken into account; these aspects are usually evaluated by simple tests such as stimulation with cotton swab, finger pressure, pinprick, cold, and warm stimuli, e.g., thermorollers kept at 20°C and 40°C, respectively *(Jensen & Finnerup, 2014)*.

Nevertheless, the primary complaint of the pain patient is **spontaneously emitted pain**. While stimulus-evoked pain is relatively reproducible in animal models of pain, often these laboratory settings do not reflect clinical reality, as the patient usually tries to avoid pain-eliciting stimuli. On the other hand, measuring spontaneous pain behavior in animal models of pain is an open issue: it remains unclear which behaviors can reveal its presence in the laboratory animal. Many measures have been proposed: analgesic self-administration, conditioned place aversion for a pain-associated chamber and preference for an analgesic-associated one, weight bearing disturbance, grip/bite force, intensification of grooming (scratching/licking/biting) behavior, writhing, limb guarding (abnormal positioning), hindpaw lifting/flinching/shaking, hypolocomotion, hypophagia, weight loss, inattention to novel stimuli, and ultrasonic vocalization. Only recently, the need of an index of spontaneous pain next to elicited-pain measures is gaining popularity *(Mogil & Crager, 2004)*.

Thus, the most used pain tests are still reflexive pain tests, which evaluate evoked behavioral responses after the application of heat, cold, mechanical, and electrical stimuli: these stimulations activate nociceptors and trigger localized, stereotyped motor responses

resulting in the withdrawal of the tested limb. If application of stimuli at the site of injury provokes a decrease of the paw withdrawal threshold, the phenomenon observed is called **primary hyperalgesia** and it is due to sensitization of nociceptive primary afferents. Enhanced sensitivity outside the site of injury, or in absence of peripheral injury, is named **secondary hyperalgesia** and is the result of central sensitization, i.e. hypersensitization of spinal secondary order neurons.

Thermal reflexive pain tests include: the Tail Flick Test, where a heat stimulus is applied to the tail of the animal and the latency to remove the tail is recorded; the Hot- or Cold-Plate Test, which evaluates the latency for withdrawing or licking the paw from the hot- or cold-plate.

Mechanical reflexive pain tests are used to measure both allodynia and hyperalgesia. They include: von Frey filaments test, where a range of nylon hairs with growing force is applied on the paw of the animal with constant pressure; the Randall-Selitto analgesiometer, which similarly consists in the application of a growing weight on the paw while the animal is restrained. The latency to withdrawal or vocalization is the measured variable *(Gregory et al., 2013)*.

2.2.2 Major animal models of chronic pain

Multiple animal models of pain have been developed. Some examples of the main categories (neuropathic pain, cancer- or chemotherapy-induced pain, post-operative pain, joint pain and inflammatory pain) are reviewed below.

Neuropathic pain is provoked by damage, trauma or disease of the nervous system. Sometimes, also ischemia or exposure to neurotoxins can lead to neuropathic pain. Central neuropathic pain can be induced in the somatosensory cortex or thalamus, by microinjection of excitotoxic agents such as picrotoxin or kainate, or directly damaging the spinal cord through contusion, surgical lesions, ischemic injury, or excitotoxicity. Though, most of the animal models of chronic pain target peripheral nerves through ligation, transection or constriction: e.g., spinal nerve ligation or transection (SNL or SNT), ligation or lesion of the sciatic nerve (chronic constriction injury, CCI; partial nerve transection), and ligation of the

distal branches (peroneal, tibial) of the sciatic nerve (spared nerve injury, SNI). Moreover, injection of an inflammatory irritant (zymosan) around the sciatic nerve has been used to induce sciatic inflammatory neuritis (SIN), while inoculation of streptozotocin leads to diabetic neuropathy.

Chronic pain conditions resulting from cancer can be directly caused by the cancer itself or by chemotherapeutic drugs administered to patients. Both the etiologies have been modeled in animals, and cancer induced peripheral neuropathy (CIPN) is often used.

Among the joint pain models, injection of collagen type II antibodies (Collagen Antibodies Induced Arthritis, CAIA) is used to model rheumatoid arthritis, while osteoarthritis is mimicked by several methods which cause the destruction of tissues surrounding the joint: e.g., transection of the anterior cruciate ligament (ACLT) or the knee medial meniscus (MMT), or injection of monosodium iodoacetate (MIA) in the knee.

Thermal hyperalgesia, mechanical hyperalgesia and spontaneous pain follow also the surgical incision of skin and muscles of the hindpaw, which results in post-operative pain, a condition often found in clinical patients *(Brennan et al 1996)*.

Inflammatory pain is reproduced in animals through the injection of irritants into the skin, paw, muscle or joints, to mimic both acute and chronic inflammatory pain. These substances act by neutrophil recruitment and, in the long period, causing macrophage infiltration. For example, injection of capsaicin into the skin, muscle or joint produces a local neurogenic inflammation; carrageenan results in an initial acute inflammation that becomes chronic by 2 weeks; formalin produces nociceptive behavior, characterized by licking and flinching of the paw. Complete Freund's adjuvant (CFA) can be injected into tail, paw, muscle and joint and results in chronic inflammatory pain, leading to thermal and mechanical hyperalgesia (both at the site of injury and in nearby areas), body weight imbalance and enhanced spontaneous pain behaviors *(Gregory et al., 2013)*.

2.2.3 The Complete Freund's adjuvant (CFA) model

Rheumatoid arthritis (RA) is an inflammatory autoimmune disorder targeting joints and cartilage with still unknown etiopathogenesis. Adjuvant-induced arthritis animal models are

widely used preclinical models to study the effects of arthritis; the most known adjuvant model for RA chronic inflammation is the CFA-induced arthritic model. The injection of CFA, composed of heat killed and dried Mycobacterium tubercolosis and adjuvant (paraffin oil and mannide monooleate) into the footpad produces localized inflammation and persistent pain, thus it is an excellent model to study chronic inflammatory pain, in addition to RA.

The mechanism of action of CFA is still not totally clear. We know that the mycobacteria in Complete Freund's adjuvant attract macrophages and other cells to the injection site which enhances the immune response. It was found that arthritogenic T cell clones recognize epitopes of the mycobacterial heat shock protein (HSP), hsp65: this led to the assumption that the pathogenesis is closely linked to the immune response to these mycobacterial antigens. Furthermore, the prolonged immune response triggered by a single CFA injection is due to the prolonged lifetime at the site of injection of protein antigens administrated in oil emulsion. Following CFA injection, dendritic cells perform a rapid uptake of adjuvant components, phagocytes start to secrete cytokines, and $CD4^+$ lymphocytes become active and start to proliferate. CFA mycobacterial agents drive T lymphocytes towards a T helper 1 (Th1) profile, so that a strong and sustained hypersensitivity against autoantigens develops (**Figure 4**) *(Billiau & Matthys, 2001)*.

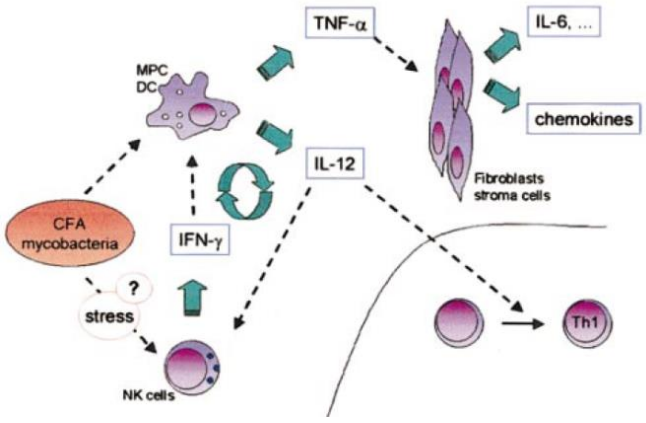

Figure 4 Schematic illustration of the inflammatory reaction triggered by CFA injection *(Billiau & Matthys, 2001)*.

After a CFA injection into the footpad, animals develop paw inflammation within a few hours, reaching the maximum peak within 5-8 h. CFA produces dose-dependent inflammatory edema, mechanical allodynia, mechanical and thermal hyperalgesia in the injected hind paw, but animals do not show weight reduction nor alterations in grooming or exploratory behavior. Symptoms persist at least for a couple of weeks, but CFA-induced inflammatory pain does not ever evolve into a systemic disease *(Zhang & Ren, 2011*). Furthermore, CFA-injected rats *(Tétreault et al., 2010*) and mice *(Griffioen et al., 2015)* decrease the use of their ipsilateral hind paws and show a reduction in the paw surface pressed against the floor, measured by the Dynamic Weight Bearing (DWB) system, a recently developed device which can measure the percentage of body weight put on each paw in freely moving animals.

In another study, the effects and progress of CFA injection in the right hind limb of male Wistar rats were followed up to one month. Animals developed arthritis within 4 h after the administration of complete Freund's adjuvant. There was rapid development of a localized inflammatory response characterized by increased vascular leakage, which resulted in higher skin temperature, and the subsequent swelling of the affected paw (**Figure 5**). Histological analyses of ankle joints showed hyperplasia of the squamous epithelium. Dermis showed dense mononuclear cells collection and pannus formation *(Snekhalatha et al., 2013)*. Collectively, these data suggest that CFA-induced chronic pain is a suitable model to study inflammatory processes in laboratory animals, specifically validated in Wistar rats.

Figure 5 CFA intraplantar injection results in paw swelling and inflammation after 4 hours.

2.3. Neurobiology of pain

2.3.1 Physiological pain

Nociceptors, the subgroup of sensory neurons specialized for the capture of pain stimuli, are classified into two main types of fibers: unmyelinated C fibers and poorly myelinated Aδ fibers. Noxious stimuli, such as extreme heat or cold, pressure and chemicals, are converted to electrical activity by transient receptor potential–generating channels (TRP channels) and purinergic channels, located on nociceptors, which in turn, stimulated by the activation of these specialized sensors, produce spikes. These nociceptive fibers, called primary afferents, mostly release glutamate onto second-order neurons in the superficial laminae (I and II) of the dorsal horn of the spinal cord. Nociceptive inputs begin to be partially processed already at the spinal level, then they are projected to the brain by several ascending pathways, mainly the spinothalamic and the spinoparabrachial tracts, which encode the sensory-discriminative and the emotional aspects of pain, respectively (**Figure 6**) *(Kuner, 2010)*.

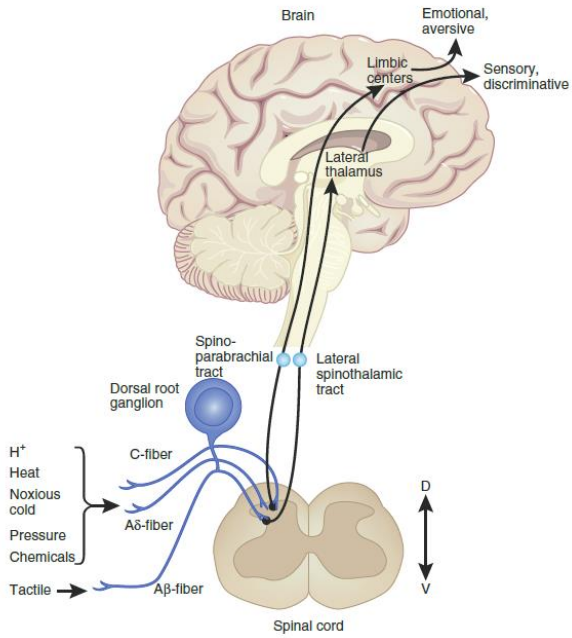

Figure 6 A schematic overview of main circuits mediating physiological pain *(Kuner, 2010).*

The experience of pain is perceived in the cortex, and information is accordingly sent to the spinal cord to enable withdrawal from the noxious stimulus.

Several brain areas project to the spinal cord and contribute to the perception of pain inhibiting spinal transmission. The noradrenergic nuclei in locus coeruleus and subcoeruleus, as well as serotoninergic areas located within the nucleus raphe magnus, extend their axons down to the spinal cord through the dorsolateral funiculus to innervate dorsal horn neurons, in particular laminae I and II *(Yoshimura & Furue, 2006)*.

2.3.2 Nociceptors: anatomy and neurobiological features

Nociceptors can be categorized basing on biochemical markers which they express or features which they show (e.g., the expression of versican, the binding partner for the isolectin B4 (IB4); the release of neuropeptides such as substance P and calcitotin-gene related peptide (CGRP)). Initial fast-onset pain is mediated by A-fiber nociceptors, myelinated fibers with conduction velocity of approximately 5–30 m/s. Most nociceptors have small diameter unmyelinated axons (C-fibers) supporting conduction velocity of 0.4–1.4 m/s, and mediate the slow-onset, less intense but more long-lasting sensation of pain.

Noxious stimuli are transduced into electrical signals in free unmyelinated nerve endings that capture information in dermis and epidermis. Painful stimuli are transformed into spikes which propagate towards the cell soma. As most of the somatosensory neurons, also nociceptors are pseudounipolar cells: a single axon comes out of the cell body in the dorsal root ganglion (DRG) and bifurcates, sending a peripheral branch to the skin and a central branch to the dorsal horn of the spinal cord.

Nociceptors activation has several consequences, both peripherally and centrally. Activity-triggered release of peptides (e.g., substance P, CGRP, somatostatin) and/or other bioactive substances from the terminals (e.g., cytokines) into the skin can exacerbate the peripheral lesion, leading to vasodilatation (reddening, via CGRP) and increased vascular permeability (edema, via substance P). These substances in turn feedback on nociceptors contributing to their sensitization. The central axon of DRG neurons enters the spinal cord via the dorsal root and sprouts branches that innervate multiple spinal segments, where synapses are also

mediated by substance P, CGRP, somatostatin, and mainly glutamate *(Dubin & Patapoutian, 2010)*.

After activation, the transduction of the signal is often carried out by second messenger-dependent pathways in most nociceptors. Ion channels, metabotropic G protein-coupled receptors (GPCRs), and receptors for neurotrophins or cytokines are commonly expressed by nociceptive neurons, and differently contribute to the transduction of the sensory signal. Ion channels include transient receptor potential (TRP) channels, NaV channels, Ca2+ and K+ channels. Excitatory GPCRs include B1 and B2 bradykinin receptors, protease-activated receptors, and receptors for prostaglandin E2. Among inhibitory GPCRs, targets for pain relief include μ, κ and δ opioid receptors.

The second-messenger pathways involved in metabotropic receptor signaling are several: some fundamental examples are the Gs- and Gi-coupled adenylate cyclase-cyclic adenosine monophosphate (cAMP)-protein kinase A (PKA), the Gq-coupled phospholipase C (PLC)-diacylglycerol (DAG)-inositol trisphosphate (IP3)-protein kinase C (PKC), and pathways involving phosphorylated extracellular signal regulated kinase and p38 mitogen activated kinase. Furthermore, consistent cross-talking between pathways, e.g. in the modulation of the TRP channel TRPV1, intriguingly complicates the picture *(Gold & Gebhart, 2010)*.

2.3.3 The transient receptor potential cation channel subfamily V member 1 (TRPV1): role in peripheral sensitization

The transient receptor potential cation channel subfamily V member 1 (TRPV1 or VR1) is a six transmembrane domains protein, non-selective cation channel that can be directly activated by capsaicin and extreme heat (with activation threshold at 43°C). However, this threshold seems to be dynamic, because it is significantly lowered under inflammation: thus, TRPV1 is thought to be involved in the establishment of **peripheral sensitization**, in which a reduction in the activation threshold and an increase in the sensitivity are observed in nociceptors. Indeed, many inflammatory substances are able to lower the activation threshold of TRPV1: some examples are medium acidification, bradykinin, nerve growth

factor (NGF), anandamide, leukotrienes, prostaglandins, adenosine triphosphate (ATP), prokineticins, polyamines and venoms (**Figure 7**) *(Szallasi et al., 2007)*.

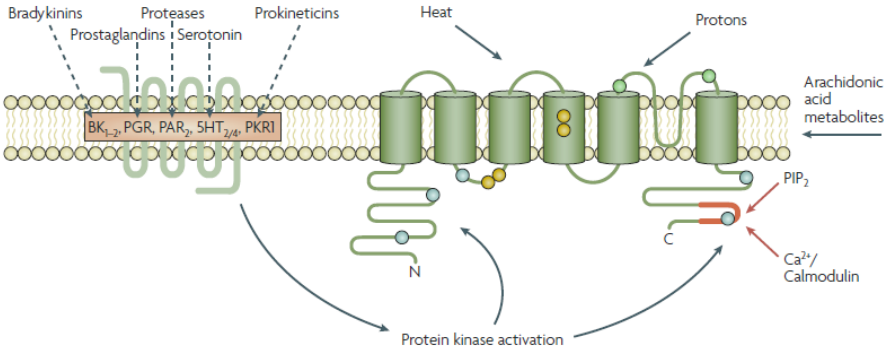

Figure 7 Schematic summary of TRPV1 signal integration in the peripheral nociceptor terminal *(Szallasi et al., 2007)*.

Usually, phosphorylation of TRPV1 by protein kinases causes sensitization: PKA and PKC (especially PKCε by a pathway that depends on cAMP-activated guanine exchange factor (EPAC)) can sensitize TRPV1. Also Ca2+-calmodulin–dependent protein kinase II (CaMKII) targets this receptor, as well as PLC-mediated pathways (**Figure 8**), making TRPV1 a clue actor in nociception.

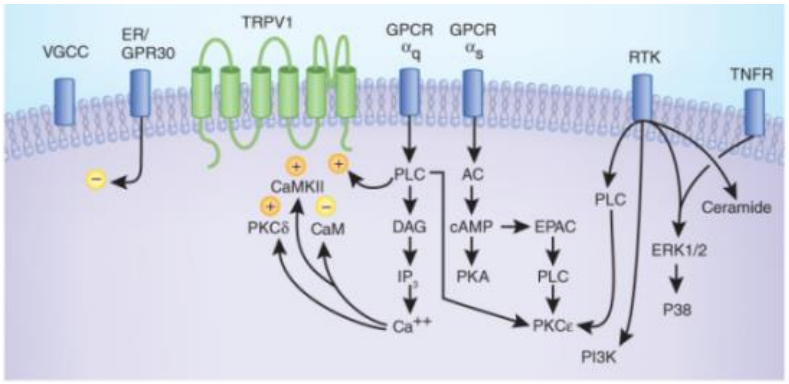

Figure 8 TRPV1 activation by intracellular pathways *(Gold & Gebhart, 2010).*

2.3.4 Protein Kinase C (PKCs) family: a leading role in pain

Protein Kinase C family is a wide family of serine/threonine kinase isoforms able to regulate several intracellular processes such as growth, differentiation, apoptosis, migration and oncogenesis. In all these isozymes, an NH2-terminal regulatory module and a COOH-terminal catalytic domain are present. Basing on the binding capability of the regulatory domain, PKC isoforms can be grouped into three major categories: the classical, or conventional, PKCs, which are calcium- and DAG-dependent (α, β, γ); the novel PKCs (δ, ε, η and θ) that are calcium-independent but DAG-dependent, and the atypical PKCs (ζ, λ and ξ) which are both calcium- and DAG-independent *(Duquesnes et al., 2011).*

Most of, if not all, PKCs are regulated by phosphorylation, even if they have different activation cascades. There are three phosphorylation sites located in the catalytic domain: the activation loop (Thr-566), the Thr-Pro turn motif (Thr-710), and the hydrophobic Phe-Ser-Tyr motif (Ser-729). Upon activation, classical and novel PKCs translocate from the cytosol, where they rest in the inactive form, to cell membrane or to specific subcellular compartments, to which they bind thanks to specific PKC-binding proteins known as RACKs (receptors for activated C-kinase) *(Newton and Messing, 2011)*.

PKCs can be found in anatomical regions that regulate pain, such as primary afferents, spinal cord (mainly in the dorsal horn), and brain, therefore they were hypothesized to be a proper target for pain therapeutics development. First experiments aimed to verify their implication in pain were based on PKC non-specific activators or inhibitors on isolated sensory neurons in vitro cultures. Nevertheless, these chemicals revealed effective on this type of cells; furthermore, they showed anti-nociceptive properties in in vivo animal models of several kinds of pain *(Velàzquez et al., 2007)*.

After the arrival of PKC-isoform k.o. animals and isozyme-selective activators and inhibitors, several PKCs have been shown to play a role in different models and kinds of pain. For example, PKC-βII, δ and ε seem to mediate paclitaxel (a chemotherapic agent)-induced neuropathic pain at the DRG level *(He and Wang, 2015)*; diabetic neuropathy *(Shangguan et al., 2003)* and inflammatory hyperalgesia *(Gu et al., 2016)* are accompanied by increased activation of PKCα; PKCε is involved in prostaglandin E2 (PGE2)-induced mechanical hypernociception *(Sachs et al., 2009)*, in paclitaxel-induced neuropathic pain *(Gao et al., 2016)* and in CFA-induced inflammatory pain *(Zhou et al., 2003)*; moreover, intraplantar

injection of ψεRACK (a direct PKCε activator) is able to prolong PGE2-induced hyperalgesia in the rat. When IB4+ nociceptors are lesioned via intrathecal administration of IB4-saporin, ψεRACK produces an initial hyperalgesia; however, the PGE2-induced prolonged hyperalgesia is absent in animals treated with toxin suggesting that priming is localized to IB4+ neurons *(Joseph and Levine, 2010)*.

Collectively, these findings support a key role for PKCε in the initiation and maintenance of nociceptor priming, therefore making this PKC isoform a key therapeutic target.

2.3.5 PKCε and TRPV1: evidences for a close relationship

Unphosphorylated PKCε has been localized to the Golgi apparatus. Following activation, it translocates to several intracellular compartments via RACK2 binding, and this interaction requires PKCε phosphorylation at Ser-729. There is evidence that activated PKCε is able to phosphorylate L-type Calcium channels, Trif related adapter molecule (TRAM, a downstream protein of toll like receptor 4, TLR-4), the GABA-A receptor and TRPV1 *(Newton and Messing, 2011)*. Upstream activators of PKCε include EPAC, GPCRs and the second messenger PLC. Epac upregulation was observed in DRGs of CFA-injected rats, and this increase was linked with purinergic P2X3 receptor potentiation mediated by EPAC-PKCε signaling *(Gu et al., 2016)*. Gαi-associated GPCRs have a role in maintaining CFA-induced hyperalgesia in the late phase (from 4 hours after the injection), and this action seems to be PKCε-mediated, while the acute inflammatory phase seems to be Gαs-regulated *(Huang et al., 2015)*. In bortezomib-induced peripheral neuropathy in rats, a chemotherapic-induced neuropathic condition, a reduction of mechanical nociceptive threshold was associated with a relative increase of TRPV1 in DRGs, and the proportion of TRPV1- and CGRP-labeled neurons increased after treatment *(Quartu et al., 2014)*. Also paclitaxel-induced peripheral neuropathy triggers heat hyperalgesia and mechanical allodynia in mice and rats. Quercetin (a polyphenolic flavonoid plant extract) administration was proved to dose-dependently counteract paclitaxel-induced hyperalgesia and allodynia, and to suppress the increased expression levels of PKCε and TRPV1 in the spinal cords and DRGs of paclitaxel-treated rats and mice *(Gao et al., 2016)*. In fact, previous studies have demonstrated that PKCε activation

in small- and medium-sized DRG neurons alters the TRPV1 function and consequently leads to hyperalgesia. In animal models of inflammatory pain, such as those induced by carrageenan *(Zhou et al., 2003)* or CFA *(Zhou et al., 2003; Yu et al., 2008; Breese et al., 2005)* injection, phosphorylation of PKCε in DRG neurons was significantly up-regulated, predominantly in TRPV1 positive small diameter DRG neurons, and was associated with thermal hyperalgesia, *(Zhou et al., 2003; Yu et al., 2008; Breese et al., 2005)* and mechanical allodynia (*Yu et al., 2008; Breese et al., 2005)*. These data indicate that functional activation of PKCε has a close relationship with the production of inflammatory hyperalgesia and the sensitization of the nociceptors. Inflammatory mediator-induced activation of PKCε and subsequent sensitization of TRPV1 to noxious stimuli by PKCε may be involved in nociceptor sensitization. Furthermore, inflammation increased the percentage of IB4-positive neurons that was TRPV1-immunoreactive in CFA-injected mice *(Breese et al., 2005)*.

2.3.6 The switch to chronicity: from peripheral to central sensitization

When peripheral nociceptors are exposed to inflammatory mediators and undergo damage or lesion, peripheral sensitization takes place, resulting in a reduction of the activation threshold and an increase of sensitivity which is restricted to the site of tissue injury. On the other hand, when **central sensitization** is established, the nociceptive system gains an abnormal responsiveness to stimuli, due to plastic neurobiological changes in the central nervous system: these include increases in membrane excitability, synaptic efficacy, or reduced inhibition, resulting in a facilitation of the nociceptive transmission *(Latremoliere & Woolf, 2010).*

Potentiation of nociceptive transmission can occur at different steps. At the synaptic level, amplification of excitatory postsynaptic potentials in response to constant neurotransmitter release takes place by insertion of glutamatergic AMPA receptors (AMPARs) into postsynaptic membranes. Otherwise, neurotransmitter release can be upregulated. Long-term potentiation of nociceptive transmission has been reported in the spinal dorsal horn *(Price & Inyang, 2015)*. At the neuronal level, the response to a nociceptive stimulus, or the entity of spontaneous activity can increase, as well as the cell receptive field, with the result

that peripheral areas previously out of the nociceptive field can now activate the neuron: this phenomenon accounts for secondary hyperalgesia. Lastly, structural plasticity can occur by changes in the synaptic spines density, aberrant connectivity and proliferation of glial cells (**Figure 9**) *(Kuner, 2010)*.

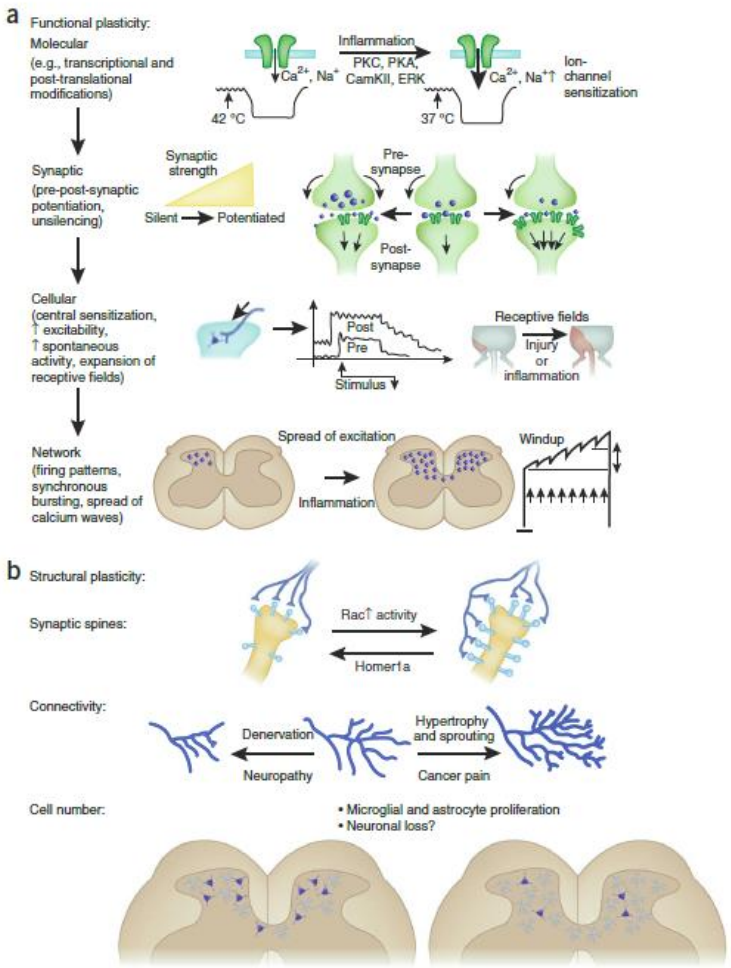

Figure 9 Disease-induced functional and structural plasticity in neural substrates of pain. **a** functional plasticity; **b** structural plasticity *(Kuner, 2010)*.

2.4. The opioid-induced tolerance: a "poppy(ing)" problem

2.4.1 The epidemy of opioids overprescription: facts and consequences

Recently, a growing epidemic phenomenon of opioids misuse and overprescription has been described by Manchikanti et al. (2017). Reports on opioids use in 2014 ascribe to the United States the consumption of the majority of opioid analgesics, as hydrocodone, morphine, oxycodone and hydromorphone. United States' and the world's opioids use doubled from 2000 to 2014. Along with this huge increase, since 2000 the rate of opioids overdoses tripled, with regard to both deaths due to opioid analgesics and the ones caused by illegal opioids consumption, such as heroin. Natural and semisynthetic opioid pain relievers, though, are still the main cause of death from opioid drugs *(Manchikanti et al, 2017)*. This trend represents without doubts an impellent clinical problem, concerning a biased chronic pain treatment towards opioid drugs prescription by physicians, but most of all, a considerable social issue that needs to be quickly addressed.

2.4.2 The neurobiology of opioids: from acute to chronic use

Opioid drugs can still be the best choice to treat acute pain thanks to their analgesic efficacy. Nevertheless, chronic treatment with opioids inevitably leads to unpleasant, and potentially dangerous, side-effects. First of all, their potential of abuse is very high, with chronic use resulting in drug-seeking and **addiction** behaviors. Besides, in the long period, opioids use leads to analgesic and pharmacological **tolerance**, which claims for an incessant increase of the dose to reach the same analgesic effect; and these drugs are potentially toxic and lethal in high doses. **Physical dependence** gets instituted and, after treatment interruption, gives rise to **withdrawal** symptoms (e.g., piloerection, chills, insomnia, diarrhea, nausea). Furthermore, chronic opioids treatment often results in aberrant hyperalgesia *(Volkow & McLellan, 2016)*.

Opioid medications primary act on μ-opioid receptors (MORs). MORs are present in cerebral areas responsible for the perception of pain (periaqueductal gray, thalamus, cingulate cortex

and insula) and in the substantia gelatinosa of the dorsal horn of the spine, where they exert their primary action in inhibiting spinal transmission (**Figure 10**).

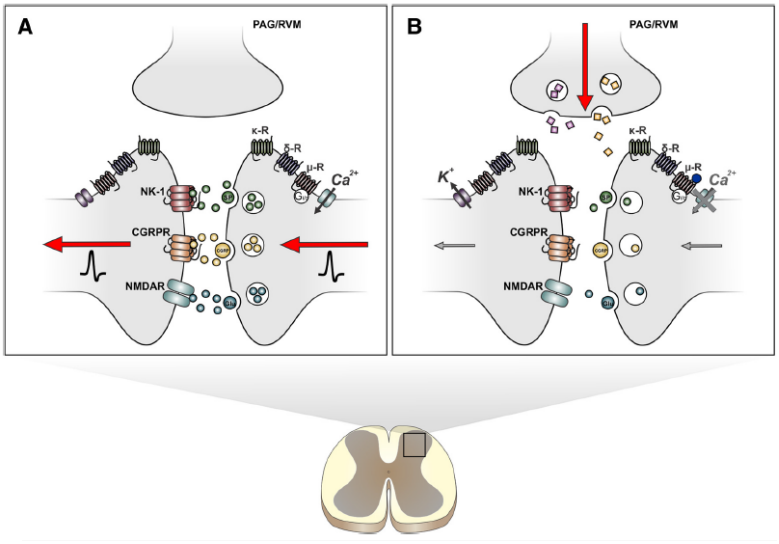

Figure 10 Spinal mechanisms of opioids analgesia. **A** Normal neurotransmission between nociceptors and second-order neurons in the dorsal horn of the spinal cord. **B** Inhibition of spinal nociceptive transmission by opioids *(Trang et al., 2015)*.

MORs are also expressed in limbic areas responsible for emotional responses and learning, such as amygdala, ventral tegmental area and nucleus accumbens. Acute opioids administration causes the activation of the reward circuits and the release of dopamine in these areas. Dopaminergic projections from ventral tegmental area to the prefrontal cortex and nucleus accumbens are responsible for the attribution of incentive salience to opioid-related contextual cues, which are learned to be associated to pain relief and pleasure. With the consolidation of these associations, drug-seeking behavior is reinforced and elicited by the perception of drug-related cues *(Garland, 2014)*.

MORs located elsewhere in the brain or in the periphery can account for the onset of opioids-induced side-effects: e.g., MORs in the brain stem cause respiratory depression, main cause of deaths by overdose; MORs in the gastric trait explain opioid-induced constipation.

Opioid receptors (μ, δ, κ) are seven transmembrane domains proteins coupled to inhibitory G proteins (**Figure 11**), whose activation leads to cAMP inhibition, deactivation of the inwardly rectifying potassium channel (Kir3), and reduction of calcium channels conductance resulting in cellular hyperpolarization *(Al-Hasani & Bruchas, 2011)*.

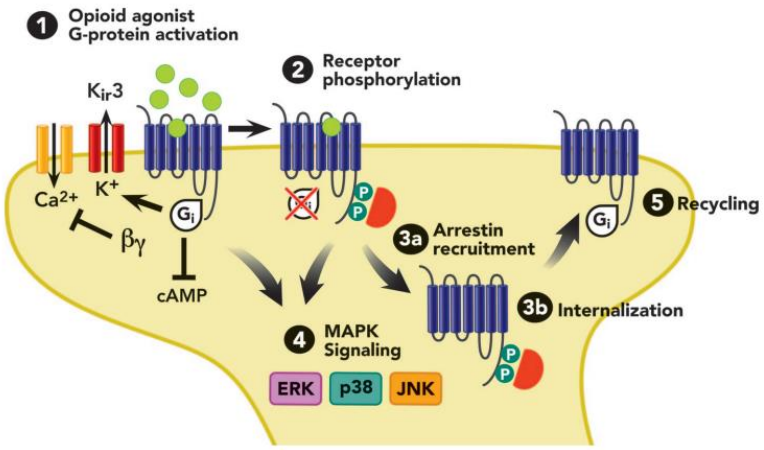

Figure 11 Summary of opioid receptor signaling *(Al-Hasani & Bruchas, 2011)*

The first neurobiological hypothesis to explain opioid tolerance was focused on receptor downregulation after chronic stimulation with agonists. However, in subsequent in vivo studies it was shown that this does not happen at the same rate with every opioid agonist, i.e. each agonist has its own ability to provoke receptor downregulation. After this finding, it was then proposed that MOR proteins may be desensitized rather than downregulated, and in this way they could get separated by their downstream signaling pathways. In fact, it was shown that chronic morphine exposure leads to an increase, instead of decrease, of cAMP levels. The physiological regulation of opioid receptors by endocytosis could be a cellular defense mechanism to prevent the development of tolerance: in fact, even if, after endocytosis, the cell is desensitized to the agonist because of the reduction of the number of receptors on the cell surface, they are kept in an active state, and thus can be recycled to the membrane. This hypothesis was confirmed by the fact that facilitating MOR endocytosis prevents tolerance. Furthermore, the lack of β-arrestin 2 prevents the development of morphine-induced analgesic tolerance, counteracting the desensitization of MOR after

chronic morphine treatment *(Bohn et al., 2000)*. The involvement of arrestins in MOR desensitization and opioid-induced tolerance is sustained by many studies. In fact, arrestin binding to MOR-associated G-protein blocks G-protein signaling promoting cellular tolerance (**Figure 12**) *(Cahill et al., 2016)*.

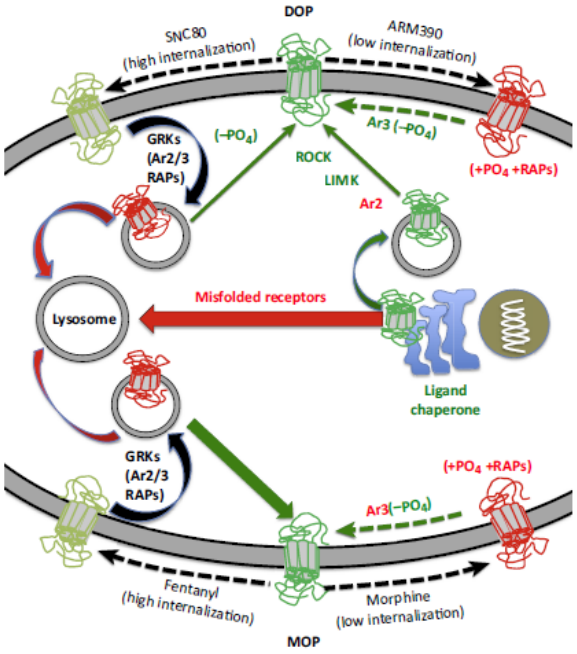

Figure 12 Differences in opioid receptor regulation by low- and high-internalizing agonists *(Cahill et al., 2016)*.

Because of the involvement of arrestins in tolerance, recently there is an effort to develop drugs able to activate MOR without recruiting either arrestin 2 or 3. Such specialized MOR agonists would be able to enlarge the therapeutic window while limiting side-effects development, first of all tolerance. Manglik and colleagues found that, of their 23 molecules, compound 12 (PZM21) had strongly biased activity for Gαi/o upon β-arrestin signaling, comparable to TRV130, a MOR agonist with similar affinity features which is currently going through clinical phase 3 *(Manglik et al., 2016; Kieffer, 2016).*

Another interesting aspect is the involvement of PKCε in morphine tolerance. In fact, morphine analgesia is enhanced in PKCε k.o. mice *(Newton et al., 2007)*. This result confirms

the hypothesis coming from previous studies showing stimulation of PKCε by MOR-specific ligands and implying the existence of a negative feedback mechanism to counteract MOR inhibition of N-type calcium channels. In PKCε k.o. mice, this putative inhibitory feedback is missing, and MORs activation keeps its analgesic efficacy. Moreover, PKCε activation was found to be fundamental in both opioids tolerance and transition to chronic pain. Joseph et al. demonstrated that repeated administration of the MOR agonist DAMGO produces hyperalgesia, and in turn, that induction of hyperalgesia by inflammation is able to facilitate opioid tolerance and dependence; both effects depend on PKCε presence in nociceptors *(Joseph et al., 2010)*.

2.4.3 The contribution of microglia

The vast majority of cells within the nervous system are not neurons but rather glia, representing 70–90% of cells, 10% of which is composed by microglial cells. In addition to implement the function of macrophages of the central nervous system, it has been shown that microglia also plays a role in the immune support for neurons and takes part to synaptic remodeling and neurotransmission. In particular, chronic pain conditions and sustained exposure to morphine actively recruit microglia, which undergoes a variety of changes in its morphology, gene expression and number. These phenomena provoke a transformation of cells from a ramified, resting to an amoeboid, activated state, in which the majority of cellular processes are retracted and somata become swollen *(Trang et al., 2015)*. Transition to this "activated" state is often referred to as microgliosis, or microglial "reactive" state, and it is traditionally identified by upregulation of several glial markers such as the C-C chemokine receptor 3/cluster of differentiation molecule 11 b (CCR3/ CD11b), the glial fibrillary acidic protein (GFAP) and the ionized calcium-binding adapter molecule 1 (IBA1), the last one being the most used marker for microgliosis. Upregulation of these factors, and phenotypical shift towards the activated state, can be found in nerve injury, inflammation, surgery, chronic opioid exposure, cancer pain and neuropathic conditions of various etiologies. Along with the morphological changes, microglia starts an overproduction of proinflammatory cytokines such as tumor necrosis factor-α (TNF-α), IL-1β (interleukin-1 β),

and IL-6 (interleukin-6), all of which contribute to sustain painful conditions, and their inhibition (not only in microglia but also in other glial cells, and even in neurons) alleviates pain and enhances morphine analgesia *(Ji et al., 2013)*. Microglia inflammation has also been reported in CCI mice, in which intrathecal administration of bone marrow stromal cells was able to reduce mechanical hyperalgesia and allodynia and to decrease spinal microglia activation via transforming growth factor-β1 (TGF-β1) secretion, an immunosuppressive cytokine *(Chen et al., 2015)*. Thus, acting on glial activation could be a valid therapeutic strategy in fighting both chronic pain and opioid tolerance.

As macrophages of the central nervous system, microglial cells are specialized to recognize and block pathogens, through their antigens-sensible receptors, the Toll-Like receptors (TLRs). These proteins can be activated not only by exogenous pathogens, but also by endogenous signals mentioned above (IL-1β, TNFα, IL-6 and nitric oxide, NO), which alert for injury, or immune danger. Activation of TLR2 in astrocytes and of TLR3 and TLR4 in microglia follows instauration of neuropathic pain, while opioids stimulate mostly TLR4. IL-1β, TNFα and IL-6 also act on DRGs and spinal cord neurons, enhancing their excitability. Chemokines are also involved in chronic pain. For example, fractalkine (chemokine C-X3-C motif ligand 1, CX3CL1), produced by neurons, binds to its receptor, CX3CR1, which is expressed mostly on microglia, and when activated triggers the production of IL-1β and IL-6. Chronic pain conditions are associated with an upregulation of CX3CR1 in microglia in pain circuits (**Figure 13**) *(Milligan & Watkins, 2009)*.

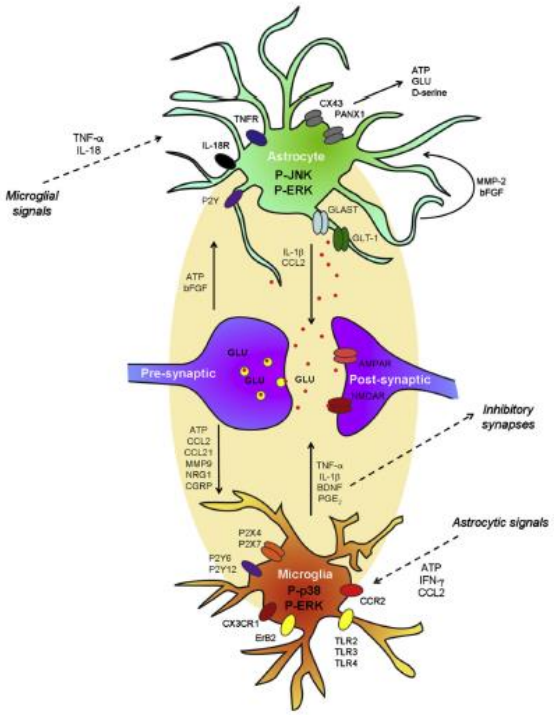

Figure 13 Schematic overview of neuronal–glial and glial–glial interactions in the spinal cord in persistent pain *(Ji et al., 2013).*

A direct link between activation of TRPV1 on nociceptive neurons and inflammation-induced microgliosis was also observed in mice models of capsaicin-induced inflammatory pain and SNL *(Chen et al., 2009)*, being this receptor necessary for the instauration of central sensitization in the dorsal horn of the spinal cord, which in turn maintains microglial activation.

As we saw, similar neuron-to-glia (and viceversa) interactions were observed in opioid tolerant animals. In fact, morphine is able to induce upregulation of microglial activation markers and proinflammatory cytokines and chemokines. Blockade or knockout of TLR4, or of any actor of the signaling cascade downstream it, leads to enhancement of opioid analgesia. These data indicate a need to review the signaling pathways so far thought to be involved in opioid analgesia, since glial TLR4 adds a new mode of action of opioid drugs to the well-known neuronal opioid receptors *(Watkins et al., 2009).*

A mechanism of action of TLR stimulation by opioids has been proposed by Merighi et al. (2013), which points out an important role for PKCε in morphine-evoked inflammatory pathways leading to chemokine and NO production. In in vitro microglial cultures stimulated

with LPS (Lipopolysaccharides, cell wall components of Gram-negative bacteria, potent activator of glia), they demonstrated that morphine-induced iNOS (cytokine-inducible nitric oxide synthase), IL-1β, TNF-α, IL-6 and NO production in primary activated microglial cells is mediated by a signaling pathway involving the activation of PKCε, Akt (also known as protein kinase B) and MAPK (mitogen-activated protein kinase) (**Figure 14**) *(Merighi et al., 2013)*.

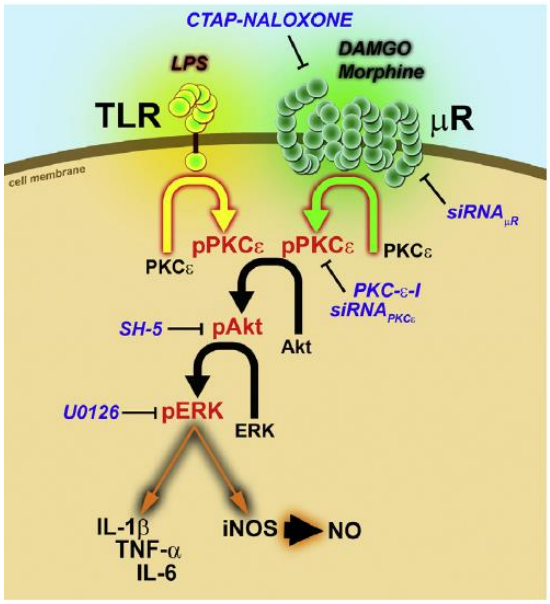

Figure 14 Schematic summary of morphine-initiated signal transduction cascade in murine microglia. Morphine binding to MOR (μR) activates PKCε, Akt and ERK kinases, which lead to subsequent expression of proinflammatory chemokines and NO *(Merighi et al., 2013)*.

2.5 Imidazoline ligands: a new perspective in treating pain

2.5.1 Imidazoline receptors and ligands: an emerging therapeutic tool for chronic pain

The term imidazoline receptors refers to the binding sites of radio-labeled adrenergic ligands such as [3H]clonidine, [3H]p-aminoclonidine and [3H]idazoxan, insensitive to norepinephrine. Subsequent binding investigations showed that these non-adrenergic

binding sites could be further subgrouped into two main categories: the binding sites for p-aminoclonidine and moxonidine and the binding sites for idazoxan and cirazoline, which were termed imidazoline 1 and 2 receptors (I1R and I2R), respectively *(Li, 2017).* To date, still I2R have not been cloned and characterized, even if some putative proteins have been identified in human and mouse brain tissue, being expressed in both neurons and astrocytes *(Keller & García-Sevilla, 2015)*. Nevertheless, thanks to the available selective I2R ligands, some insights have been achieved in the signaling and function of these proteins.

In vitro studies located I2Rs primarily on the outer membrane of mitochondria. Furthermore, it was shown from affinity studies that they may be novel allosteric binding sites of monoamine oxidases (MAO) A and B *(Jones et al., 2007)*.

One consistent finding is that I2R ligands are effective for tonic and chronic pain (inflammatory and neuropathic pain) but ineffective for acute phasic pain (nociceptive stimulus-evoked reflexive responses). Agmatine, a polyamine resulting from the metabolism of arginine, is the first I2R ligand studied. Agmatine is present in mammalian brain and binds to a number of targets including I1R, I2R and adrenergic α2 receptors, for which it has been pointed at as endogenous I2R ligand, despite its actually moderate affinity at adrenergic and imidazoline binding sites. Nevertheless, agmatine administration was able to provoke significant analgesia in animal models of tonic inflammatory and chronic neuropathic pain, but not in acute phase pain models (*Li & Zhang, 2011)*.

As agmatine, other I2R ligands were shown to have analgesic properties in several animal models of chronic pain. For example, selective I2R agonists 2-BFI, BU224, tracizoline and CR4056 significantly counteracted mechanical and thermal hyperalgesia, measured by Von Frey filaments and plantar test, respectively, in rat models of inflammatory (CFA model) and neuropathic pain (CCI model). The antihyperalgesic effects of these drugs was totally blocked by co-administration of I2R antagonist idazoxan. Similarly, morphine also dose-dependently attenuated mechanical and thermal hyperalgesia. Furthermore, at a dose that effectively attenuated hyperalgesia, 2-BFI, BU224 and CR4056 all markedly attenuated the place escape/avoidance behavior, demonstrating that I2R ligands are also effective in counteracting the affective component of pain *(Li et al., 2014)*. Furthermore, the selective imidazoline I2R agonists 2-BFI, BU224, and CR4056 produced antinociceptive effects in the formalin test *(Thorn et al., 2016)*.

I2R ligands also showed to serve as discriminative stimuli in rats: CR4056 was recognized by animals as a specific discriminative stimulus, and BU224, phenyzoline and tracizoline were able to substitute for the discriminative stimulus effects of CR4056 *(Qiu et al., 2014; 2015)*. This phenomenon demonstrates high pharmacological specificity and appears to be mediated by I2Rs. Both morphine and methadone produced dose-dependent and partial substitution for CR4056 and the effects were antagonized by naltrexone, suggesting that MORs might be involved in the discriminative stimulus effects of CR4056; however, naltrexone did not alter the effects of CR4056, thus suggesting possible secondary, but excluding primary, interactions with MORs.

2.5.2 The contribution of I2R ligands to the opioid tolerance issue

I2R ligands were also found to counteract morphine-induced tolerance and to potentiate morphine antinociception. For example, acute injection of agmatine can reduce tolerance to chronic morphine administration *(Regunathan, 2006)*. Moreover, agmatine does not enhance morphine-induced constipation in combined administration *(Kolesnikov et al., 1996)*. Furthermore, agmatine has been shown to reduce symptoms of withdrawal from morphine as measured by physical dependence in animal models: chronic exposure of rats for 7 days to morphine resulted in marked naloxone-induced withdrawal symptoms and co-administration of agmatine with morphine significantly decreased the withdrawal symptoms *(Aricioglu et al., 2004)*.

Several further I2R ligands showed similar effects on the modulation of opioid-induced tolerance. Phenyzoline was able to produce significant morphine analgesia enhancement in the tail-flick and hot-plate test. These effects proved to be mediated by I2R, since they were completely reversed by the I2R/α2-adrenoceptor antagonist idazoxan, but not by the I1R/α2-adrenoceptor antagonist efaroxan, nor by the selective α2-adrenoceptor antagonist yohimbine *(Gentili et al., 2006)*. Morphine administration for 7 days produced analgesic tolerance, which was reverted by co-administration with 2-BFI, BU224 or CR4056 *(Thorn et al., 2016)*. Oxycodone-induced tolerance, measured by the Von Frey filaments in CFA or CCI rats, was not associated with cross-tolerance to phenyzoline and vice versa. Combined

treatment of oxycodone and phenyzoline for was able to delay the onset of analgesic tolerance *(Thorn et al., 2017)*.

Similarly, 3 synthetic imidazoline compounds (providing preferential recognition of α2-adrenoceptors, I2R or both systems) were tested on morphine tolerance in CFA-injected rats. Interestingly, all compounds significantly reduced the induction of morphine tolerance. In particular, a sub-chronic 4 days treatment with the I2R-selective compound, administered twice a day 15 minutes before each morphine administration, significantly restored morphine analgesic response at day 4 *(Caprioli et al., 2015)*.

These findings strongly suggest I2R ligands as candidate drugs to treat chronic pain conditions, both alone or combined with opioids to counteract the onset of opioid-induced analgesic tolerance, given that many studies underline I2R potentiating effects without exacerbating opioid-induced side-effects (**Figure 15**).

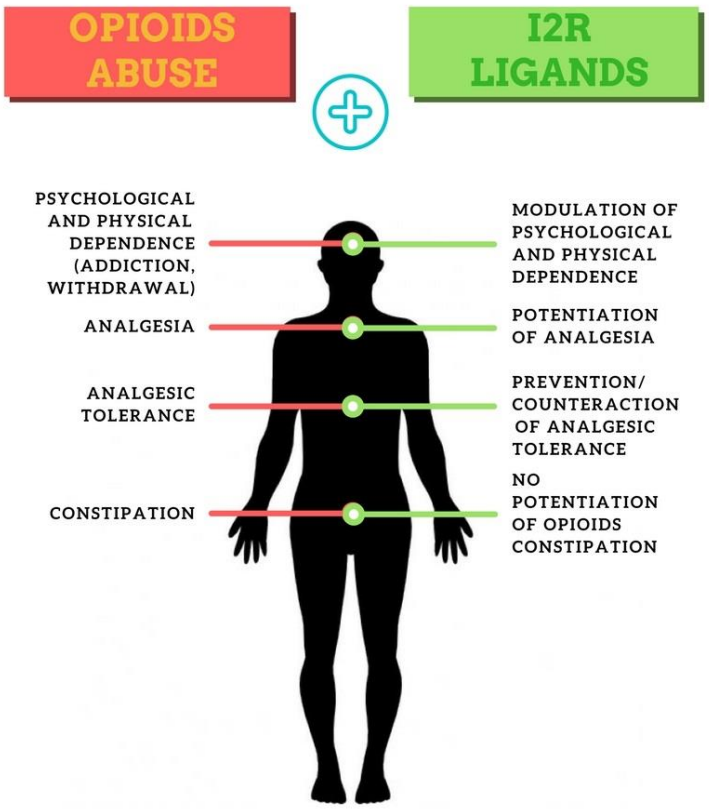

Figure 15 Potential effects of I2R ligands co-administration with opioid drugs on human opiate abuse outcomes.

2.6 CR4056

2.6.1 CR4056: a new I2R agonist analgesic drug. Biochemical features

CR4056 (2-phenyl-6-(1H-imidazol-1yl) quinazoline) is a new synthetic drug with high selectivity for I2 binding sites (molecular formula $C_{17}H_{12}N_4$; molecular weight 272.31 Da) (**Figure 16**).

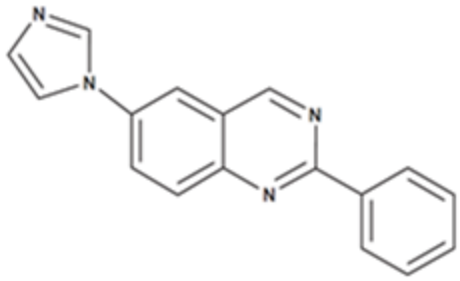

Figure 16 Chemical structure of CR4056.

CR4056 is a competitive agonist of I2 binding sites, and via this interaction allosterically modulates human recombinant and rat MAO-A activity. Moreover, CR4056 is provided with strong analgesic activity, proved in different animal models of inflammatory, chronic and neuropathic pain *(Ferrari et al., 2011; Meregalli et al., 2012; Lanza et al., 2014).* To date, CR4056 is going through phase 2 clinical trials for the treatment of chronic pain. "If approved, CR4056 would be the first I2R mechanism-based pharmacotherapy, which naturally would become one of the most important milestones in imidazoline receptor research" *(Li, 2017)*.

2.6.2 In vitro pharmacology: binding and affinity studies

In in vitro screening assays, the pharmacological selectivity of CR4056 was evaluated by testing several receptors, ion channels, transport sites and enzymes. CR4056, at the concentration tested (10 µM), was inactive in all assays except for I2R and monoamine oxidases A (MAO-A), for which showed an affinity for more than 90% *(Ferrari et al., 2011).*
CR4056 binding to I2R was then investigated on rat whole-brain membranes labeled with the specific radioligand [3H]2-BFI, using different concentrations of CR4056 and several reference compounds (2-BFI, BU224, idazoxan, clonidine). CR4056 inhibited [3H]2-BFI binding with an affinity value (IC_{50}) of 596 ± 76 nM (**Table 1**) (*Ferrari et al., 2011*); tested at equivalent concentrations, CR4056 did not show significant effect on I1R binding sites, confirming its selectivity for I2R.

Compounds	IC_{50} (nM)
CR4056	596 ± 76 *(n=3)*
2-BFI	10.3 ± 2.4 *(n=3)*
BU224	8.7 ± 2.1 *(n=2)*
Idazoxan	11.4 ± 3.4 *(n=3)*
Clonidine	8320 ± 258 *(n=2)*

Table 1 Effect of CR4056 and reference compounds on [3H]2-BFI binding to imidazoline-2 receptor subtype in rat cerebral membranes *(Ferrari et al., 2011).*

Performing a standard binding assay protocol, 3 µM CR4056 co-incubated with the labeled radioligand [3H]2-BFI induced a significant inhibition of specific binding to I2R. To test whether CR4056 binding to I2R was reversible, a pre-incubation of 3 µM CR4056 on rat whole-brain membranes was introduced before starting the equilibrium binding assay, followed by two washes: in this case, a two-fold decrease of the inhibitory effect of CR4056 was observed, suggesting a reversible binding of CR4056 towards I2R (**Figure 17**).

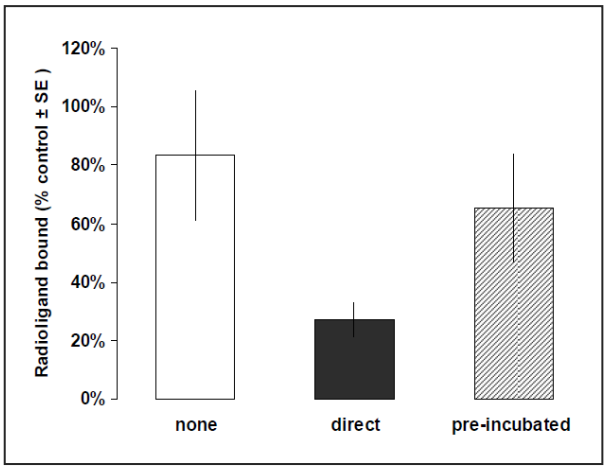

Figure 17 Effect of CR4056 co-incubation or pre-incubation with rat whole-brain membranes (i.e. I2R) on the [3H]2-BFI specific binding.

Additional experiments were performed to deepen and clarify the effect of CR4056 with regard to the specific binding to high and low affinity I2 binding sites, showing that CR4056 is a competitive ligand for I2 high affinity binding sites, and has little or no effect on low affinity binding sites (**Table 2**).

	No compound	1µM CR4056
Kd_H	3.8±0.1 nM	12.5±5.5 nM ($p<0.05$, Student's t-test vs no compound)
$Bmax_H$	0.4±0.05 pmol/mg protein	0.7±0.2 pmol/mg protein
Kd_L	32.4±9.4 nM	15.2±9.7 nM
$Bmax_L$	1.2±0.3 pmol/mg protein	0.5±0.1 pmol/mg protein

Table 2 CR4056 effect on kinetic parameters of [3H]2-BFI specific binding.

The affinity of CR4056 for MAO-A and MAO-B was then studied in receptor binding assays in rat cortical membranes, using clorgyline and (R)-deprenyl as standard compounds for MAO-

A and MAO-B. CR4056 significantly inhibited MAO-A specific binding, while inhibition of MAO-B was only obtained at very high concentrations (**Figure 18**) *(Ferrari et al., 2011).*

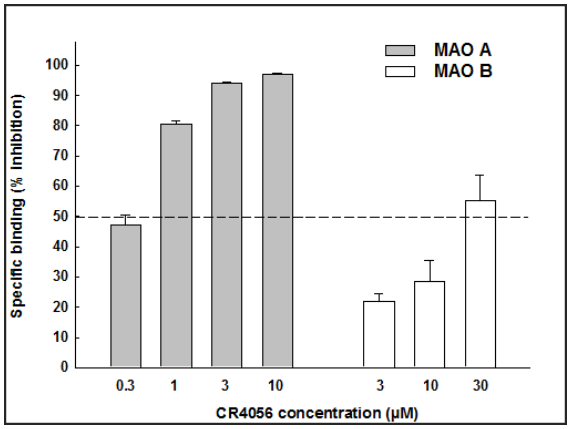

Figure 18 Inhibition of MAO-A and MAO-B binding; dose-response curve of CR4056.

To confirm these data, CR4056 and the reference compounds modulation of MAO-A and MAO-B was also tested on human recombinant enzymes, through a fluorimetric assay. Similarly to the binding study, CR4056 selectively inhibited the enzymatic activity of MAO-A (**Table 3**) *(Ferrari et al., 2011).*

Compound	IC_{50}, nM	
	MAO-A	MAO-B
CR4056	202.7 ± 10.3 *(n=2)*	>10000 *(n=2)*
Clorgyline	19.5 ± 1.1 *(n=3)*	45300 *(n=1)*
Deprenyl	19100 *(n=1)*	347 ± 32.5 *(n=2)*
2-BFI	10µM= -57%	10µM= -61%

Table 3 Effect of CR4056 and reference compounds on the enzymatic activity of human recombinant MAO-A and MAO-B *(Ferrari et al., 2011).*

The effects of 1 µM CR4056 on the modulation of MAO-A was also assessed in rat cerebral mitochondrial membranes, using serotonin as substrate, where it was shown to inhibit MAO-A in an allosteric way (**Figure 19, panel A**). On the other hand, CR4056 (0.3 µM-1 µM) tested on human recombinant MAO-A activity suggested a mixed (competitive-allosteric) mechanism of action (**Figure 19, panel B**). The gap observed between human and rat MAO-A could be explained by the existing differences between MAO-A and I2R proteins across species.

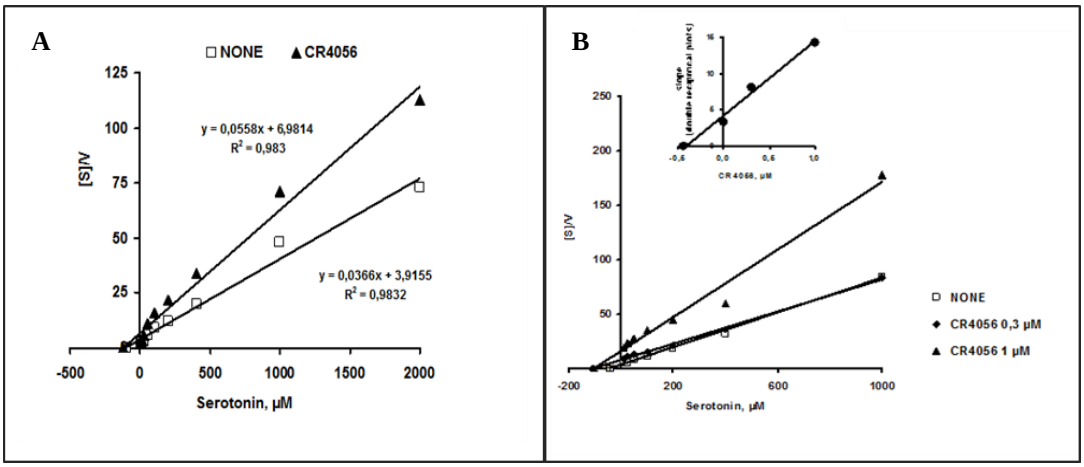

Figure 19 A: CR4056 effect on rat cerebral MAO-A activity; **B**: CR4056 effect on human recombinant MAO-A activity (Hanes-Woolf plot). S=substrate initial concentration; V=reaction velocity.

2.6.3 In vivo pharmacology

Given in vitro results on CR4056's ability to inhibit MAO-A, the effects of this I2R ligand were also tested in vivo. It is known that monoamines such as serotonin and noradrenaline are crucial components of the central descending inhibitory pathways which can modulate spinal nociception; therefore, selective inhibitors of synaptic reuptake of noradrenaline, serotonin, or both (e.g., duloxetine) are currently used in the treatment of chronic pain conditions (*Yoshimura & Furue, 2006*; *Pertovaara, 2013*). MAOs are enzymatic inactivators of

monoamines at synaptic spines; therefore, inhibition of MAOs activity should imply an increase in the available levels of monoamines.

To assess if CR4056 in vivo administration successfully inhibits MAO-A, and consequently increases the levels of monoamines in the tissues, norepinephrine (NE) was quantified in parieto-occipital cortex and lumbar spinal cord (L4-L6) of male rats, after either acute or sub-acute (4 days) treatment. Acute 20 mg/kg CR4056 oral administration significantly increased the levels of noradrenaline in the parieto-occipital cortex, but also in the spinal cord a similar trend was found (**Figure 20**). On the other hand, the 4-days sub-acute CR4056 treatment at the same dose significantly increased noradrenaline levels, both in cerebral cortex and in the lumbar spinal cord. No effect was found in plasma samples (**Figure 21**) *(Ferrari et al., 2011).*

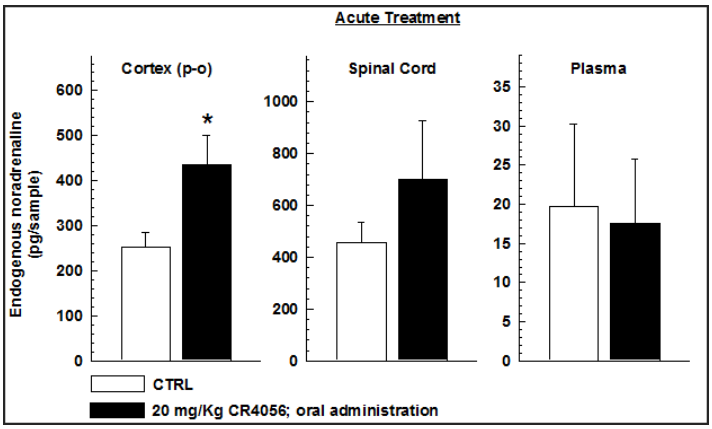

Figure 20 Effects of acute oral treatment with 20 mg/kg CR4056 on endogenous NE levels in rat parieto-occipital cortex, lumbar spinal cord (L4–L6) and plasma *(Ferrari et al., 2011).*

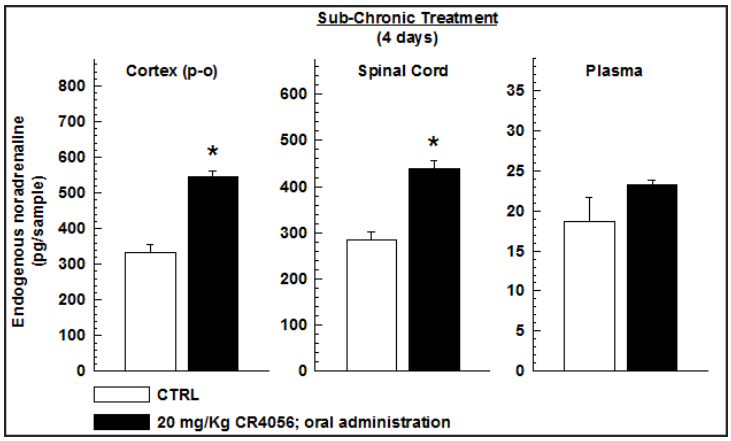

Figure 21 Effects of sub-acute oral treatment (4 days, once daily) with 20 mg/kg CR4056 on endogenous NE levels in rat parieto-occipital cortex, lumbar spinal cord (L4–L6) and plasma *(Ferrari et al., 2011).*

2.6.4 Analgesic activity in animal models of pain

CR4056, orally administered, showed analgesic effects in several experimental animal models of pain.

Inflammatory pain, induced in rats by either CFA or capsaicin sub-plantar injection, provoked the onset of secondary mechanical hyperalgesia, which was reversed by acute administration of CR4056 (6, 20 or 60 mg/kg) in both CFA- (**Figure 22**) and capsaicin- (**Figure 23**) induced inflammatory pain, the 60 mg/kg dose revealing hypoalgesic properties (i.e. increase of the paw withdrawal threshold above control levels) *(Ferrari et al., 2011).*

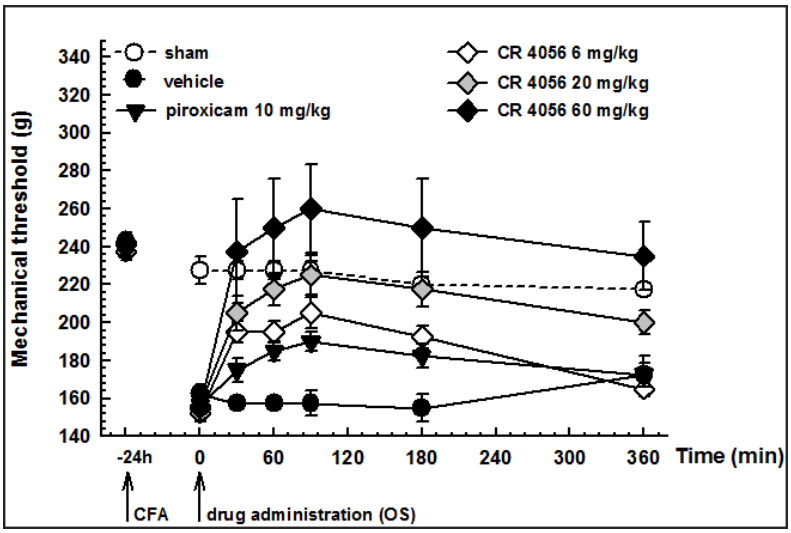

Figure 22 Antinociceptive effects of increasing doses of CR4056 on CFA-induced inflammatory pain in rats (Randall-Selitto test). CR4056 was orally administered 24h after CFA injection in the right paw of the rats. Piroxicam (10 mg/kg; oral) was used as positive control *(Ferrari et al., 2011).*

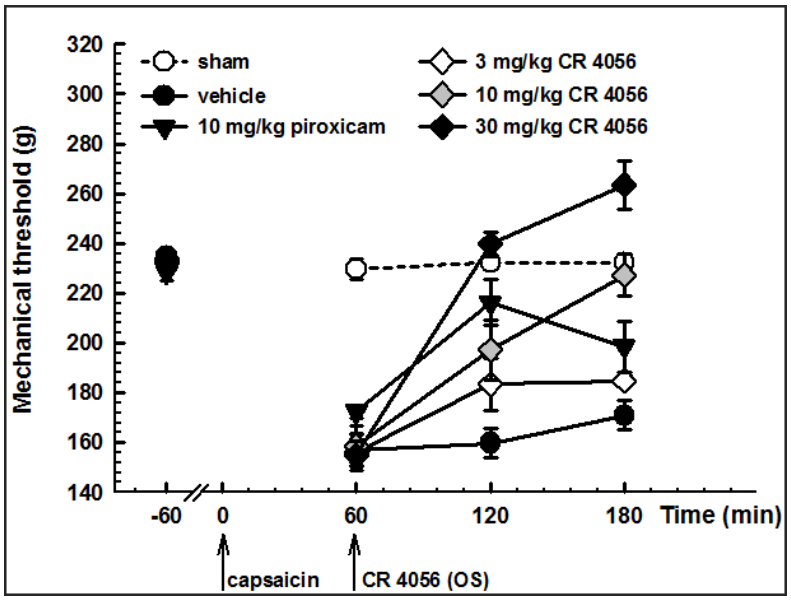

Figure 23 Antinociceptive effect of increasing doses of CR4056 on capsaicin-induced inflammatory pain (Randall-Selitto test). CR4056 was orally administered 1h after the sub-plantar injection of capsaicin in the rats right paw. Piroxicam (10 mg/kg; oral) was used as positive control *(Ferrari et al., 2011).*

Moreover, in the Brennan's model of post-operative pain (**Figure 24**), in which a surgical incision through skin, fascia and muscle of the rat hind paw causes secondary mechanical hyperalgesia, the analgesic efficacy of a single oral administration of CR4056 (1, 3 or 10 mg/kg) was confirmed, the higher dose being hypoalgesic also in this case *(Lanza et al., 2014).*

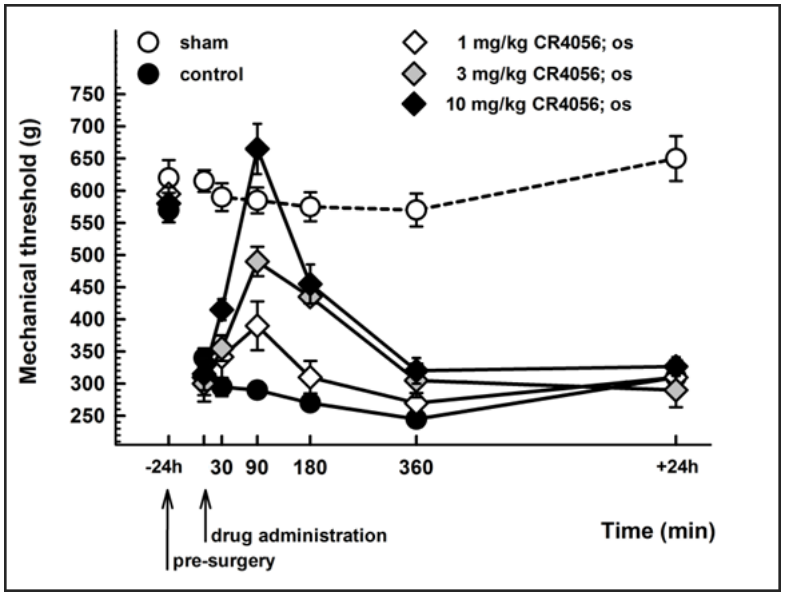

Figure 24 Anti-hyperalgesic effect of CR4056 on postoperative pain-induced mechanical hyperalgesia in rats (Randall-Selitto test). CR4056 was orally administered 24h after surgery *(Lanza et al., 2014).*

To prove that CR4056 in vivo analgesic efficacy is performed acting on I2R, in the capsaicin-induced pain model several imidazoline and/or adrenergic receptors antagonists were administered 15 minutes before CR4056 (30 mg/kg) administration. Efaroxan (a non-selective I1R and α2 adrenoceptors antagonist), yohimbine (a selective α2 antagonist) and prazosin (a selective α1 antagonist) did not alter CR4056 analgesic efficacy in this model. Conversely, idazoxan (3 mg/kg; a non-selective I2R and adrenergic α2 receptors antagonist) significantly reduced the analgesic activity of CR4056 (**Figure 25, panel A**), in a dose-dependent manner (**Figure 25, panel B**). Furthermore, naloxone (a MOR antagonist) antagonized the slight hypoalgesic effect caused by high doses of CR4056, without abolishing the analgesic property (**Figure 25, panel A**). Therefore, the hypoalgesic component of

CR4056 analgesic activity may be explained by the activity of endogenous endorphins on MORs, but the binding at I2R sites is the primary mechanism of CR4056 analgesic efficacy *(Ferrari et al., 2011).*

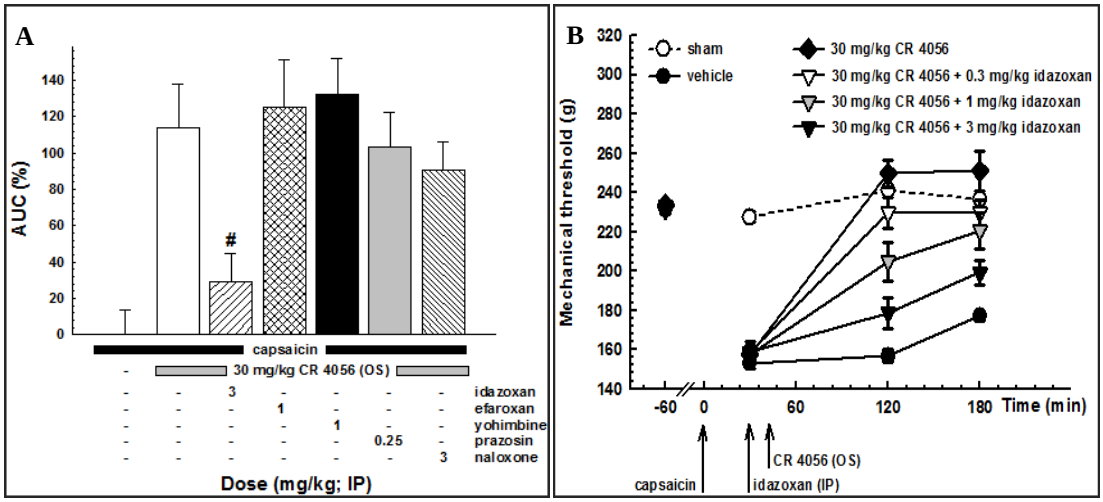

Figure 25 Capsaicin-induced neurogenic/inflammatory pain in rats (mechanical hyperalgesia). **A**: effect of different receptor antagonists on the analgesic activity induced by 30 mg/kg CR4056. **B**: dose-dependent effect of idazoxan on the analgesic activity induced by oral CR4056 *(Ferrari et al., 2011).*

Also in Brennan's model of post-operative pain, idazoxan, but not efaroxan nor naloxone, completely suppressed the analgesic activity of CR4056. On the other hand, in this model, yohimbine significantly reduced the effect of CR4056 (**Figure 26**). This phenomenon could be explained by the increased levels of noradrenaline, induced by CR4056 allosteric inhibition of MAO-A, which could also activate presynaptic α2 autoreceptors. Yohimbine, blocking α2 sites, could counteract this process *(Lanza et al., 2014).*

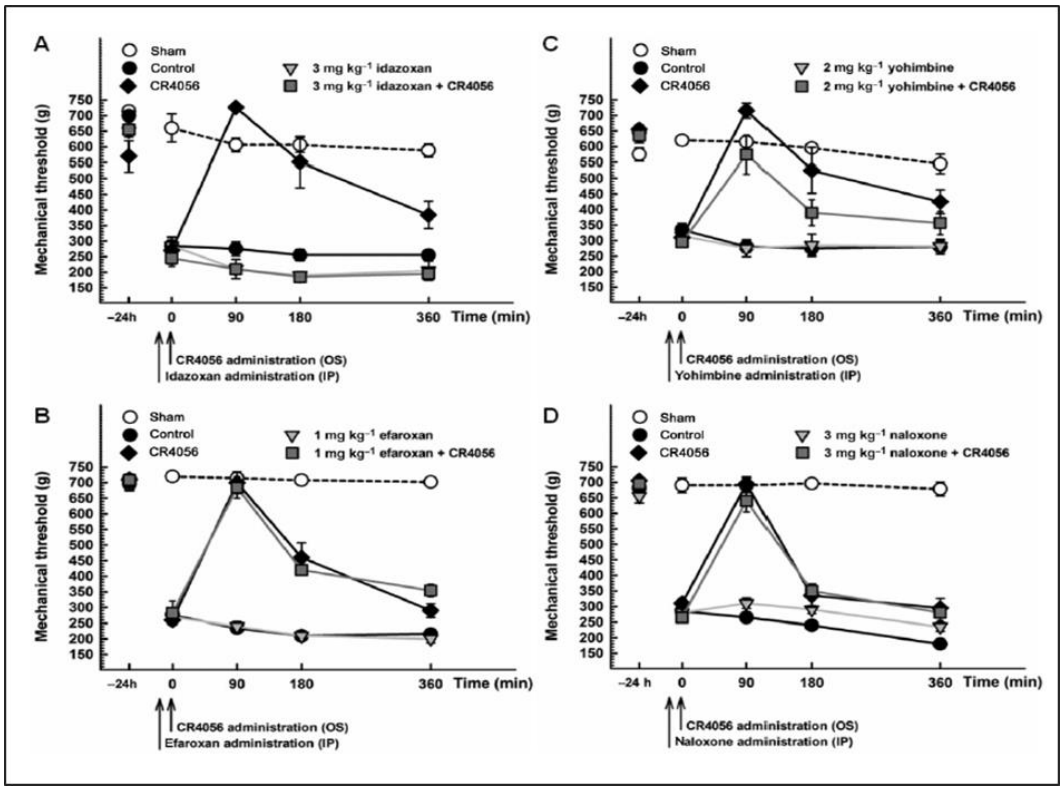

Figure 26 Effects of idazoxan (A), efaroxan (B), yohimbine (C) and naloxone (D) on the analgesic activity induced by 10 mg/kg oral CR4056 CR4056 on post-operative pain-induced mechanical hyperalgesia (Randall-Selitto test) *(Lanza et al., 2014).*

CR4056 was then tested in additional animal models of pain. Acute CR4056 dose-dependently decreased both streptozotocin-induced diabetic secondary mechanical hyperalgesia (**Figure 27**) and acidic saline-induced fibromyalgia-like mechanical allodynia (**Figure 28**) *(Ferrari et al., 2011).*

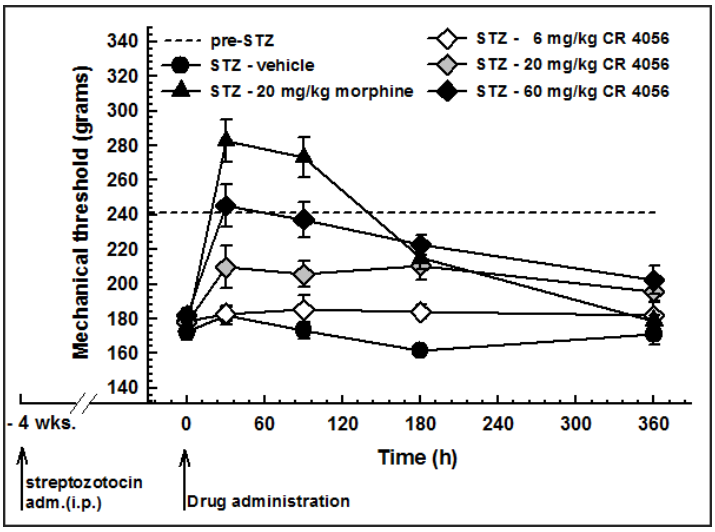

Figure 27 Streptozotocin (STZ)-induced neuropathic (diabetic, type I) pain in rats: effects of increasing oral doses of CR4056 (Randall–Selitto test). CR4056 was orally administered four weeks after the STZ injection. Morphine (20 mg/kg; sc) was used as positive control *(Ferrari et al., 2011).*

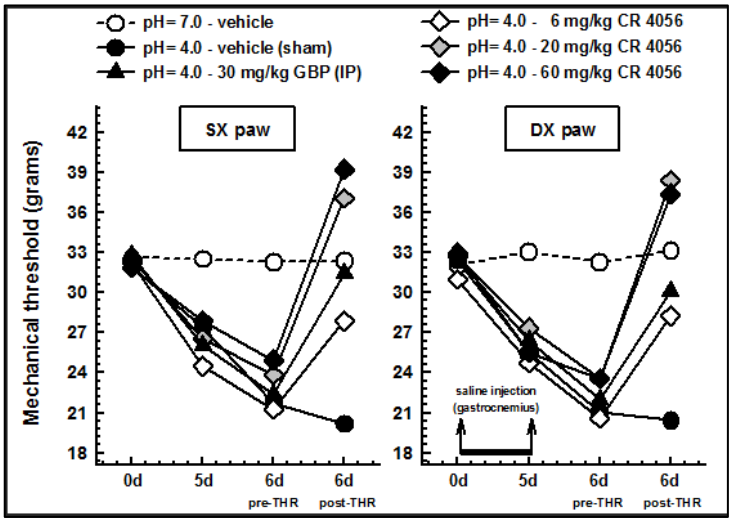

Figure 28 Antiallodynic effects of CR4056 in the acid-induced muscle allodynia model in rats (Dynamic Plantar Aesthesiometer). Six days after the induction, CR4056 was orally administered two hours before testing. Gabapentin (GBP; 30 mg/kg; ip) was used as positive control *(Ferrari et al., 2011).*

Moreover, a chemotherapy-induced neuropathic pain model was also selected for the compound in vivo testing. Bortezomib chronic treatment in rats produces mechanical allodynia. CR4056, in particular the optimal dose of 6 mg/kg, completely reversed

bortezomib-induced mechanical allodynia, administered and monitored up to 3 weeks (**Figure 29**) *(Meregalli et al., 2012).*

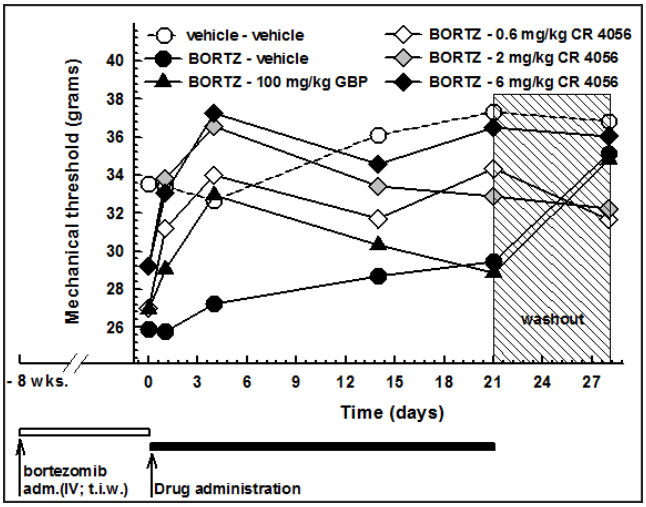

Figure 29 Bortezomib-induced neuropathic pain in rats: effect of increasing oral doses of CR4056 (0.6, 2, 6 mg/kg) on mechanical allodynia (Dynamic Plantar Aesthesiometer). CR4056 was administered once daily for 3 weeks, starting after the treatment with bortezomib (BORTZ; 0.2 mg/kg iv; three times a week for 8 weeks). Gabapentin (GBP; 100 mg/kg os) was used as positive comparator *(Meregalli et al., 2012).*

2.6.5 CR4056 and morphine: a clear and striking synergic action

Lastly, the interaction between CR4056 and the opioid system was further investigated both in the model of neurogenic inflammation obtained by capsaicin sub-plantar injection and in the post-operative pain model, given several evidences of I2R ligands modulation of the opioid system.

Morphine (0.03–3 mg/kg, subcutaneously), CR4056 (0.3–30 mg/kg, orally) and their combined acute administration produced a significant, dose-dependent antihyperalgesic effect in capsaicin-injected rats. Isobolographic analysis revealed a significant synergistic interaction between morphine and CR4056. When these agents were combined, the doses

needed to reach the median effective dose were about 4-fold lower than those seen after administration of each drug alone (**Figure 30**) *(Ferrari et al., 2011)*.

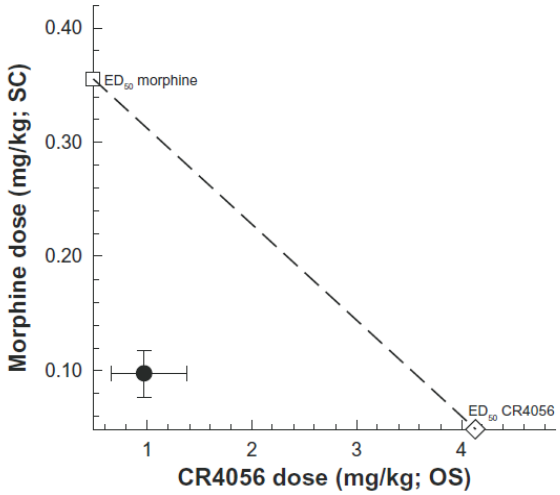

Figure 30 Isobologram for the effects of CR4056 and morphine, alone or in combination, in capsaicin-induced neurogenic/inflammatory pain in rats. Filled circle corresponds to the experimental co-treatment ED50 with 95% confidence limits; open square corresponds to the experimental ED50 for morphine alone, and open diamond corresponds to the experimental ED50 for CR4056 alone *(Ferrari et al., 2011)*.

In the post-operative pain model, effects of co-administered morphine and CR4056 were evaluated in both male and female Sprague Dawley rats. Drugs combination produced a significant, dose-dependent analgesic effect 24 h after surgery both in male (**Figure 31, panel A**) and in female rats (**Figure 31, panel B**) *(Lanza et al., 2014)*.

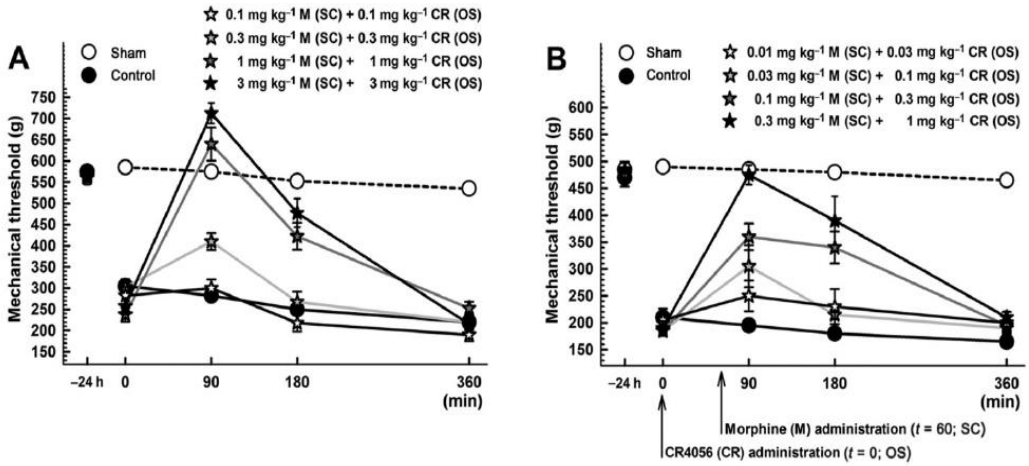

Figure 31 Anti-hyperalgesic effect of the combination CR4056/morphine on postoperative pain-induced mechanical hyperalgesia (Randall-Selitto test) in male (**A**) and female (**B**) rats. Mechanical hyperalgesia was measured 90, 180 and 360 min after CR4056 administration corresponding to 30, 120 and 300 min after morphine administration. Data represent the mean withdrawal threshold expressed in grams ± SEM (*n* = 6 per group). OS, oral administration; SC, subcutaneous administration *(Lanza et al., 2014)*.

Isobolographic analysis revealed a significant synergistic interaction independent of sex. In fact, when CR4056 and morphine were combined, their ED50 values were about fivefold lower than those measured after administration of each drug alone, both in male rats and in female rats, and significantly lower than the ED50 values predicted assuming an additive effect, both in male (**Figure 32, panel A**) and female (**Figure 32, panel B**) rats *(Lanza et al., 2014)*.

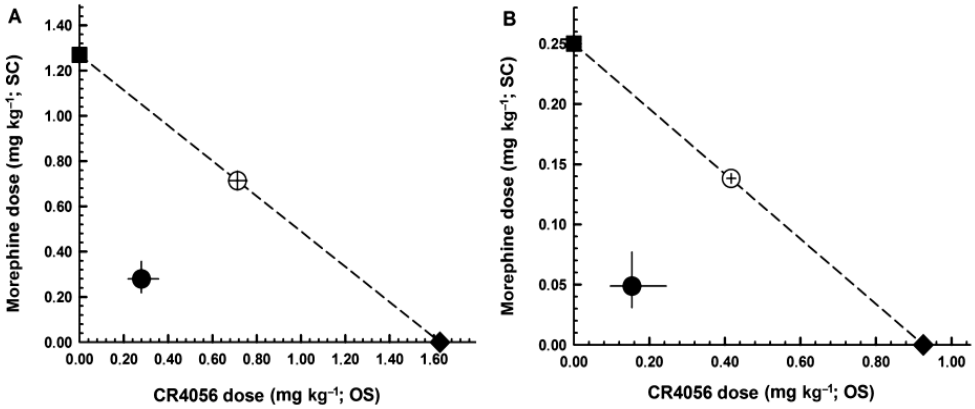

Figure 32 Isobolograms for the combination of oral CR4056 with subcutaneous morphine in male (A) and female (B) rat models of post-operative pain. Open circles correspond to the theoretical ED50 with 95% CI; filled circles corresponds to the experimental co-treatment ED50 with 95% CI; filled square corresponds to the experimental ED50 for morphine alone; and filled diamond corresponds to the experimental ED50 for CR4056 alone. OS, oral administration; SC, subcutaneous administration *(Lanza et al., 2014)*.

2.7 In vitro testing of analgesic drugs

2.7.1 TRPV1 sensitization by PKCε translocation: a possible in vitro screening assay for analgesic drugs

In in vitro studies, it was found that PKC could directly sensitize TRPV1, in a different manner to heat-, anandamide-, protons- or capsaicin-induced sensitization: in fact, while these agents are direct activators of the channel, PKC seems to act through phosphorylation of the receptor, thus being able to enhance their agonist action. In HEK293 cells transiently transfected with TRPV1, acidification of the medium provoked the activation of the channel; the application of phorbol ester (phorbol myristate-acetate, PMA), a PKC activator, caused a significant increase of the pH-gated current, selectively in transfected cells (**Figure 33**) *(Vellani et al., 2001)*.

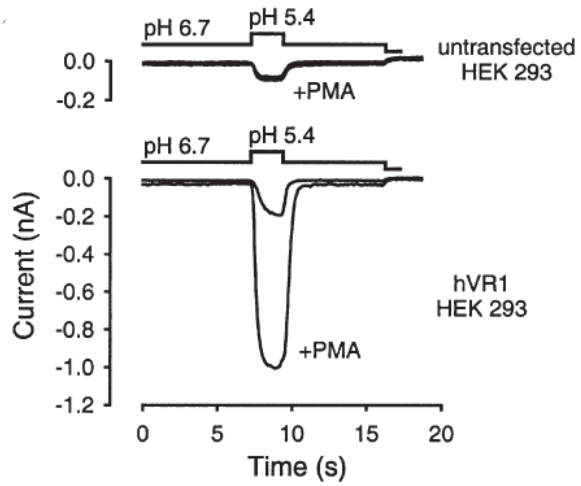

Figure 33 pH-gated current. Acidification from pH 6.7 to 5.4 activated a sustained inward current that was larger in TRPV1-transfected than in untransfected HEK293 cells. PMA enhanced the current in transfected cells but had little effect in untransfected cells *(Vellani et al., 2001)*.

Subsequently, it was shown that TRPV1 sensitization is mainly performed by PKCε through phosphorylation, which is acted after translocation of this kinase from the cytoplasm to the cell membrane (**Figure 34**). In primary cultures of rat DRGs, application of inflammatory agents such as bradykinin (BK) or thrombin (THR) caused a significant increase of the number of cells displaying PKCε translocation. In this in vitro model of inflammation, several analgesic drugs have been tested to prove their efficacy in counteracting inflammation, which in this case was evaluated by their ability to inhibit such translocation. Application of paracetamol and nimesulide, but not of other NSAIDs, significantly decreased PKCε translocation (**Figure 35**) *(Vellani et al., 2011; 2013)*.

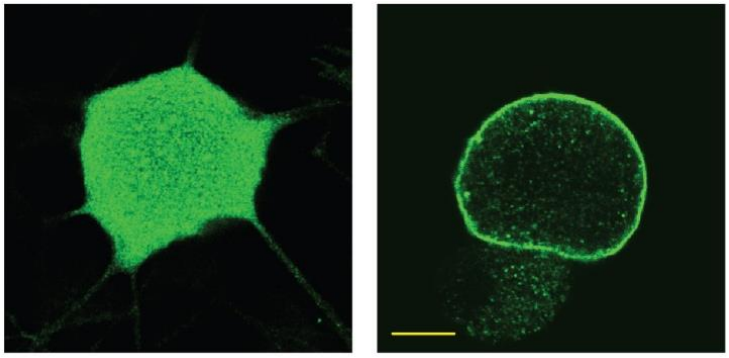

Figure 34 Confocal optical sections of cultured sensory neurons treated with THR and stained for PKCε. **A** typical neuron showing no response; **B** typical THR-responsive neuron with translocation of PKCε to the plasma membrane *(Vellani et al., 2013)*.

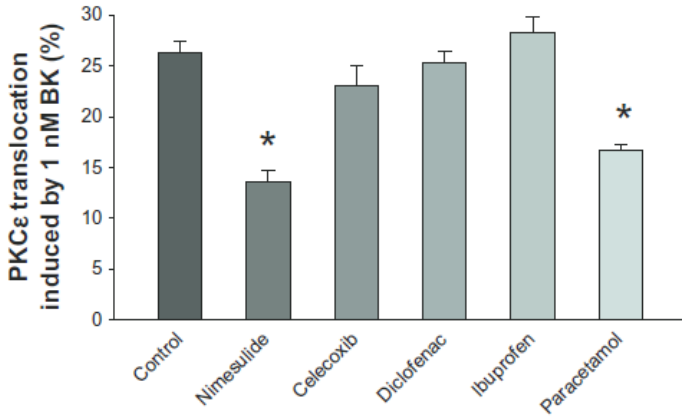

Figure 35 The effects of NSAIDs and paracetamol on translocation induced by BK (1 µM) for 30 seconds. Translocation induced by BK was significantly reduced in the presence of nimesulide and paracetamol, while celecoxib, diclofenac, and ibuprofen were ineffective *(Vellani et al., 2013)*.

Moreover, also gabapentin significantly reduced PKCε translocation induced by the pronociceptive peptides bradykinin and prokineticin 2; when co-applied with paracetamol in the same in vitro model, they showed additive effects on the inhibition of translocation *(Vellani & Giacomoni, 2016)*.

Collectively, these data point out a new screening tool using an in vitro model of inflammation which could be useful in the assessment and validation of analgesic antinflammatory drugs.

2.7.2 CR4056 and morphine: in vitro screening and synergy

Since several analgesic drugs were shown to have inhibitory effect on PKCε translocation in cultured rat DRGs treated with inflammatory agents, the effects of CR4056 and morphine application were also tested in the same in vitro model (unpublished data). In a first set of experiments, time-courses of morphine (2 µM) or CR4056 pre-application were carried out for 24h on cells treated with bradykinin (**Figure 36**) or prokineticin 2 (10 nM) 30 seconds before rapid fixation, and at each time point PKCε translocation from the cytoplasm to cell membrane was quantified. Inhibition of PKCε translocation induced by morphine starts one hour after application and peaks at 3 hours with about 50% reduction in translocation percentage; after that, a gradual tachyphylaxis starts, which leads to a complete reversal of morphine effect at about 12h of exposure. This effect is completely blocked by naloxone (100 µM) co-application, indicating that morphine-induced PKCε translocation inhibition is totally mediated by opioid receptors.

On the other hand, CR4056 effect is instantaneous, starting within a few seconds after application, and persists for 24h with a slight gradual increase of effect. Even with no pre-application (co-application with inflammatory agent), CR4056 displays a significant reduction of PKCε translocation.

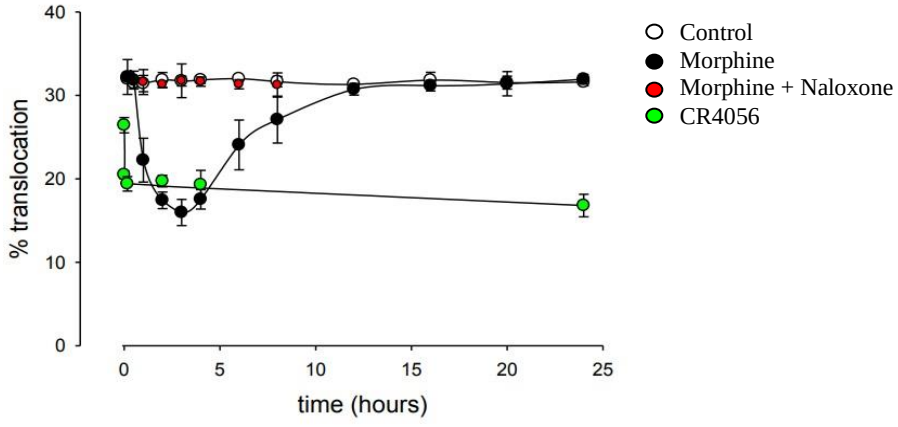

Figure 36 Effect of pre-application of morphine (2 µM) alone, morphine and naloxone (100 µM) or CR4056 on cultured rat DRG neurons, studied along a 24h period between day 2 and 3 in vitro. At each time point, bradykinin was added for 30 seconds before fixation. Data represent % of cells displaying PKCε translocation *(Vellani et al., personal communication).*

When co-applied with naloxone, CR4056's effect on translocation is not modified in the bradykinin (**Figure 37**) and in the prokineticin 2 models, indicating that CR4056-induced PKCε translocation inhibition is not mediated by opioid receptors, and that opioid receptors do not modulate per se PKCε activity.

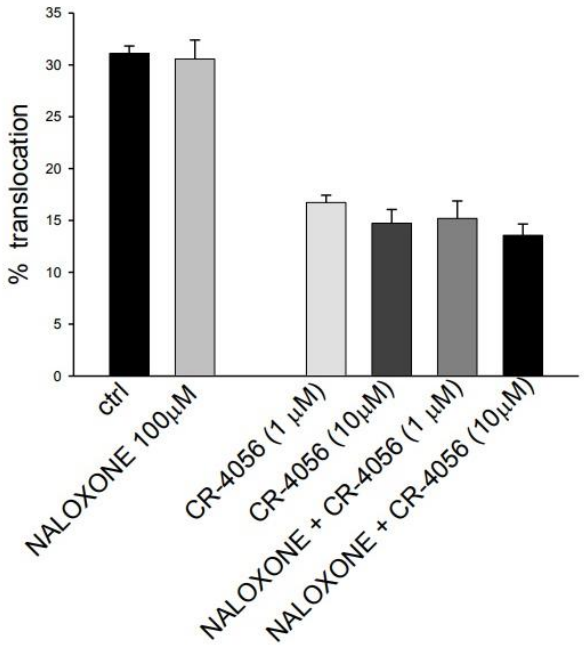

Figure 37 Effects of naloxone (100 µM) pre-application overnight, alone or before co-application of CR4056 (1 µM and 10 µM for 10 minutes), or application of CR4056 (1 µM and 10 µM for 10 minutes) alone, on the percentage of cells displaying PKCε translocation. After pre-treatment, bradykinin was applied for 30s before fixation *(Vellani et al., personal communication).*

Since CR4056 peaks a few seconds after application, in a different set of experiments it was applied just for 10 minutes and then cells were washed out in PBS and DMEM 10% serum. Effect of CR4056 was followed up to 10 hours after complete removal from extracellular solution. PKCε translocation inhibition was unaffected 10 minutes after CR4056 wash out, and it slowly returned to control levels 2 hours after drug removal (**Figure 38**).

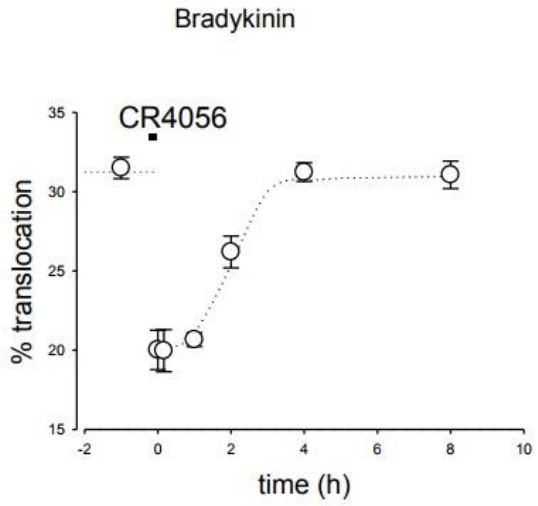

Figure 38 Effect of CR4056 (10 µM) 10 min application on the percentage of cells displaying PKCε translocation in the bradykinin model. Evaluation of translocation was first investigated before application of CR4056. Time 0 refers to cells fixed exactly at the end of the 10 min application of the drug. The following symbols display translocation observed at increasing times after complete removal of CR4056 *(Vellani et al., personal communication).*

CR4056 effect on bradykinin- (**Figure 39, left panel**) or prokineticin 2-induced PKCε translocation was then extensively investigated. Being CR4056 a selective I2R agonist, its activity was compared to a standard I2R-ligand, 2-BFI. Counting of DRG neurons showing translocation reported the usual inhibitory effect of CR4056, but no effect caused by 2-BFI (1-10-100 µM), neither alone nor in co-application with CR4056. Moreover, 2-BFI did not affect translocation even when pre-applied overnight (**Figure 39, right panel**).

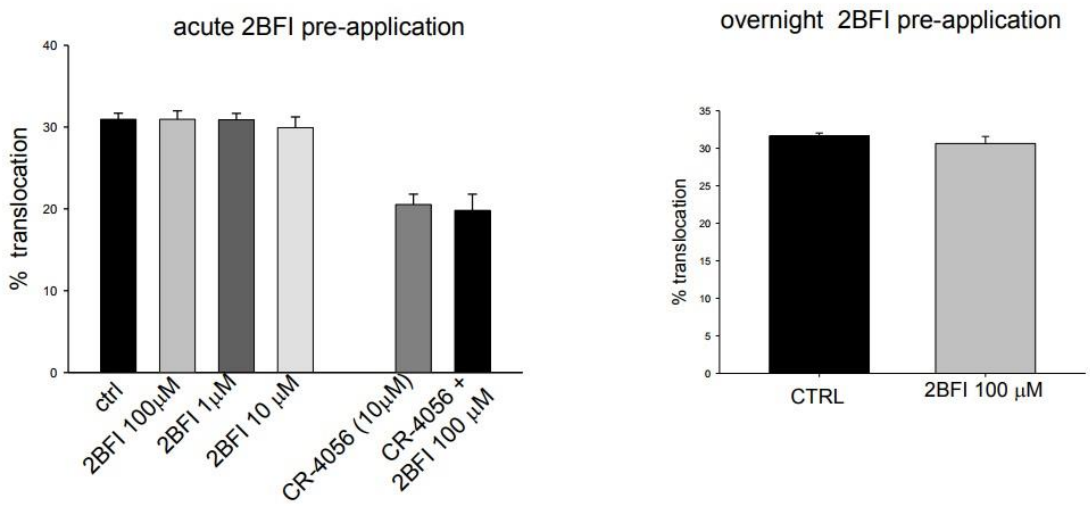

Figure 39 Effect of 2-BFI (1-10-100 µM) alone and CR4056 (10 µM) alone or in combination with 2BFI (100 µM) 10 min pre-application before bradykinin 30s application on the percentage of cells displaying PKCε translocation (**left panel**). Effect of 2-BFI (100 µM) overnight pre-application was also evaluated (**right panel**) *(Vellani et al., personal communication).*

Besides, application of idazoxan (10-100 µM), an I2R antagonist, had no effect on PKCε translocation, neither alone nor in co-application with CR4056, on bradykinin- (**Figure 40**) or prokineticin 2-stimulated cultured DRGs. Therefore, these results suggest that I2Rs are not involved in the modulation of PKCε induced by bradykinin or prokineticin 2. CR4056's ability to act on the PKCε pathway could be due to peculiar properties, for example related to structural features, which make it different from other I2R ligands.

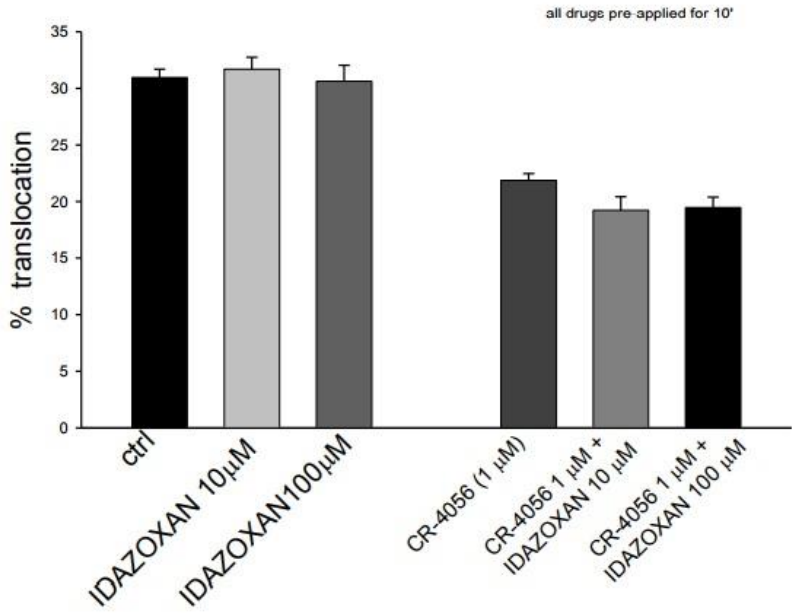

Figure 40 Effect of idazoxan (10-100 µM) alone and CR4056 (1 µM) alone or in combination with idazoxan (10-100 µM) 10 min pre-application before bradykinin 30s application on the percentage of cells displaying PKCε translocation *(Vellani et al., personal communication).*

Since CR4056 analgesic effect was shown to be slightly, but not significantly, suppressed by α2-adrenoceptor antagonists (yohimbine and atipamezole) in the Brennan's animal model of post-operative pain *(Lanza et al., 2014),* the role of these receptors was also deepened in this in vitro model. Yohimbine (1000 µM), a selective α2 antagonist, was applied alone or in combination with CR4056 (1-10 µM) on bradykinin- (**Figure 41**) or prokineticin 2-treated cultured sensory neurons. Percentage of DRG neurons with PKCε translocation was dose-dependently decreased by CR4056, but no effect was caused by the presence of yohimbine, despite the very high concentration used. Therefore, α2 receptors are not involved in the modulation of PKCε translocation in this in vitro inflammatory model.

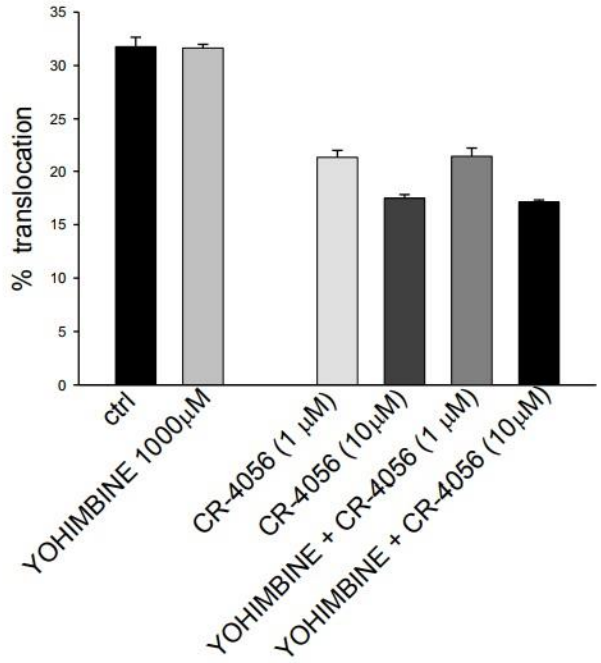

Figure 41 Effect of yohimbine (1000 µM) alone and CR4056 (1-10 µM) alone or in combination with yohimbine (1000 µM) 10 min pre-application before bradykinin 30s application on the percentage of cells displaying PKCε translocation *(Vellani et al., personal communication).*

It was then hypothesized that CR4056 could exert its effect on PKCε translocation via G-protein-coupled receptors (GPCRs) different from opioid receptors. For this purpose, pertussin toxin (PTX), a cAMP inhibitor, was used to block GPCRs activity. As expected, since opioid receptors are coupled to Gαi proteins, morphine-induced inhibition of PKCε translocation was completely blocked by co-application with PTX (500 ng/ml). Interestingly, also CR4056-induced inhibition of translocation was abolished by PTX co-application (**Figure 42**). Therefore, CR4056 may act on a GPCR different from opioid receptors.

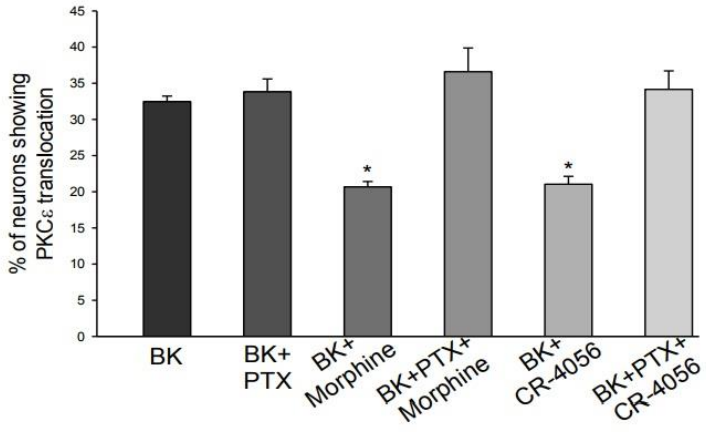

Figure 42 Effect of PTX (500 ng/ml) co-application with morphine or CR4056 on percentage of cells showing PKCε translocation induced by bradykinin *(Vellani et al., personal communication).*

On the contrary, GPCR-independent analgesics such as nimesulide are shown to inhibit PKCε translocation in a PTX-insensitive fashion (**Figure 43**).

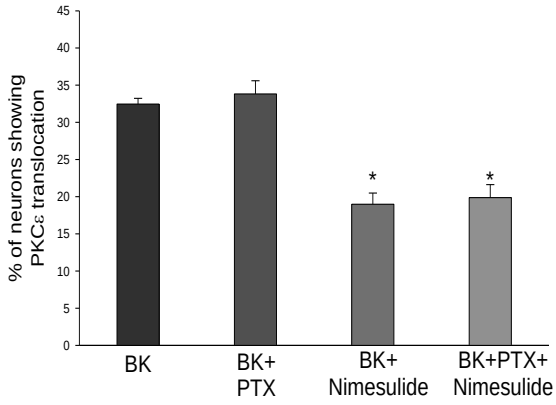

Figure 43 Effect of PTX (500 ng/ml) co-application with nimesulide on percentage of cells showing PKCε translocation induced by bradykinin *(Vellani et al., personal communication).*

Nevertheless, when CR4056 was co-applied with PMA, it did not show any effect on PKCε translocation, already caused in the majority of neurons by PMA alone (**Figure 44**). Translocation was visible at or above 10^{-10} M PMA concentration in the vast majority of neurons. The presence of CR4056 (20 μM), preapplied for 30 minutes, did not change the

effect of PMA. Therefore, CR4056 is inactive when PKCs are directly activated without the mediation of GPCRs.

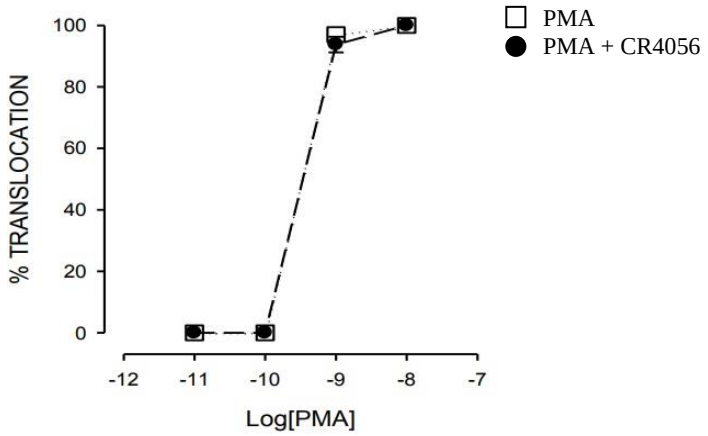

Figure 44 Effect of PMA at different concentrations, alone or in combination with CR4056 (20 μM), preapplied for 30 minutes on percentage of cells showing PKCε translocation induced by bradykinin *(Vellani et al., personal communication).*

Given these results, morphine and CR4056 effects in co-application were investigated. Compared to ED50 of single drugs dose-response quantification of morphine (**Figure 45**) or CR4056 (**Figure 46**), potency of both drugs is increased by a $>10^3$ factor when co-applied at respective time peaks (morphine for 3 hours and CR4056 for 10 minutes), showing a marked synergism (**Figure 47**).

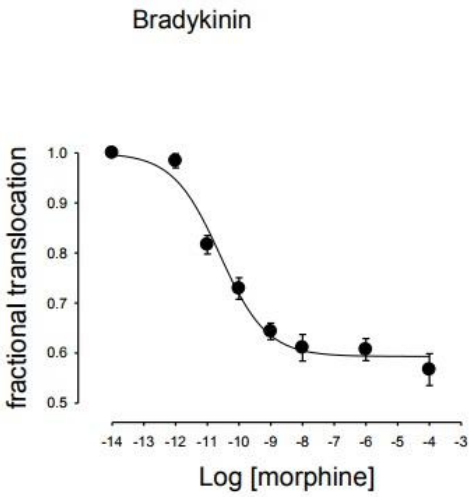

Figure 45 Effect of morphine application, at different concentrations, on bradykinin -induced PKCε translocation *(Vellani et al., personal communication).*

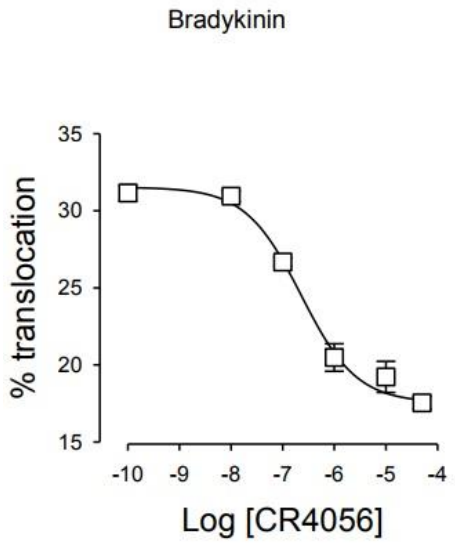

Figure 46 Effect of CR4056 application, at different concentrations, on bradykinin-induced PKCε translocation *(Vellani et al., personal communication).*

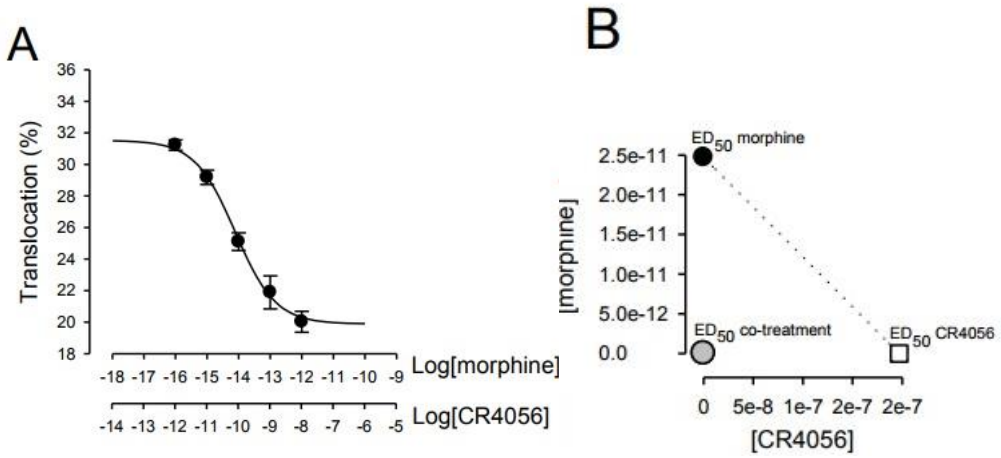

Figure 47 Effect of morphine or CR4056 application, at different concentrations, on bradykinin-induced PKCε translocation (left panel); isobologram of combined application of CR4056 and morphine on the same in vitro model (right panel) *(Vellani et al., personal communication).*

Interestingly, synergy is also evident with another μ agonist, DAMGO, and also this response is blocked by naloxone (**Figure 48**).

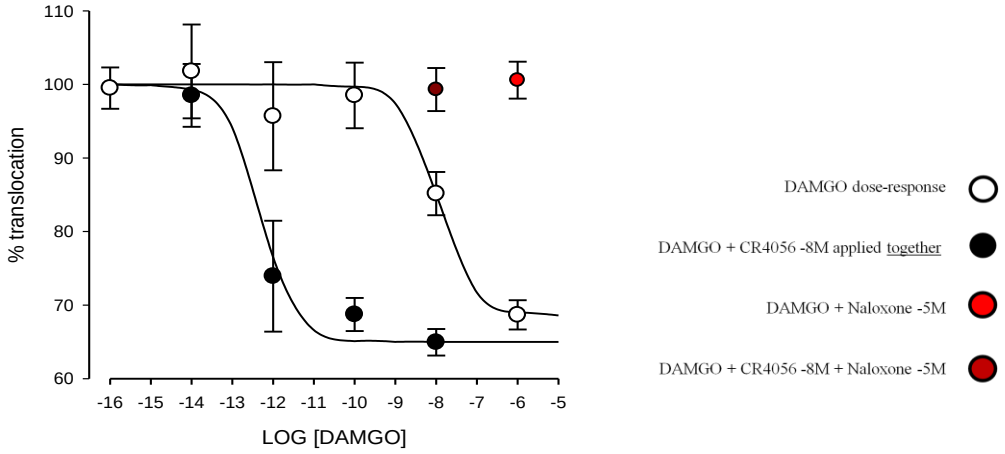

Figure 48 Effect of DAMGO application, at different concentrations, alone or in combination with CR4056 and naloxone on bradykinin-induced PKCε translocation *(Vellani et al., personal communication).*

Collectively, these data highlight some in vitro details of the synergy observed also in vivo between CR4056 and morphine, providing further insights in the subcellular mechanisms shared by the two drugs, and individuating PKCε as a main downstream target.

3. Aims

I2R agonist drugs have been shown to be a useful alternative tool in the treatment of chronic pain, especially in combination with opioid drugs, in order to strengthen their efficacy over time and to limit their side-effects. The aims of my study were thus oriented to deepen our knowledge on the interaction between morphine and CR4056, a promising novel I2R agonist, especially regarding the effect of the latter on opioid tolerance, and trying to understand the mechanistic basis of this pharmacological interaction. In this set of experiments, an animal model of chronic inflammatory pain was chosen, the CFA model, given the fact that it is widely used in literature on analgesics screening and provides several neurobiological features of chronic inflammation.

1. First aim of this study was to validate the CFA-induced chronic inflammatory model by evaluating pain features such as mechanical hyperalgesia, mechanical allodynia and spontaneous pain. The effects of acute administration of morphine or CR4056 was assessed by potential relief of these behavioral pain markers.

2. Moreover, the effects of acute administrations of morphine or CR4056 were also assessed in the spinal cord, by evaluation of CFA-induced microgliosis and potential effect of treatments on it.

3. Then, the hypothesis that CR4056 could ameliorate morphine-induced analgesic tolerance was tested, in the short and in the long period. First, I wondered if CR4056 could prevent the development of opioid tolerance in the CFA pain model.

4. In the second place, I wanted to assess if CR4056 could restore an already established opioid tolerance, thus if it had an effect on tolerance expression.

5. Moreover, it is known that morphine-induced analgesic tolerance is related to chronic spinal microgliosis. Therefore, I evaluated microglia activation in tolerant rats and in animals subjected to combined CR4056-morphine treatment.

6. Furthermore, I also took care of ruling out the possibility that CR4056 administration, in combination with opioid drugs, could worsen opioid-induced side-effects; for this purpose, I evaluated constipation after single administration in naïve rats.

7. Given in vitro preliminary data on possible shared subcellular mechanisms of action of morphine and CR4056, the effects of acute administrations of morphine or CR4056 were also evaluated in ex vivo DRGs from CFA-treated rats, by quantification of PKCε phosphorylation and TRPV1 expression.

8. In a small subgroup of animals, I also aimed to verify if changes in pPKCε and TRPV1 expression found in lumbar DRGs were related to cells receiving directly from the peripheral site of lesion, by retrograde labeling DRGs somata injecting a fluorescent dye in the injured paw.

4. Materials and Methods

4.1. Animals

Male Wistar Han rats (Charles River, Calco, LC, Italy) weighing 175-300 g at the time of arrival were housed 2 (if weighing >250 g) or 3 per cage in polycarbonate cages (42,5 x 26,6 x 18,5 cm) with ad libitum access to food (Teklad rodent diet 2018, Harlan Laboratories, S. Pietro al Natisone, UD, Italy) and water, in a temperature and humidity controlled room (20°C ± 2°C and relative humidity within the range of 55% ± 10) with a 12 h light/dark cycle (7:00-19:00), at least 1 week before the tests. All the experimental procedures described herein were in compliance with national and international laws and policies (Italian Legislative Decree 26/2014 of 4th March 2014 which transposed the EU Directive 2010/63/EU on the protection of animals used for scientific purposes), authorized by the Italian Ministry of Health (ministerial authorization n° 561/2017-PR) and were approved by the Rottapharm Biotech review board. All studies involving animals are reported in accordance with the ARRIVE guidelines for reporting experiments involving animals *(Kilkenny et al., 2010; McGrath et al., 2010)*. The animal house is authorized by and in compliance with the same laws and policies above. Number of animals used in each experimental group is the minimum number used in analogous experiments described in the International literature. Choice is also based on previous experiments in which the same experimental techniques were used, and is in any case sufficient to limit experimental variability in order to obtain statistically significant results.

4.2. Complete Freund's Adjuvant (CFA) – induced inflammatory pain model

Rats were anesthetized with isofluorane (the level of anesthesia was assessed by loss of paw withdrawal reflex) and received intraplantar injection of complete Freund's adjuvant 1mg/ml (CFA) (100 µl, sc, diluted in sodium chloride, NaCl 0,9% 1:1; Sigma) into the right hindpaw. Control rats received an equivolume saline injection *(Okun et al., 2011)*.

4.3. Pharmacological treatments

All drugs were administered in 5 ml/kg volume.

CR4056 (2-phenyl-6-(1H-imidazol-1yl) quinazoline; Rottapharm Biotech, Monza, Italy) was suspended in 0.5% hydroxyl-propyl-carboxymethyl cellulose (HPMC) and administered orally at doses 0.1-0.3-1-6 mg/kg.

Morphine (Morphine HCl, Salars) was dissolved in NaCl 0,9% and administered subcutaneously 5-10 mg/kg.

2-BFI (2-(2-benzofuranyl)-4,5-dihydro-1H-imidazole hydrochloride, CR4868; Rottapharm Biotech, Monza, Italy) was dissolved in NaCl 0,9% and administered intraperitoneally at doses 0.003-0.03 mg/kg.

Codeine (Salars, Italy) was dissolved in NaCl 0,9% and administered subcutaneously at dose 12 mg/kg.

4.4. Induction of tolerance: short paradigm

Morphine analgesic tolerance was induced as previously described *(Beaudry et al., 2015)* with minor modifications. Morphine hydrochloride was injected subcutaneously starting from 24 hours after CFA injection, twice a day for 3 days and as single treatment on day 4 (seven injections). CR4056 at different doses was orally administered 15 minutes before each morphine administration. In this experiment, 6 animals (250-300 g) per group were used, and 6 experimental groups were included; this paradigm was performed twice, to test effect on morphine tolerance of both 2-BFI and CR4056, for a total number of 72 animals.

4.5. Induction of tolerance: long paradigm

Morphine hydrochloride was injected subcutaneously starting from 24 hours after CFA injection, twice a day for 13 days and as single treatment on day 14. CR4056 1 mg/kg was orally administered 15 minutes before each morphine administration for 14 days (effect on

tolerance development) or for 7 days, starting 1 week after daily morphine treatment (effect on *tolerance expression*). In this experiment, 6 animals (250-300 g) per group were used, and 5 experimental groups were included; this paradigm was performed twice, to test effect of CR4056 on both morphine tolerance development and expression, for a total number of 60 animals.

4.6. Evaluation of opioid-induced constipation

The experiments have been performed according to the procedure described by Harada and colleagues *(Harada et al., 2017)*. Rats were housed 2 per cage. Drugs were administered 2 hours before the dark cycle onset; the feces per cage were collected and counted 17 hours after drug treatment. Feces number per cage was divided by 2 to obtain the number of feces per rat, assuming a similar course of defecation between rats housed in the same cage. CR4056 was administered 15 minutes before codeine or morphine to the group treated with the drug association. In this experiment, 6 animals (250-275 g) per group were used, and 4 experimental groups were included; this paradigm was performed twice, to test effect of CR4056 on both morphine and codeine induced constipation, for a total number of 48 animals.

4.7. Behavioral assessments

4.7.1. Mechanical hyperalgesia

Mechanical hyperalgesia was measured as the hind paw withdrawal threshold to a noxius mechanical stimulus and was determined using the paw pressure technique (Randall & Selitto method). For this purpose, an analgesymeter (7200 Ugo Basile, Italy) was used. After 30 minutes of habituation in the experimental room, animals were gently restrained and steadily increasing pressure was applied to the dorsal surface of the CFA-injected paw by a

dome-shaped plastic tip. The threshold was determined when the rat exhibited a stereotyped flinch response and remove the foot from the apparatus; cut-off was set at 350 g.

In opioid tolerance experiments, a baseline measurement was performed before and 24 hours after CFA injection. In the short paradigm, the analgesic effect of morphine was evaluated 24 and 96 hours after CFA injection. In the long paradigm, the analgesic effect of morphine was evaluated 1, 7 and 14 days after CFA injection. Mechanical hyperalgesia was measured 30, 60 and 180 minutes after morphine administration, which corresponds to 45, 75 and 195 minutes after CR4056 or 2-BFI administration.

In all other experiments, a baseline measurement was performed before and 72 hours after CFA injection. Mechanical hyperalgesia was measured 30 minutes after acute morphine administration or 90 minutes after CR4056 acute administration.

4.7.2. Mechanical allodynia

Mechanical allodynia was assessed measuring mechanical withdrawal threshold of both the ipsilateral and contralateral hind paw using a Dynamic Plantar Aesthesiometer (Ugo Basile S.r.l., Gemonio, VA, Italy), which generated a linearly increasing mechanical force. On each day of testing, rats were placed in a Plexiglas chamber (28 × 40 × 35 cm) equipped with a wire mesh floor, 20 cm above the bench, for a 30 minutes acclimatization period followed by testing. A non-noxious mechanical stimulus, represented by an automatic pointed metallic filament of 0.5 mm diameter, was positioned under the plantar surface of the hind paw, exerting a progressively increasing punctuate pressure, reaching up to 50 g within 20 seconds. A clear spontaneous hind paw withdrawal response caused by the punctuate pressure was recorded automatically. The results defined the minimum pressure (in grams) required to elicit a robust and immediate withdrawal reflex of the paw. Stimuli were applied alternately on each posterior paw every 2 minutes on three repeated measures to obtain a mean value representing the mechanical allodynic threshold. In this experiment, 6 animals (200-225 g) per group were used, and 4 experimental groups were included, for a total number of 24 animals; these animals were also used for Dynamic Weight Bearing evaluation.

4.7.3. Dynamic Weight Bearing

The Dynamic Weight Bearing (DWB) system (Bioseb, Boulogne, France) is a non-invasive method used to obtain the weight distribution and surface area of all four paws in a freely moving animal, as indirect index of spontaneous pain. The system consists of a Plexiglas enclosure (22 × 22 × 30 cm) with a floor sensor composed of 44 × 44 sensors. A camera is affixed to the top of the enclosure to align the sensor directionally during the analysis phase. Raw pressure and live video recordings are transmitted to a tablet PC via a USB interface at a sampling frequency of 10 Hz. The data were analyzed using the DWB software, version 1.4.2. Zone parameters were set for the analysis as follows: ≥ 1,5 g for one sensor and a minimum of two adjacent sensors ≥ 1 g (to be considered a valid zone). For each time segment that was stable for more than 1 second, zones meeting the above criteria were validated and assigned as either right or left and front or rear paw. Mean values for the weight of each zone were calculated over the entire testing period based on the length of time for each validated segment. For each testing period, the animals were placed into the chamber and the data were collected over a period of 5 minutes. The animals were subjected to the test without previous adaptation, since exploratory movements improve data capture. The operator manually "validated" each test period by ensuring that each paw print corresponded to the appropriate paw, using the video footage as a reference. The following parameters were measured for each limb separately and for both the front and hind limb combined: body weight (g), weight put on the limb (g) and percentage of weight placed on the limb.

4.8. Immunofluorescence assay

Animals dedicated to ex vivo sample collection were 6 per group (175-200 g), and 4 experimental groups were included, for a total number of 24 animals.

Rats were sacrificed 72 hours after CFA injection and 30 minutes after acute morphine administration or 90 minutes after CR4056 acute administration. Briefly, after behavioral assessment (Randall-Selitto test), rats were deeply anesthetized with an overdose of

urethane (1,5 g/kg, ip), and then transcardially perfused with 250 ml 0.9% saline containing 1% heparin (5000 UI/ml), followed by 500 ml 10% formalin (4% paraformaldehyde, Bio-Optica Spa, Milan, Italy). L5 segments of the lumbar spinal cord and L4-L5 dorsal root ganglia were dissected and post-fixed in the same fixative (10% formalin) for 24 hours at 4 °C. After that, samples were switched to a 0.01% NaN3 (Sodium Azide, Sigma) 1M Phosphate Buffered Saline (PBS; Phosphate Buffered Saline tablets, Sigma).

Each sample was then dehydrated through a graded series of ethanol solutions, cleared in xylene (BioClear, Bio-Optica Spa, Milan, Italy), and embedded in paraffin blocks for sectioning. Samples were sliced with a fully automated rotary microtome (RM2255, Leica Microsystem Srl, Milan, Italy) at 5 µm thickness and mounted on poly-L-lysine coated slides (Thermo Fisher Scientific, Waltham, MA, USA). The slides were kept at room temperature (RT), before immunofluorescence staining.

Before starting immunofluorescence assay, sections were cleared with xylene and rehydrated through a graded series of ethanol solutions. Antigen unmasking was performed using 0.05 % Tween (Tween20, Sigma) 10 mM Citrate Buffer pH 6.0 (Citric Acid, Sigma) at 95°C.

Sections were then washed in PBS and PBST (0.3% Triton X-100, Sigma), blocked in 10% Normal Donkey Serum (Donkey Serum, Sigma) PBST and incubated overnight at 4°C with primary antibodies in 2% Normal Donkey Serum PBST. DRG sections were stained for phosphorylated PKCε (rabbit anti-PKC ε (phospho S729), Abcam, 1:25), VR1 receptor (mouse anti-VR1 (E8), Santa Cruz Biotechnology, 1:25) and FITC-conjugate IB4 (Lectin from Bandeiraea simplicifolia (Griffonia simplicifolia), Isolectin B4 (BSI-B4), FITC conjugate, lyophilized powder, Sigma, 5mg/ml). Spinal cord sections were stained for IBA1 (rabbit anti-IBA1, Wako's, 1:350). After primary antibodies incubation, sections were washed again in PBS and PBST and incubated with secondary antibodies, 1:400 in 2% Normal Donkey Serum PBST (Alexa Fluor 594 donkey anti-rabbit IgG (H+L), Invitrogen, 1:400; Alexa Fluor 488 donkey anti-rabbit IgG (H+L), Thermofisher, 1:400; Alexa Fluor 488 donkey anti-mouse IgG (H+L), Thermofisher, 1:400). Sections were than dehydrated again and coverslipped with DAPI mounting media (Fluoroshield with DAPI, Sigma) or not (Fluoromount Aqueous Mounting Medium, Sigma) and then visualized with Invitrogen EVOS FL Auto Cell Imaging System (Thermo Fisher Scientific, Waltham, MA, USA).

4.9. Immunofluorescence cell counting

In DRG slides, one section containing L4 and L5 DRGs was considered for the right hind limb and one for the left one. For each animal, whole DRGs were considered, taking progressive pictures at 20x magnification (picture area of 578 µm x 434 µm); a mean percent value was calculated for the two DRGs referring to the right and to the left side. Cells were counted as follow: percentage of pPKCε or IB4 positive cells was obtained normalizing the number of cells for the total number of DAPI positive neurons (i.e. with a clearly visible nucleus); for colocalization studies, percentage of VR1 and pPKCε positive cells was normalized for the total number of VR1 positive cells, while percentage of VR1 and IB4 positive cells was normalized for the total number of IB4 positive cells.

In spinal cord slides, six sections of the L5 trait were considered per animal. A small cut was operated in the contralateral ventral area in order to identify sections sides. For each section, a representative area of the dorsal horn of ipsilateral and contralateral side was considered, at 20x magnification (picture area of 578 µm x 434 µm), using consistent exposure times across all sections. Laminae I-III were identified taking as reference the rat brain atlas of Paxinos and Watson *(Paxinos & Watson, 1982)*. IBA1 positive cells were counted only if colocalized with DAPI staining and if displaying an "active" phenotype (clearly swollen body, short processes); number of active microglial cells in ipsilateral side was normalized for the number obtained in the contralateral side.

In both experiments, animals whose samples or slides were damaged were excluded from statistical analyses,

4.10. Retrograde labeling of DRGs nuclei of sensory cells receiving from the hind paw

To assess if changes in labeled antigens expression were actually referring to paw-related cells, a small group of animals (1 per experimental group (175-200 g), for a total number of 4 rats) was saved for retrograde labeling of DRGs nuclei. Animals received an intraplantar

injection of 20 µl of 1% True Blue (TB, True Blue Diaceturate Salt, Sigma) into the right hind paw, 7 days before perfusion, to let the retrograde tracer spread properly along axons to DRGs nuclei. The needle was left in site for 10 minutes. 3 days later, they received CFA injection into the same paw and joined the major group of animals.

4.11. Statistical analyses

GraphPad Prism 7 (GraphPad Software, Inc., La Jolla, CA, USA) was used for the data statistical analysis. Animals were randomly assigned to each group. In morphine tolerance paradigms, data analysis was performed on the area under the curve (total AUC) of mechanical thresholds measured at the established time points after drugs administration. The AUC mean value ± standard error of the mean (SEM) was calculated and corrected by the mean AUC of the vehicle treated group. The percentage of maximum possible effect of the drugs (% MPE) was calculated as the percentage of the difference between the measured response and the baseline response post-CFA, divided by the difference between the baseline response post-CFA and the baseline response before CFA injection. Data were analyzed by two-way repeated measures (RM) analysis of variance (ANOVA) and Tukey's post hoc comparisons test, with $P < 0.05$ considered statistically significant.

In the other experiments, data were analyzed by one-way or two-ways ANOVA, except for behavioral data, which were analyzed by RM two-way ANOVA, with $p<0.05$ accepted as significant. Differences between experimental groups were assessed by Sidak's, Dunnett's or Tukey's multiple comparisons tests ($p<0.05$ accepted as significant). Data are presented as the mean ± SEM.

5. Results

5.1. Behavioral assessments of pain features in the CFA model and effects of acute administration of morphine or CR4056

CFA-induced chronic pain triggered mechanical hyperalgesia in the ipsilateral paw measured by Randall-Selitto analgesymeter, 72 hours after the injection, compared to sham animals. Morphine (5 mg/kg, sc) or CR4056 (6 mg/kg, os) acute administration caused a significant increase in the paw withdrawal threshold (g) measured at drugs peak times (**Figure 49**).

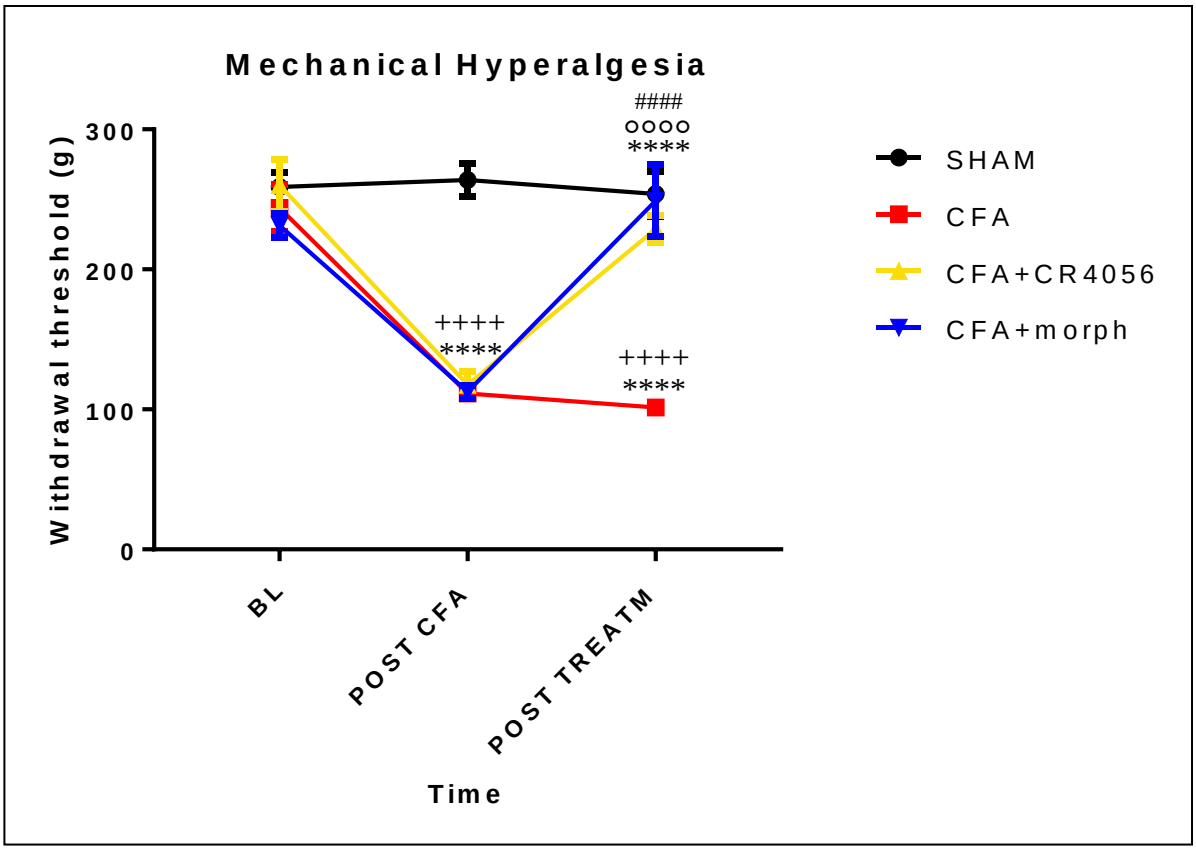

Figure 49 Effect of acute CR4056 (6 mg/kg, os) or morphine (5 mg/kg, sc) administration on CFA-induced mechanical hyperalgesia 72 hours after CFA injection. Data represent withdrawal thresholds expressed in grams ± SEM, measured before CFA injection (baseline, "BL"), after 72h ("POST CFA") and after drugs treatments ("POST TREATM"); n = 6 per group. ****p<0,0001; * vs BL; ° vs POST CFA; + vs sham; # vs CFA; Two-way RM ANOVA (Time: F (2, 40) = 59,88, p<0.0001; Group: F (3, 20) = 27,92, p<0.0001; Interaction: F (6, 40) = 16,61, p<0.0001), Tukey's multiple comparisons test.

In the same animals, CFA-induced chronic pain triggered mechanical allodynia in the ipsilateral paw measured by Von Frey test, 72 hours after the injection, compared to sham

animals. Morphine (5 mg/kg, sc) acute administration caused a significant increase in the paw withdrawal threshold (g) measured at drugs peak times. Also CR4056 (6 mg/kg, os) partly reversed the allodynia being the withdrawal threshold of this group indistinguishable from that of sham operated animals and not significantly different from the baseline value (**Figure 50**).

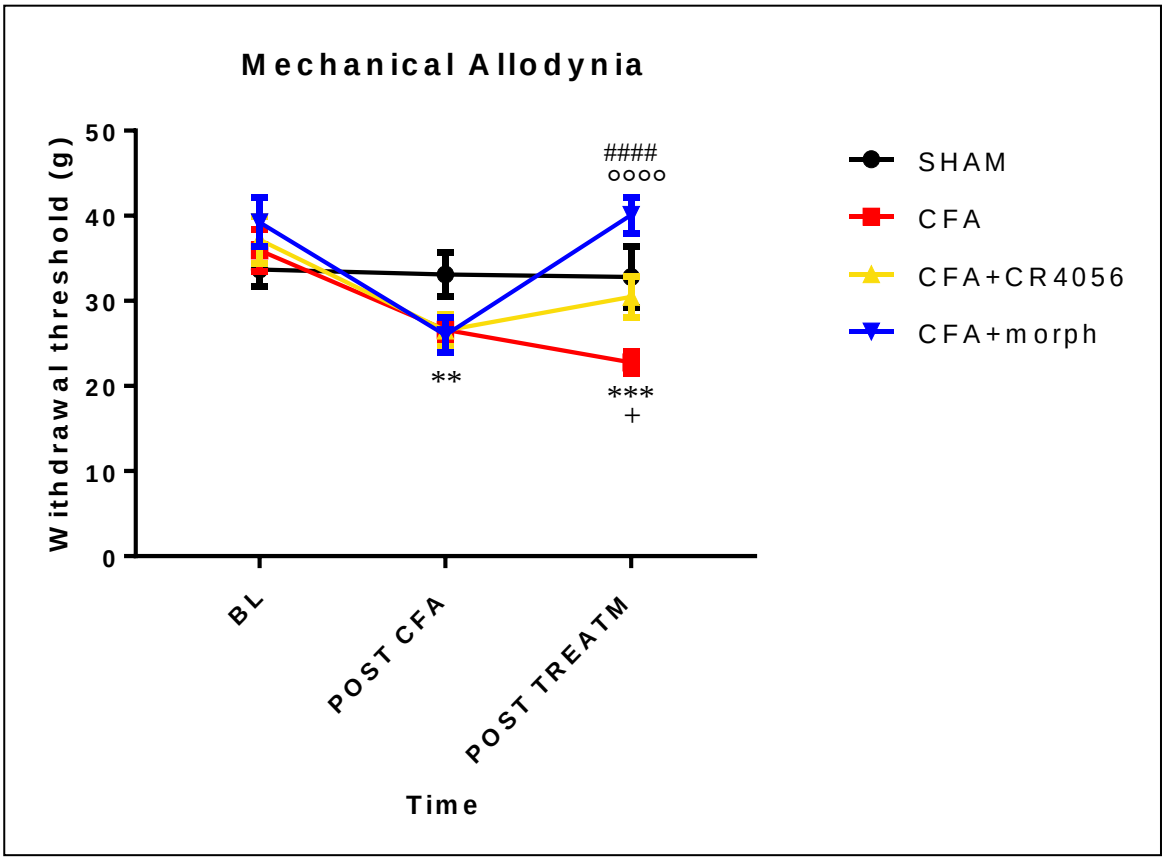

Figure 50 Effect of acute CR4056 (6 mg/kg, os) or morphine (5 mg/kg, sc) administration on CFA-induced mechanical hyperalgesia 72 hours after CFA injection. Data represent mean of 3 repeated measurements for timepoint of withdrawal threshold expressed in grams ± SEM, measured before CFA injection (baseline, "BL"), after 72h ("POST CFA") and after drugs treatments ("POST TREATM"); n = 6 per group. ****p<0,0001; ***p<0,001; **p<0,01; *p<0,1; * vs BL; ° vs POST CFA; + vs sham; # vs CFA; Two-way RM ANOVA (Time: F (2, 40) = 16,79, p<0.0001; Group: F (3, 20) = 2,959, p = 0.057; Interaction: F (6, 40) = 5,058, p = 0.0006), Tukey's Multiple comparisons test.

In the same animals, ongoing pain was evaluated by Dynamic Weight Bearing. CFA-induced chronic pain caused a significant shift of the body weight distribution to the contralateral

rear paw, 72 hours after the injection. Morphine (5 mg/kg, sc) but not CR4056 (6 mg/kg, os) acute administration caused a significant increase of the body weight put on the injured limb, measured at drugs peak times (**Figure 51**), even if also this drug was not able to completely reverse the imbalance induced by CFA.

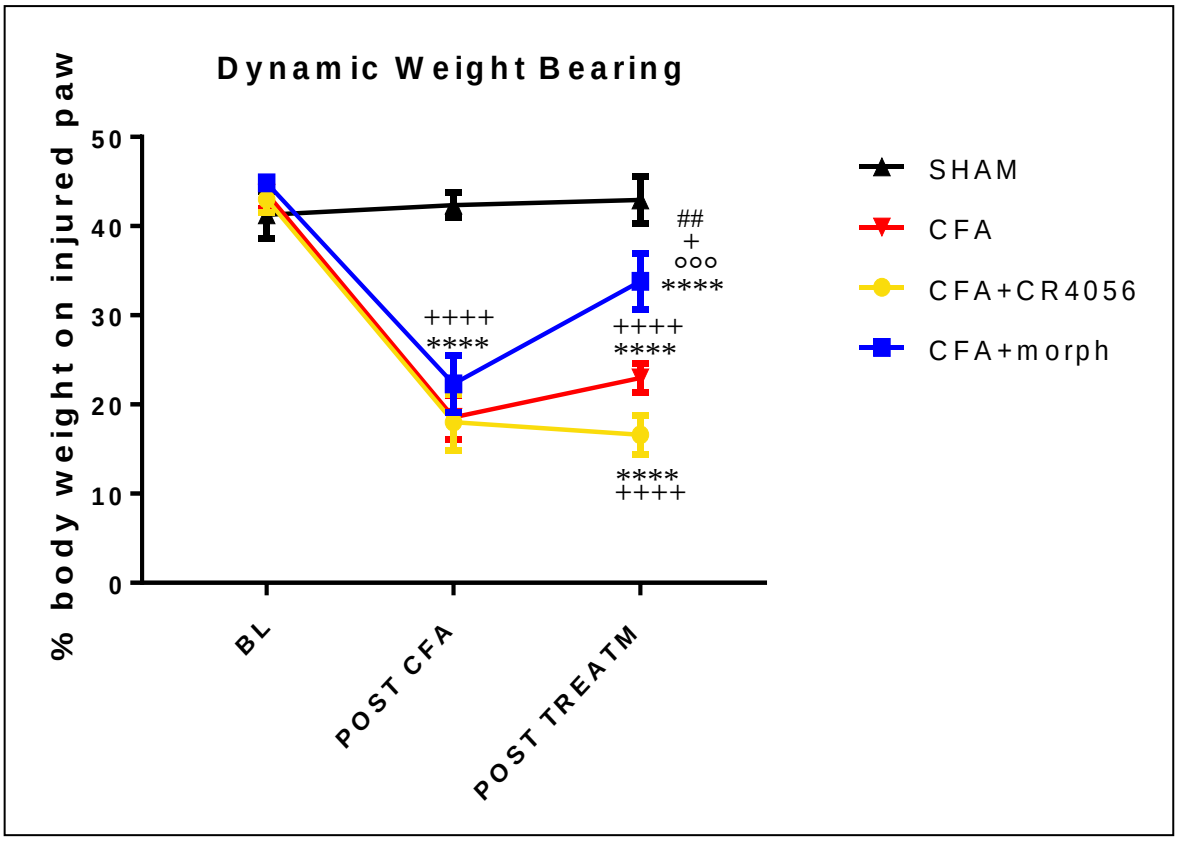

Figure 51 Effect of acute CR4056 (6 mg/kg, os) or morphine (5 mg/kg, sc) administration on CFA-induced body weight imbalance 72 hours after CFA injection. Data represent mean percentage of body weight put on the ipsilateral paw ± SEM, measured before CFA injection (baseline, "BL"), after 72h ("POST CFA") and after drugs treatments ("POST TREATM"); n = 6 per group. ****p<0,0001; ***p<0,001; **p<0,01; *p<0,1; * vs BL; ° vs POST CFA; + vs sham; # vs CFA; Two-way RM ANOVA (Time: F (2, 40) = 93,9, p<0.0001; Group: F (3, 20) = 18,12, p<0.0001; Interaction: F (6, 40) = 15,18, p<0.0001), Tukey's multiple comparisons test.

5.2. Effects of CR4056 or morphine acute administration in CFA-treated rats on spinal microglia activation

CFA-induced inflammation was associated with increased IBA-1 expression in microglial cells in the dorsal horn of the L5 spinal cord trait ipsilateral to CFA injection. Ipsilateral vs contralateral IBA1 expression percent ratio was 100% in sham animals and 150% in CFA-injected animals after 72 hours. Moreover, acute treatment with CR4056 (6 mg/kg, os) but not with morphine (5 mg/kg, sc) was able to reduce ipsilateral expression of IBA-1 (**Figures 52 and 53**).

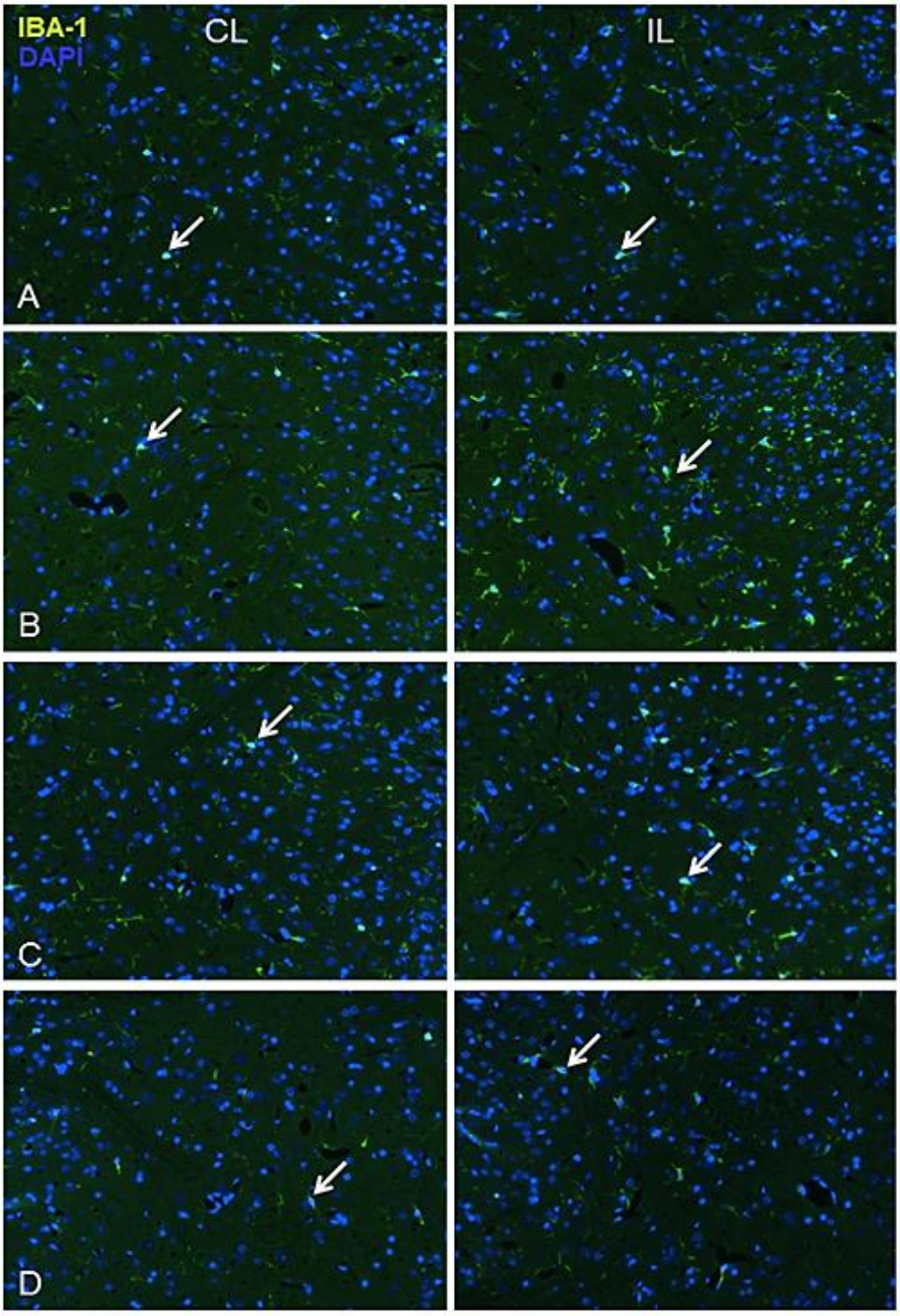

Figure 52 Immunofluorescence staining for IBA-1 in laminae I-III of contralateral (CL) and ipsilateral (IL) dorsal horn of L5 spinal cord. Pictures show representative images of IBA-1 immunoreactivity counterstained with DAPI. Arrows point examples of double-stained cells. **Row A**: sham animals; **row B**: vehicle-treated CFA-injected animals; **row** C: morphine (5 mg/kg, sc)-treated CFA-injected animals, 30 minutes after single administration; **row D**: CR4056 (6 mg/kg, os)-treated CFA-injected animals, 90 minutes after single administration.

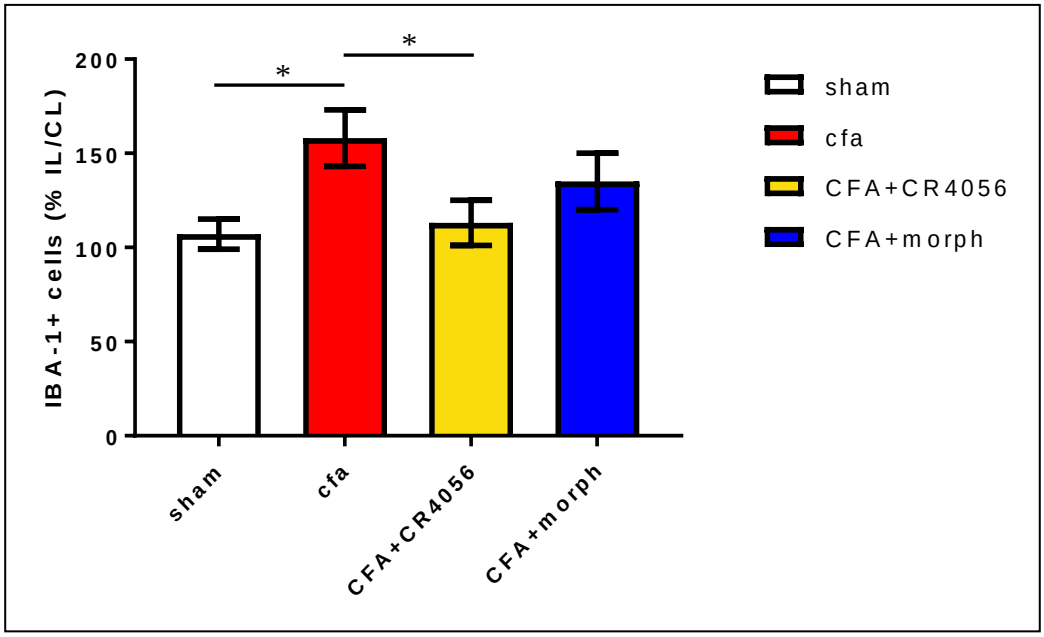

Figure 53 Quantification of IBA-1 expression in the dorsal horn of L5 spinal cord of sham or CFA-injected rats at 72 hours, acutely treated either with vehicle (MC 0,5%), morphine (5 mg/kg, sc) or CR4056 (6 mg/kg, os). Data represent mean percent ratio of IBA-1 positive cells in the ipsilateral (IL) dorsal horn of the spinal cord, normalized for the contralateral (CL) side (Sham n = 6; CFA n = 6; CFA+morphine n = 5; CFA+CR4056 n = 6). *p<0,05; One-way ANOVA ($F(3,19) = 3,491$; $p = 0,0359$), Holm-Sidak's multiple comparisons test.

5.3. Effects of imidazoline agonists on morphine tolerance development in an animal model of CFA-induced inflammatory pain

CFA-induced inflammation triggered mechanical hyperalgesia and the acute administration of 5 mg/kg morphine produced a robust time-dependent alleviation of CFA-induced mechanical hyperalgesia, with maximal effect at 30 minutes post-treatment. CR4056 (0.1-0.3-1 mg/kg, os) (**Figure 54**) and 2-BFI (3-30 µg/kg, ip) (**Figure 55**), administered 15 minutes before morphine (5 mg/kg, sc), at doses devoid of analgesic effect, only slightly modified the acute response to morphine. The dose ratio between CR4056 and 2-BFI inactive doses is in agreement with the affinity difference of the two compounds to I2R, evaluated by binding receptor assay (596 µM vs 10.3 µM respectively). Following 4 days of morphine treatment (7 administrations), the analgesic effect of the drug was significantly reduced; interestingly, when CR4056 (**Figure 54**) or 2-BFI (**Figure 55**) were administered 15 minutes before each

morphine administration, we observed a dose-dependent prevention of morphine analgesic tolerance.

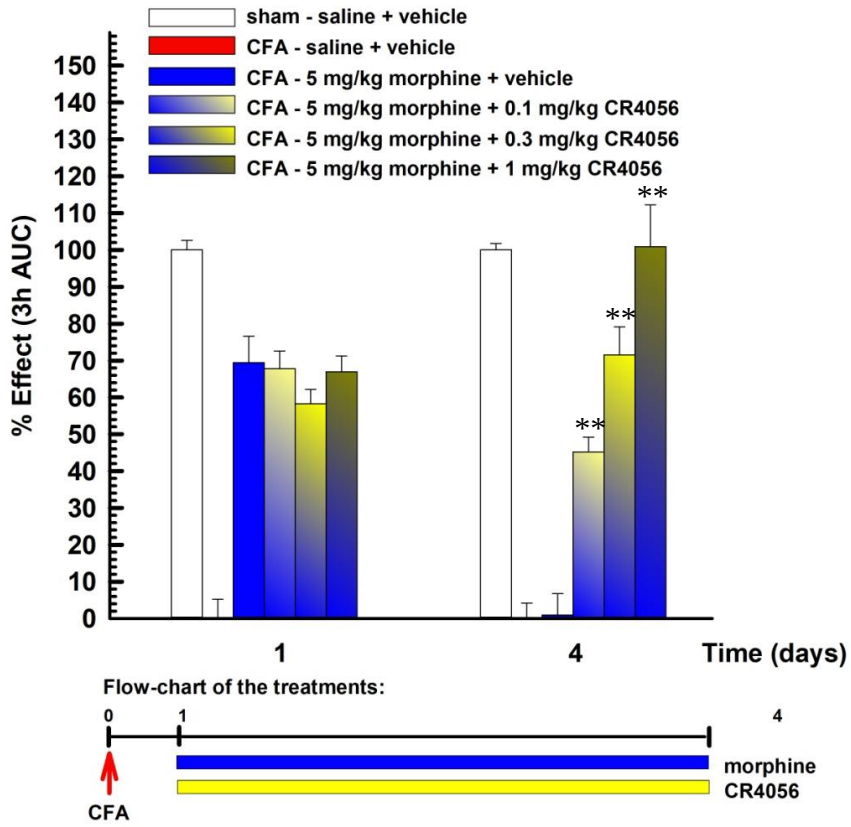

Figure 54 Effect of CR4056 (dose range 0.1-0.3-1 mg/kg, os)-morphine (5 mg/kg, sc) co-treatment on the development of morphine analgesic tolerance. Data represent the mean area under the curve (AUC) ± SEM of mechanical withdrawal threshold time course (0 – 3 hours) after drug administrations, on day 1 and on day 4 (n = 6 per group). **p<0.01 vs morphine alone treated group; One-way ANOVA ($F(4,25) = 36{,}54$; $p<0{,}0001$), Tukey's multiple comparisons test.

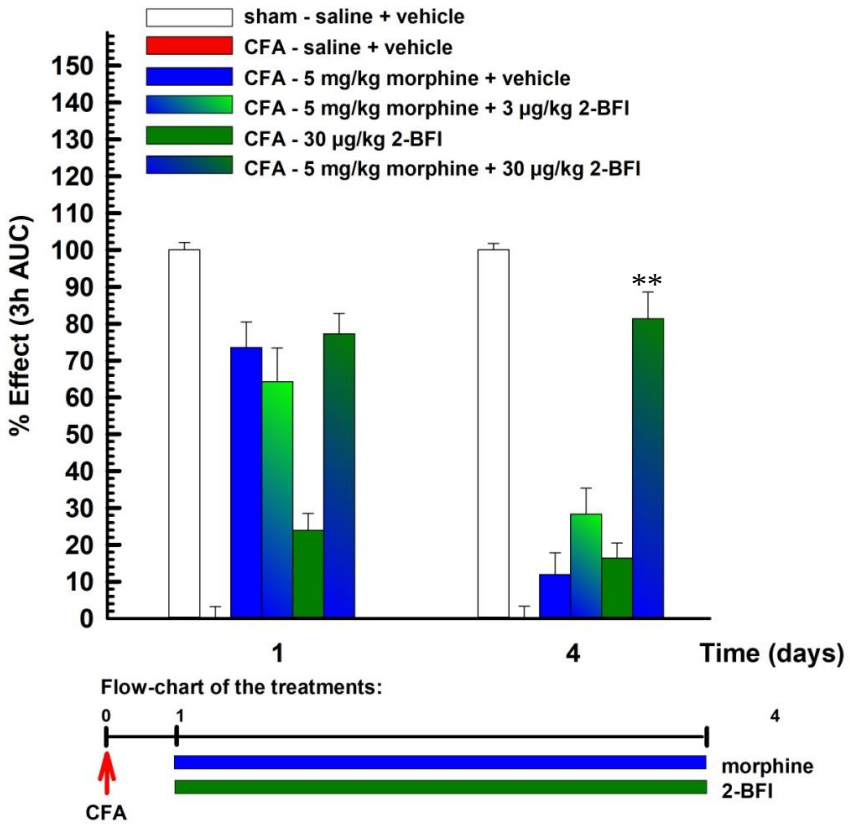

Figure 55 Effect of 2-BFI (dose range 3-30 µg/kg, ip)-morphine (5 mg/kg, sc) co-treatment on the development of morphine analgesic tolerance. Data represent the mean area under the curve (AUC) ± SEM of mechanical threshold time course (0 – 3 hours) after drug administrations, on day 1 and on day 4 (n = 6 per group). **p<0.01 vs morphine alone treated group; One-way ANOVA (F (3,20) = 30,42; p<0,0001), Tukey's multiple comparisons test.

Following 14 days of morphine (5 mg/kg, sc) treatment the analgesic effect of the drug was negligible; interestingly, when CR4056 (1 mg/kg, os) was administered 15 minutes before each morphine administration, we observed a reduction of morphine analgesic tolerance and a partial recovery of morphine analgesic effect (**Figure 56**).

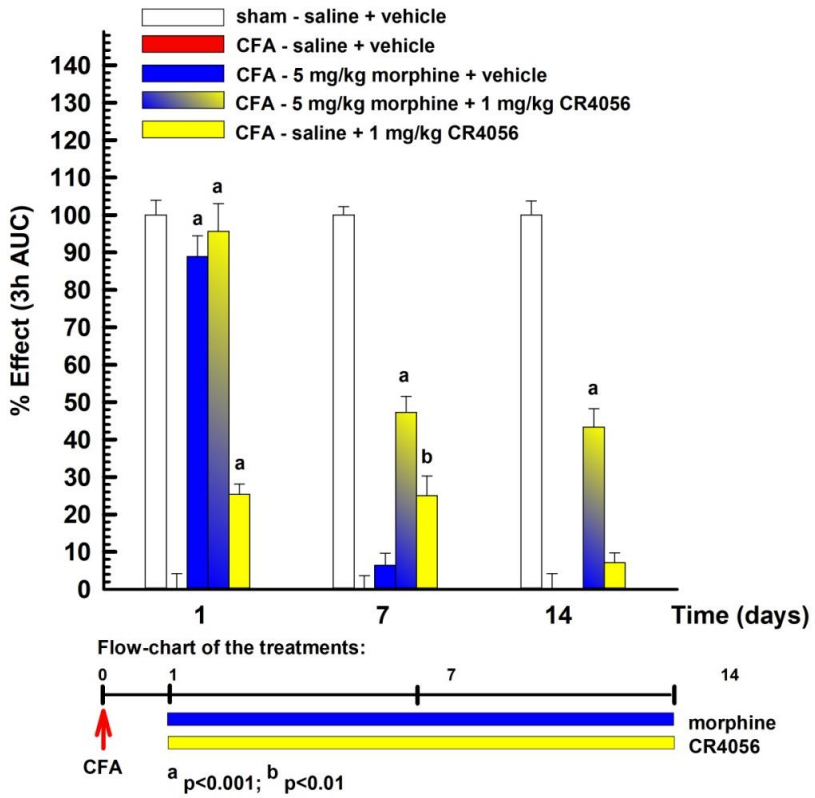

Figure 56 Effect of CR4056 (1 mg/kg, os)-morphine (5 mg/kg, sc) co-treatment on the development of morphine analgesic tolerance. Data represent the % effect of the drugs on the area under the curve (AUC) ± SEM of mechanical threshold time course (0 – 3 hours) after drug administrations, on day 1, day7 and day 14 (n = 6 per group). [a] p<0.001, [b] p<0.01 vs vehicle treated group; Two-way ANOVA RM (Time: F (2,40) = 33,09, p<0,0001; Group: F (3,20) = 34,33, p<0,0001; Interaction: F (6,40) = 25,45, p<0,0001), Tukey's multiple comparisons test.

5.4. Effects of CR4056 on already established morphine tolerance in an animal model of CFA-induced inflammatory pain

As previous experiment, CFA-induced inflammation triggered mechanical hyperalgesia and the acute administration of morphine (5 mg/kg, sc) produced a robust time-dependent alleviation of CFA-induced hyperalgesia. Following 7 days of morphine treatment the analgesic effect of the drug was negligible; after 7 days, CR4056 (1 mg/kg, os) was co-administered with morphine in already tolerant rats and it partially re-established the analgesic activity of the drug on the first day of co-administration; continuing the combined treatment for another week, CR4056 further improved the recovery of morphine analgesic

activity (**Figure 57**). Moreover, CR4056 extended the time course of morphine induced analgesia from 30 minutes to 75 minutes after drugs administration.

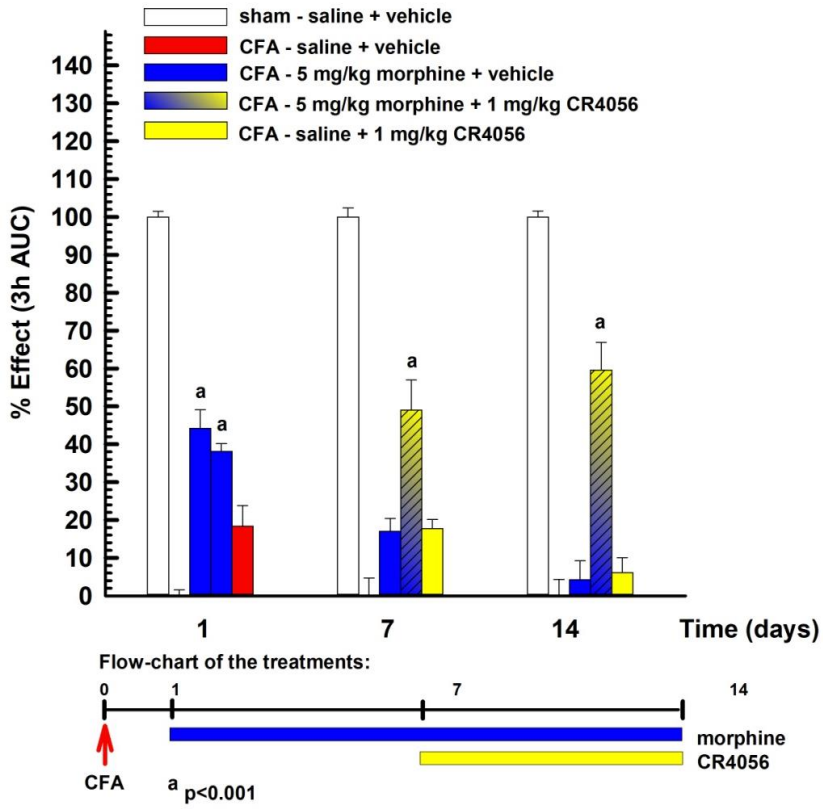

Figure 57 Effect of CR4056 (1 mg/kg, os)-morphine (5 mg/kg, sc) co-treatment on morphine tolerance expression. Data represent the % effect of the drugs on the area under the curve (AUC) ± SEM of mechanical threshold time course (0 – 3 hours) after drug administrations, on day 1, day 7 and day 14 (n = 6 per group). [a] p<0.001 vs vehicle treated group; Two-way ANOVA RM (Time: F (2,40) = 9,86, p<0,0001; Group: F (3,20) = 53,84, p<0,0001; Interaction: F (6,40) = 16,86, p<0,0001), Tukey's multiple comparisons test.

5.5. Effect of CR4056 on morphine tolerance-induced spinal microgliosis

In animals described under 5.4 paragraph, spinal microglia activation was also analyzed. 2 hours after the last drug treatment, rats were sacrificed on day 14, and microglial cells showing an "activated" phenotype were counted in the dorsal horn of the spinal cord

ipsilateral to CFA (or saline) injection. Percent value of IBA-1 positive cells found in the ipsilateral dorsal horn normalized for the contralateral side was significantly higher in CFA-injected animals treated either with vehicles or with morphine alone. Interestingly, CFA-injected animals treated either with morphine and CR4056 or CR4056 alone were not significantly different from the control group (**Figure 58 and 59**).

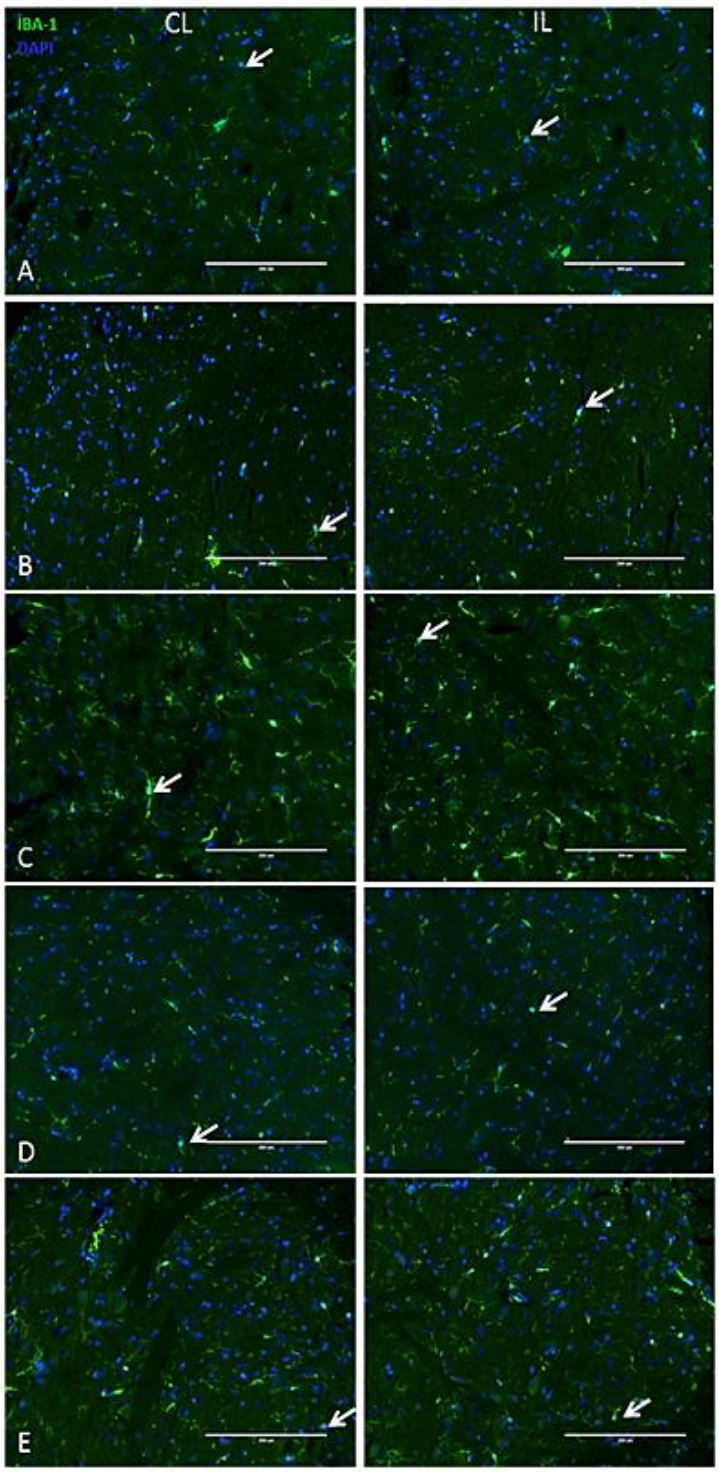

Figure 58 Immunofluorescence staining for IBA-1 in laminae I-III of contralateral (CL) and ipsilateral (IL) dorsal horn of L5 spinal cord. Pictures show representative images of IBA-1 immunoreactivity counterstained with DAPI. Arrows point examples of double-stained cells. **Row A**: sham animals; **row B**: vehicle-treated CFA-injected animals; **row C**: morphine (5 mg/kg, sc)-treated CFA-injected animals, at 14th day of chronic administration; **row D**: CR4056 (1 mg/kg, os)-treated CFA-injected animals, at 7th day of chronic administration; **row E**: morphine (5 mg/kg, sc) and CR4056 (1 mg/kg, os)-treated CFA-injected animals, at 14th day of morphine chronic administration, CR4056 being co-administrated in days 7-14.

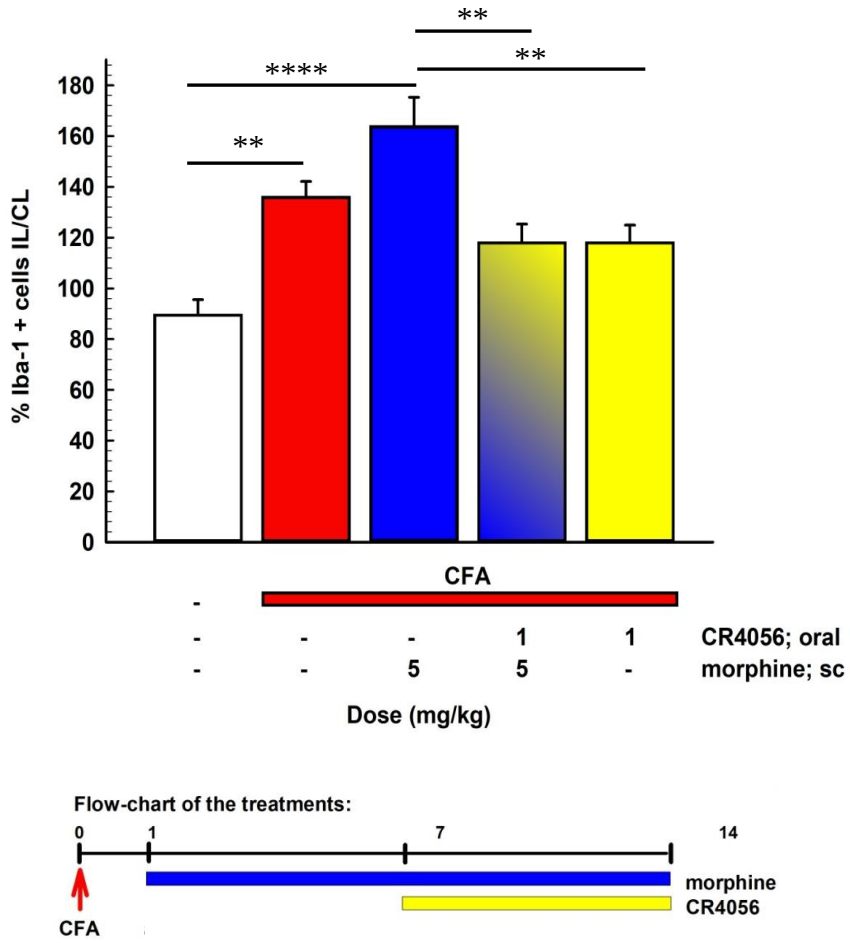

Figure 59 Quantification of IBA-1 expression in the dorsal horn of L5 spinal cord of sham or CFA-injected rats, either treated with: vehicles (saline; MC 0,5%); morphine (5 mg/kg, sc) 2/die for 14 days of chronic administration; CR4056 (1 mg/kg, os) 2/die for 7 days of chronic administration; morphine (5 mg/kg, sc) and CR4056 (1 mg/kg, os), morphine being administered 2/die for 14 days and CR4056 being co-administrated in days 7-14. Data represent mean percent ratio of IBA-1 positive cells in the ipsilateral (IL) dorsal horn of L5 spinal cord, normalized for the contralateral (CL) side (n = 4 per group). ****p<0,0001; **p<0,01; One-way ANOVA (F (4,15) = 11,7; p = 0,0002), Tukey's multiple comparisons test.

5.6. Effects of CR4056 on opioid-induced constipation

Acute administration of codeine (12 mg/kg, sc) and morphine (10 mg/kg, sc) to healthy rats induced a significant constipation compared to vehicle; this effect was compared to CR4056 6 mg/kg which slightly and not significantly decreased defecation. The association of CR4056

with codeine (**Figure 60**) or morphine (**Figure 61**), at the same doses, did not show a synergistic or additive modulation of this opioid adverse side-effect.

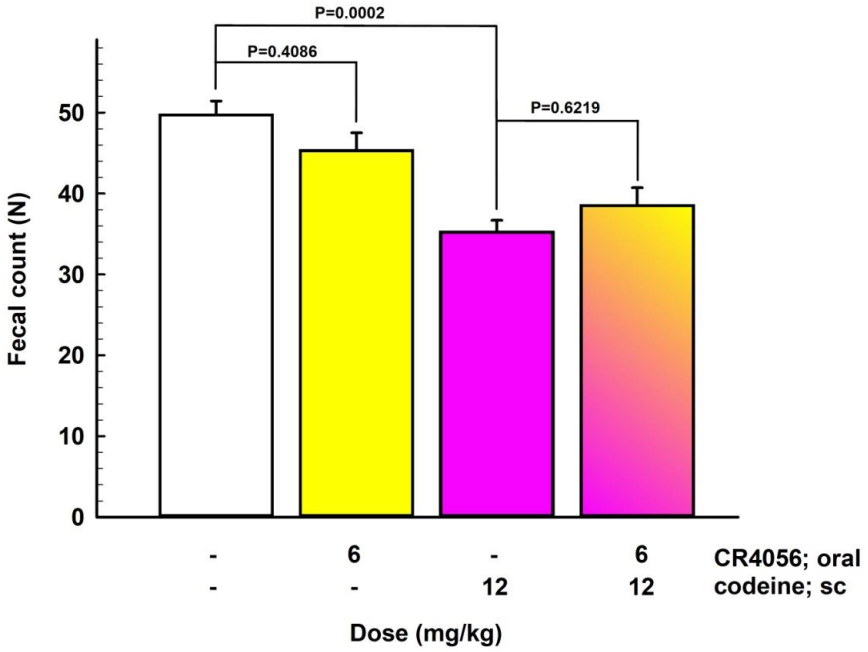

Figure 60 Effect of acute oral administration of CR4056 (6 mg/kg, os) on defecation in normal rats, in comparison to codeine (12 mg/kg, sc) alone and to CR4056-codeine combination treatment. Data represent the mean faecal number ± SEM (n = 6 per group); One-way ANOVA (F (3,20) = 11,49; p<0,0001), Tukey's multiple comparisons test.

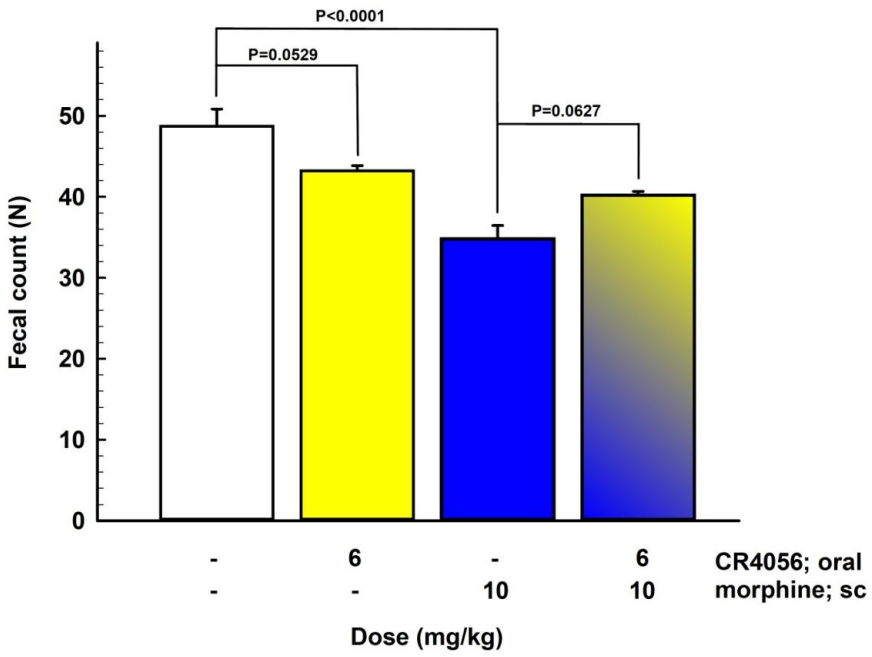

Figure 61 Effect of acute oral administration of CR4056 (6 mg/kg, os) on defecation in normal rats, in comparison to morphine (10 mg/kg, sc) alone and to CR4056-morphine combination treatment. Data represent the mean faecal number ± SEM (n = 6 per group); One-way ANOVA (F (3,20) = 16,96; p<0,0001), Tukey's multiple comparisons test.

5.7. Effects of CR4056 or morphine acute administration in CFA-treated rats on PKCε phosphorylation and TRPV1 expression in L4-L5 DRG neurons

In a different set of experiments, chronic hind limb inflammation induced by intraplantar CFA administration in rats was again associated with marked mechanical hyperalgesia (data not shown) and with a significant increase in PKCε phosphorylation in the ipsilateral L4-L5 DRG neurons compared to contralateral DRG and to control rats, 72 h after injection. Moreover, a single acute treatment with morphine (5 mg/kg, sc) or CR4056 (6 mg/kg, os) was able to increase paw withdrawal threshold and to reduce PKCε phosphorylation in ipsilateral L4-L5 DRG neurons. No significant difference was detected between ipsi- and contralateral L4-L5 DRG of sham, CR0456- or morphine-treated groups animals, nor between sham animals and CR0456- or morphine-treated groups (**Figures 62 and 63**).

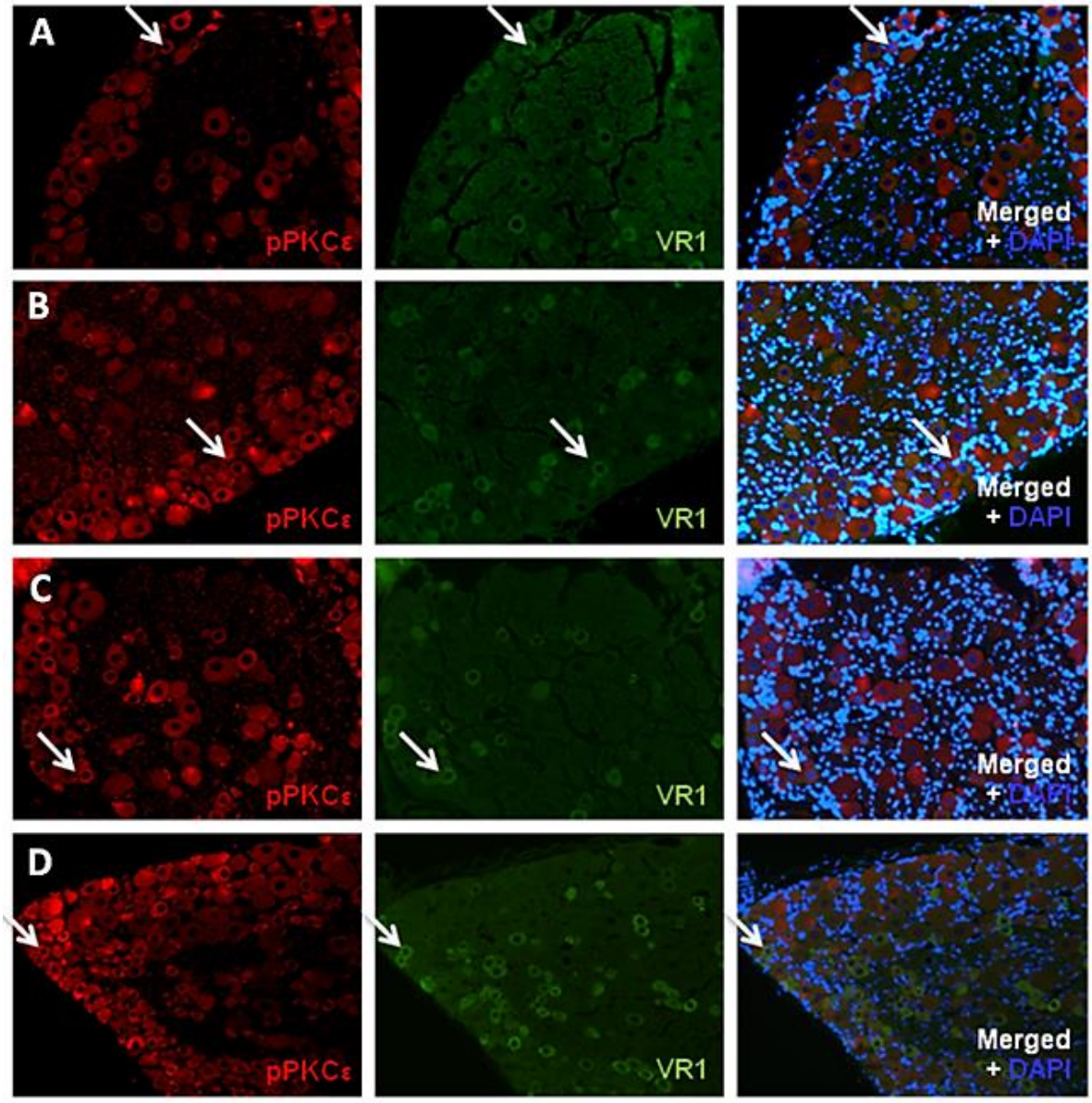

Figure 62 Immunofluorescence staining for pPKCε and VR1 in L4-L5 ipsilateral to lesion DRG sections of CFA- injected rats at 72 hours. Pictures show representative images of pPKCε immunoreactivity (**first column**), VR1 immunoreactivity (**second column**) and colocalization counterstained with DAPI. Arrows point examples of double-stained cells. **Row A**: sham animals; **row B**: vehicle-treated CFA-injected animals; **row C**: morphine (5 mg/kg, sc)-treated CFA-injected animals, 30 minutes after single administration; **row D**: CR4056 (6 mg/kg, os)-treated CFA-injected animals, 90 minutes after single administration.

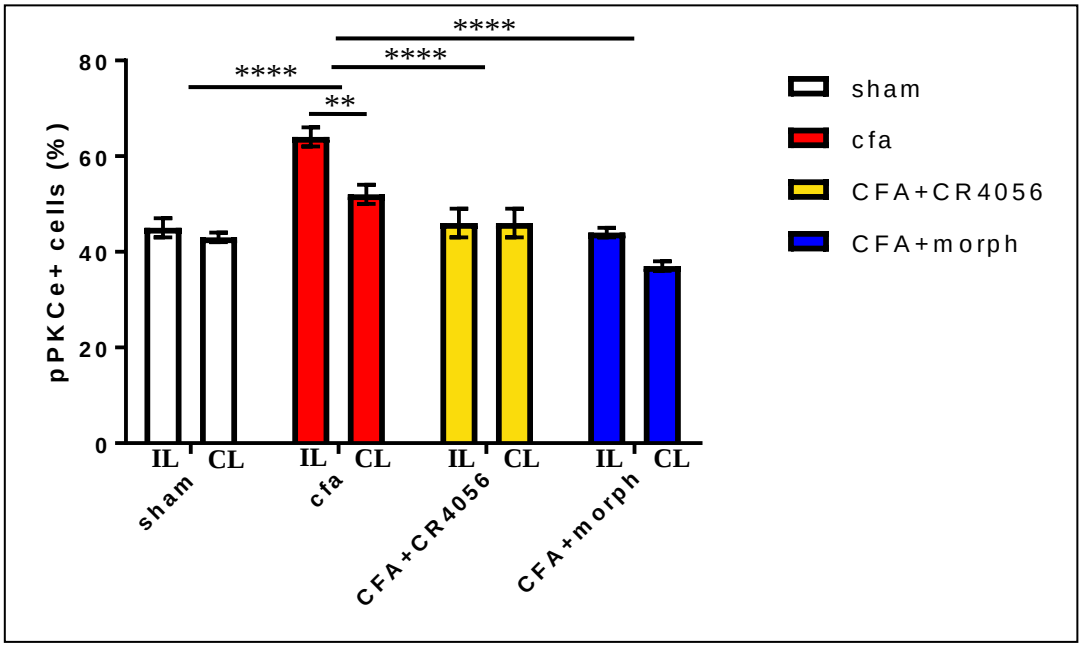

Figure 63 Quantification of pPKCε expression in L4-L5 DRG sections ipsilateral (IL) and controlateral (CL) to lesion of sham or CFA-injected rats at 72 hours, acutely treated either with vehicle (MC 0,5%), morphine (5 mg/kg, sc) or CR4056 (6 mg/kg, os). Data represent mean percentage of pPKCε positive cells normalized for the total number of cells (Sham n = 6; CFA n = 4; CFA+morphine n = 6; CFA+CR4056 n = 6). ****p<0,0001; **p<0,01; Two-way ANOVA (Side: F (1,36) = 9,13, p = 0,0011; Group: F (3,36) = 57,39, p<0,0001; Interaction: F (3,36) = 7,19, p = 0,0318), Holm-Sidak's multiple comparisons test.

In the same animals, CFA-induced inflammation was not associated with remarkable differences in TRPV1 expression *tout court* (data not shown). Conversely, the colocalization ratio between pPKCε and TRPV1 expression, normalized for the total number of TRPV1 positive cells, was influenced by inflammatory insult and acute treatment: it was increased in CFA-treated animals after 72 hours, and acute treatments with morphine (5 mg/kg, sc) or CR4056 (6 mg/kg, os) were able to reduce it (**Figure 64**).

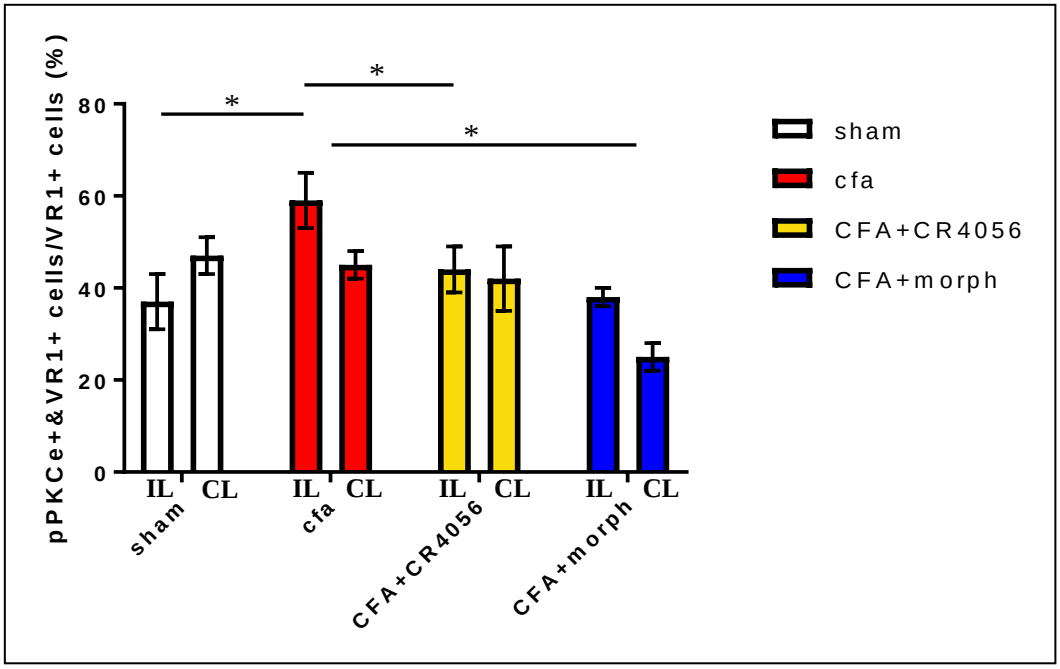

Figure 64 Quantification of pPKCε and TRPV1 (VR1) colocalization in L4-L5 DRG sections ipsilateral (IL) and controlateral (CL) to lesion of sham or CFA-injected rats at 72 hours, acutely treated either with vehicle (MC 0,5%), morphine (5 mg/kg, sc) or CR4056 (6 mg/kg, os). Data represent mean percentage of pPKCε and TRPV1 positive cells normalized for the total number of TRPV1 positive cells (Sham n = 6; CFA n = 4; CFA+morphine n = 6; CFA+CR4056 n = 6). *p<0,05; Two-way ANOVA (Side: F (1,36) = 2,93, p = 0,1835; Group: F (3,36) = 27,43, p<0,0026; Interaction: F (3,36) = 12,3, p = 0,0691), Holm-Sidak's multiple comparisons test.

Exploring TRPV1 expression in the IB4 positive neuronal subpopulation, though, I found no influence of CFA injection at 72h, nor of acute treatments with morphine (5 mg/kg, sc) or CR4056 (6 mg/kg, os), contrary to what expected according to literature (**Figure 65**).

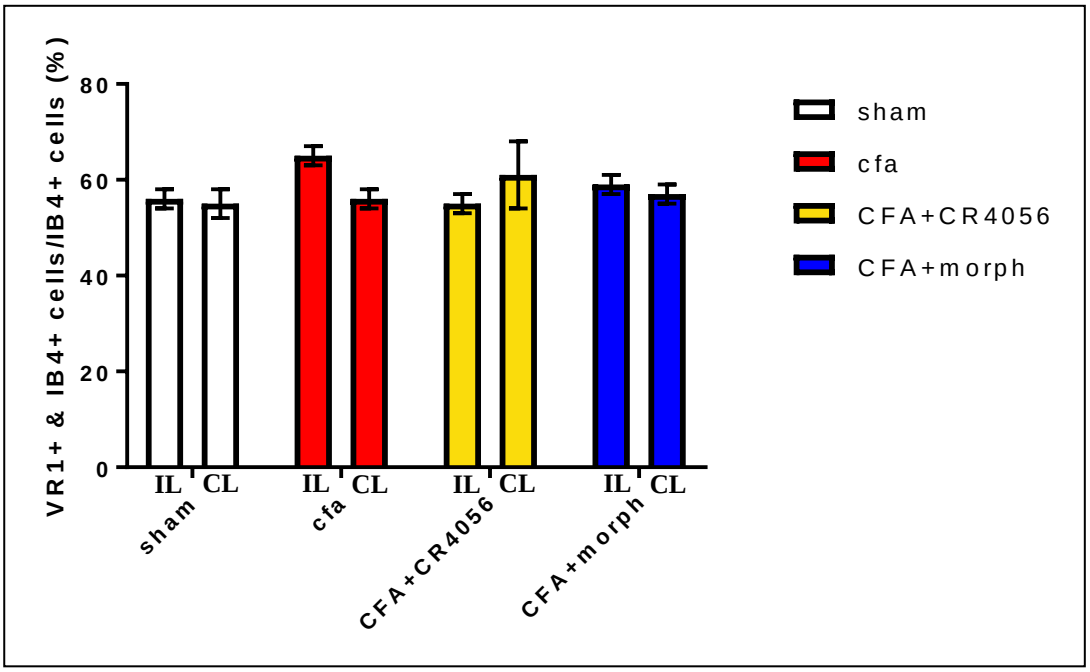

Figure 65 Quantification of IB4 and TRPV1 (VR1) colocalization in L4-L5 DRG sections ipsilateral (IL) and controlateral (CL) to lesion of sham or CFA-injected rats at 72 hours, acutely treated either with vehicle (MC 0,5%), morphine (5 mg/kg, sc) or CR4056 (6 mg/kg, os). Data represent mean percentage of IB4 and TRPV1 positive cells normalized for the total number of IB4 positive cells (Sham n = 5; CFA n = 4; CFA+morphine n = 6; CFA+CR4056 n = 6). Two-way ANOVA (Side: F (1,34) = 0,8889, p = 0,5503; Group: F (3,34) = 4,938, p<0,5738; Interaction: F (3,34) = 11,16, p = 0,226).

5.8. Retrograde labeling of DRGs nuclei of sensory cells receiving from CFA-injected paw

In a different batch of animals, I assessed if phenomena observed in DRGs nuclei of the hind paw ipsilateral to inflammation were specifically taking place in somata of cells receiving information from the CFA-injected paw. To do so, cells were retrogradely labeled with TB, then DRGs were collected and postfixed for immunofluorescence. TB+ cells, in most cases, were also pPKCε and VR1 positive (**Figure 66**).

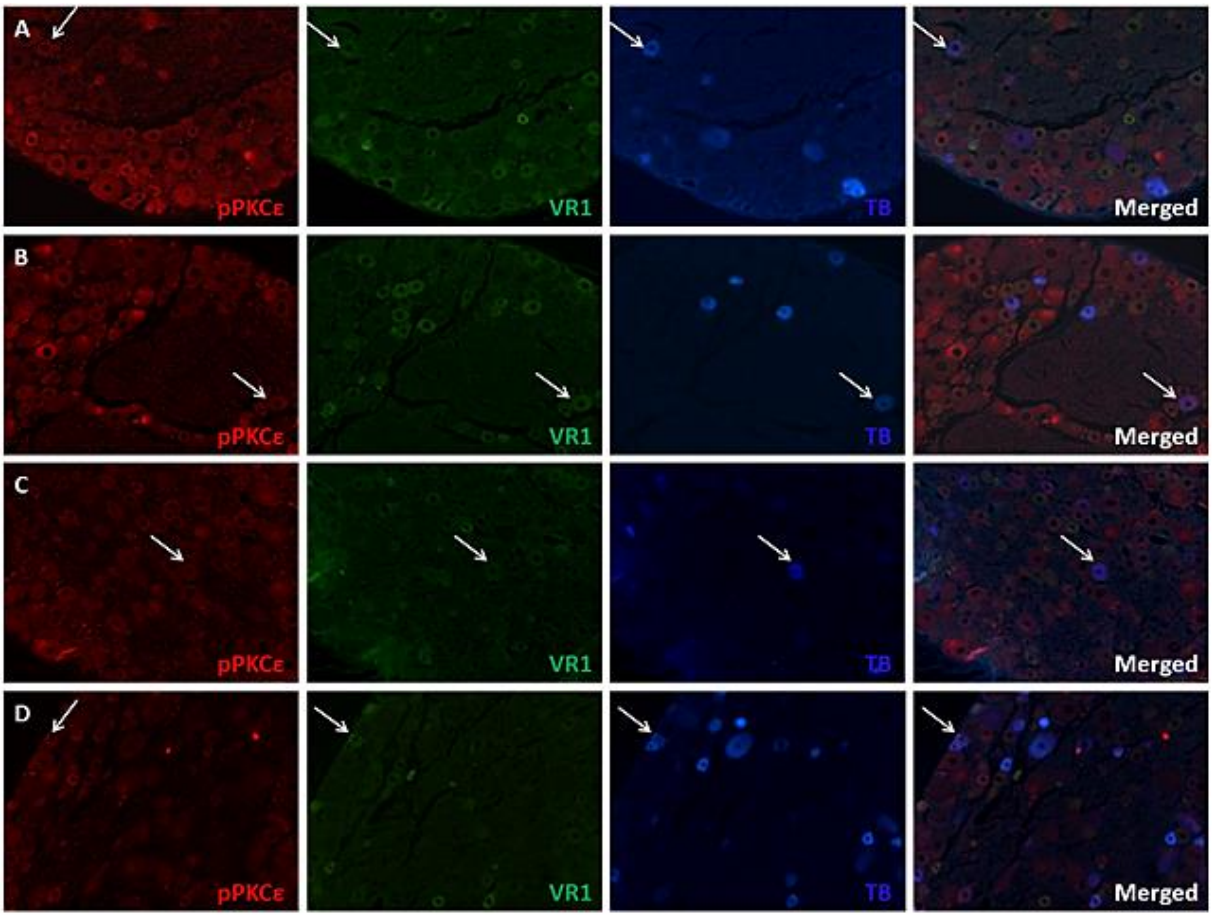

Figure 66 Immunofluorescence staining for pPKCε (red) and VR1 (green) in L4-L5 ipsilateral to lesion DRG sections of TB (blue)-injected rats, 7 days after tracer injection in the hind paw that eventually received also CFA injection (-72h from sacrifice). Pictures show representative images of pPKCε immunoreactivity (**first column**), VR1 immunoreactivity (**second column**), TB fluorescence (**third column**) and colocalization. Arrows point examples of triple-stained cells. **Row A**: sham animals; **row B**: vehicle-treated CFA-injected animals; **row C**: morphine (5 mg/kg, sc)-treated CFA-injected animals, 30 minutes after single administration**; row D**: CR4056 (6 mg/kg, os)-treated CFA-injected animals, 90 minutes after single administration.

6. Discussion

Chronic pain is a cross-pathology symptom that affects 20% of European population, and 12 to 25% of U.S.A. citizens *(Goldberg & McGee, 2011)*. The difficulty of dealing with this life-interfering disease is its high co-morbidity with a wide variety of diseases and its long-lasting persistence (7 years in average). Moreover, mental and physical stress at work, socioeconomic conditions and education are considered influencing variables, leading to the need of adopting a biopsychosocial model in the evaluation of pain *(Priest & Hoggart, 2002).* In clinical patients, two major symptoms of chronic pain are allodynia (i.e., pain elicited by a stimulus that normally does not cause pain) and hyperalgesia (i.e., an increased pain response produced by a stimulus that normally causes pain), in the clinical setting difficult to clearly differentiate in the individual patient. However, the primary complaint of the pain patient is mostly spontaneously emitted pain. Several animal models of chronic pain have been developed, in order to reproduce clinical symptoms and to study their mechanisms. While stimulus-evoked pain is relatively reproducible in animal models of pain, often laboratory settings do not reflect clinical reality, as the patient usually tries to avoid pain-eliciting stimuli. On the other hand, measuring spontaneous pain behavior in animal models of pain is an open issue: it remains unclear what behaviors can reveal its presence in the laboratory animal *(Mogil & Crager, 2004)*. So, pain modeling and pain therapeutics testing in the animal need a broad-spectrum evaluation in order to try to analyze all possible variables implied.

Complete Freund's Adjuvant (CFA)-induced chronic pain is one of the adjuvant-induced animal models, which mimic chronic inflammatory pain *(Gregory et al., 2013)*. CFA injection into the footpad produces dose-dependent inflammatory edema, mechanical allodynia, mechanical and thermal hyperalgesia in the lesioned paw, but animals do not show weight reduction nor alterations in grooming or exploratory behavior. Symptoms persist at least for a couple of weeks, but CFA-induced inflammatory pain does not ever evolve into a systemic disease *(Zhang & Ren, 2011*). Furthermore, CFA-injected rats *(Tétreault et al., 2010*) and mice *(Griffioen et al., 2015)* decrease the use of their ipsilateral hind paws and show a reduction in the paw surface pressed against the floor, thus showing a body weight imbalance.

In line with these and many other findings *(Zhang & Ren, 2011; Caprioli et al., 2015; Ferrari et al., 2011)*, in the present study, a single intraplantar injection of 100 µl of CFA in the right hindlimb of rats provoked the onset, measured at day 3 from the induction, of mechanical

hyperalgesia and allodynia, measured by the Randall-Selitto analgesymeter and the Von Frey Test, respectively, as well as a significant reduction of the body weight put on the injured paw.

On this animal model, two main analgesic drugs have here been tested: the well-known opioid morphine and the new imidazoline-2 ligand CR4056. Opioid medications primary act on μ-opioid receptors (MORs), which are present in cerebral areas responsible for the perception of pain (periaqueductal gray, thalamus, cingulate cortex and insula) and in the substantia gelatinosa of the dorsal horn of the spine, where they exert their primary action in inhibiting spinal transmission. MORs are seven transmembrane domains proteins coupled to inhibitory G proteins, whose activation leads to cAMP inhibition, deactivation of the inwardly rectifying potassium channel (Kir3), and reduction of calcium channels conductance resulting in cellular hyperpolarization *(Al-Hasani & Bruchas, 2011)*.

On the other hand, imidazoline receptors still have not been cloned and fully characterized yet, even if some putative proteins have been identified in human and mouse brain tissue, being expressed in both neurons and astrocytes *(Keller & García-Sevilla, 2015)*. In vitro studies located imidazoline 2 receptors (I2R) primarily on the outer membrane of mitochondria. Furthermore, it was shown from affinity studies that they may be novel allosteric binding sites of monoamine oxidases (MAO) A and B *(Jones et al., 2007)*. Thus, the mechanism of action of I2R ligands may be more complex and intriguing than the one of opioid drugs. One consistent finding is that I2R ligands are effective for tonic and chronic pain (inflammatory and neuropathic pain) but ineffective for acute phasic pain (nociceptive stimulus-evoked reflexive responses). For example, agmatine administration was able to provoke significant analgesia in animal models of tonic inflammatory and chronic neuropathic pain (*Li & Zhang, 2011)*. The selective I2R agonists 2-BFI, BU224, tracizoline and CR4056 showed significant effect, totally blocked by co-administration of I2R antagonist idazoxan, in counteracting mechanical and thermal hyperalgesia, measured by Von Frey filaments and plantar test, respectively, in rat models of inflammatory (CFA model) and neuropathic pain (CCI model); furthermore, they markedly attenuated the place escape/avoidance behavior, demonstrating that I2R ligands are also effective in counteracting the affective component of pain *(Li et al., 2014)*.

In the present work, morphine (5 mg/kg, sc) or CR4056 (6 mg/kg, os) acute administration caused a significant increase in the paw withdrawal threshold, measured at drugs peak times

by the Randall-Selitto and the Von Frey tests. CR4056 and morphine analgesic efficacy in counteracting mechanical hyperalgesia and allodynia was already observed in several animal models of pain *(Ferrari et al., 2011; Lanza et al., 2014; Meregalli et al., 2012; Caprioli et al., 2015)*, including the CFA model; furthermore, CR4056 dose (6 mg/kg) was selected as the optimal dose for the relief of hyperalgesia and allodynia without deviating into hypoalgesic effects, and it is equivalent to the CR4056 dose for humans *(Ferrari et al., 2011).* Morphine dose (5 mg/kg) was selected for the same reasons, and furthermore, to compare this set of experiments to the subsequent tests on morphine-induced tolerance, given that morphine 5 mg/kg was already shown to be an optimal dose to induce analgesic tolerance in a relatively brief period *(Caprioli et al., 2015; Beaudry et al., 2015).*

Morphine (5 mg/kg) acute administration, but not CR4056 (6 mg/kg), could partly, but significantly, increase the percentage of body weight put on the paw ipsilateral to the CFA injection. Using a similar device for measuring plantar pressure distribution on freely moving rats (Tekscan Walkway), it was demonstrated that, in the monosodium-iodoacetate (MIA) model of osteoarthritis, only acute morphine 5 mg/kg, and not naproxene, was able to significantly recover the pain-induced body weight imbalance *(Gregersen et al., 2013).* The authors conclude that naproxene probably needs chronic administration to be able to exert its analgesic activity in spontaneous pain. Even if MIA-induced chronic pain is different from the CFA model, we can still compare some of the pain features they share, such as chronicity and elicitation of mechanical hyperalgesia and allodynia, as well as spontaneous pain behaviors. In another study *(Ferreira-Gomes et al., 2012)*, spontaneous pain in the MIA model was evaluated by the Knee-Bend and the Cat-Walk assays, which analogously measure body weight distribution: also in this case, morphine was the best-acting analgesic, compared to the slight effects of diclofenac and lidocaine. My hypothesis is that CR4056 would influence body weight distribution if administered in chronic, therefore we set out to verify this assumption in further experiments.

Moreover, several I2R ligands showed effects on the modulation of opioid-induced tolerance and proved to potentiate opioid antinociception. For example, agmatine administration could reduce tolerance to chronic morphine administration *(Regunathan, 2006)* and naloxone-induced withdrawal symptoms *(Aricioglu et al., 2004)*, without enhancing morphine-induced constipation *(Kolesnikov et al., 1996)*. Phenyzoline was able to produce significant morphine analgesia enhancement in the tail-flick and hot-plate test *(Gentili et al.,*

2006). Oxycodone-induced tolerance, measured by the Von Frey filaments in CFA or CCI rats, was delayed by the co-administration of phenyzoline *(Thorn et al., 2017)*. Morphine-induced antinociceptive tolerance was attenuated by co-administration with 2-BFI, BU224 or CR4056 *(Thorn et al., 2017)*. Furthermore, in capsaicin-injected rats *(Ferrari et al., 2011)* and in the post-operative pain model *(Lanza et al., 2014)*, morphine, CR4056 and their combination produced a significant, dose-dependent antihyperalgesic effect. Isobolographic analyses revealed a significant synergistic interaction between morphine and CR4056. When these agents were combined, the doses needed to reach the median effective dose were about 4-fold lower than those seen after administration of each drug alone. These data underline a possible therapeutic use of I2R ligands as adjuvants in opioid-based treatment, which we aimed to validate for the novel imidazoline-2 ligand CR4056.

In fact, chronic exposure to opioids is a relevant clinical and social problem in the current pain management, since the repeated administration of any opioid almost inevitably results in the development of tolerance, physical dependence and addiction *(Cahill et al., 2016)*. In addition, unwanted side-effects emerge during a chronic opioid treatment, such as constipation or respiratory depression. To date, this represents a huge clinical problem in the pain field.

Chronically stimulated MORs may be desensitized and are separated by their downstream signaling pathways, giving rise to antinociceptive tolerance and unwanted side-effects, attributed to the recruitment of arrestins. In fact, the lack of β-arrestin 2 prevents the development of morphine-induced analgesic tolerance, counteracting the desensitization of MOR after chronic morphine treatment *(Bohn et al., 2000)*; on the other hand, the Gαi pathway, which leads to cAMP inhibition and cell hyperpolarization, is thought to mediate the analgesic properties of MORs.

In the present work, I showed that CR4056 significantly and dose-dependently inhibits morphine-induced analgesic tolerance development, in combined chronic administration with morphine, both in the short period (4 days) and in the long period (14 days). Following 4 days of morphine treatment (7 administrations), the analgesic effect of the drug was significantly reduced, and rats showed analgesic tolerance, as already observed in other studies *(Beaudry et al., 2015; Caprioli et al., 2015)* using the same paradigm. Interestingly, when CR4056 or 2-BFI were administered 15 minutes before each morphine administration, I observed a dose-dependent prevention of morphine analgesic tolerance. Also when tested

in a longer period (14 days of administration), CR4056 (1 mg/kg, os) combined administration with morphine was able to reduce morphine analgesic tolerance and to partly recover morphine analgesic effect, compared to morphine alone treated group, which was completely tolerant. These results are in line with other studies in literature which tested the effect of I2R ligands on morphine-induced analgesic tolerance, as phenyzoline *(Gentili et al., 2006)*, 2-BFI, BU224 and CR4056 *(Thorn et al., 2017).* Moreover, I demonstrated that CR4056's optimal dose for the combined administration with morphine is 1 mg/kg, confirming the isobolographic analyses already performed on the capsaicin-induced neurogenic pain model *(Ferrari et al., 2011)*.

Another new finding of the present study is the demonstration that CR4056 is also able to counteract morphine-induced analgesic tolerance when already established. In fact, when CR4056 (1 mg/kg, os) was co-administered with morphine in already tolerant rats (which underwent 7 days of morphine alone treatment), it partially re-established the analgesic activity of the drug on the first day of co-administration; continuing the combined treatment for another week, CR4056 further improved the recovery of morphine analgesic activity, reverting the antinociceptive tolerance.

Moreover, these animals also showed a significant reduction of spinal microgliosis following CR4056 and morphine combined treatment, compared to the morphine alone treated group, evaluated by "amoeboid" phenotype and IBA1 expression *(Trang et al., 2015; Ji et al., 2013)*, the most used marker for reactive microglia. It is known that morphine tolerance is associated with spinal microglia inflammation and activation, and that inhibition of these cells alleviates the symptoms of morphine-induced analgesic tolerance *(Watkins et al., 2009; Ji et al., 2013)*. Therefore, this finding suggests that CR4056 could also act on microglial I2 binding sites, inhibiting the reactive process and thus potentiating morphine analgesic effect.

Of great therapeutic interest, CR4056 did not worsen opioid-induced constipation. In fact, the combined acute administration of CR4056 with codeine (12 mg/kg, sc) or morphine (10 mg/kg, sc) in healthy rats did not show a synergistic or additive effect on constipation, which was significant in codeine or morphine alone treated animals, compared to vehicle. This result is comparable to what Kolesnikov et al. found, observing that agmatine, another I2R ligand, did not worsen morphine-induced constipation *(Kolesnikov et al., 1996)*.

These findings strongly suggest CR4056 as a valid therapeutic tool to recover opioid-induced analgesic tolerance, as well as a suitable candidate for a preventive combined administration therapy from the beginning. CR4056 was found to be effective in the management of several kinds of chronic pain, and in the present study, it was shown to enhance morphine analgesia, even in the long period, ameliorating a pain and tolerance hallmark such as spinal microgliosis, without exacerbating a common adverse side-effect such as constipation. Therefore, the use of CR4056 in pain clinics could significantly widen the opioid therapeutic window, while not aggravating the well-known unwanted effects of these commonly used drugs, thus acting in combination with morphine as a functionally biased opiate agonist, in a similar way to some recently developed molecules (e.g., PZM21 *(Manglik et al., 2016)* or TRV130 *(Kieffer, 2016)*), engineered in the effort of activating MORs without recruiting either arrestin 2 or 3.

Given the striking synergy observed in the relief of pain and in the inhibition of the development and the expression of analgesic tolerance, the mechanism of action and interaction of CR4056 and morphine was deepened through in vitro studies. PKCε phosphorylation is linked to the upregulation of TRPV1, known to be involved in the establishment of peripheral sensitization *(Szallasi et al., 2007)*; following activation, pPKCε translocates to the cell membrane, where it sensitizes the receptor *(Vellani et al., 2011; 2013).* Since several analgesic drugs were shown to have inhibitory effect on PKCε translocation in cultured rat DRGs treated with inflammatory agents such as bradykinin *(Vellani et al., 2011; 2013; Vellani & Giacomoni, 2016)*, the effects of CR4056 and morphine application were also tested in the same in vitro model (unpublished data). CR4056 and morphine, separately applied to bradykinin-treated DRG cells, inhibited PKCε translocation in the majority of neurons. Compared to ED50 calculated for each drug dose-response curve, the potency both of morphine and of CR4056 is increased by a $>10^3$ factor when co-applied at respective time peaks, showing a marked synergism, which seems to be independent from idazoxan-sensitive I2R and α2-adrenoceptors, and to act via a GPCR different from μ opioid receptor *(Vellani et al., unpublished data)*.

The surprising synergy observed in in vitro DRGs, and its extent much greater than the one observed in in vivo isobolographic analyses (increase of a $>10^3$ factor in vitro versus a 4 factor in vivo) and in the evaluation of the antinociceptive effect, suggest that the effect on

PKCε phosphorylation and translocation could be the way through CR4056 and morphine act their synergy.

As a matter of fact, in vivo PKCε involvement in chronic inflammatory pain at the DRG level, and consequently, in the expression of pain-like behaviors, is now unanimous. Carrageenan *(Zhou et al., 2003)* or CFA *(Zhou et al., 2003; Yu et al., 2008; Breese et al., 2005)* injection produce a significant phosphorylation of PKCε in DRG neurons, predominantly in TRPV1 positive small diameter DRG neurons, and this is associated with thermal hyperalgesia, *(Zhou et al., 2003; Yu et al., 2008; Breese et al., 2005)* and mechanical allodynia (*Yu et al., 2008; Breese et al., 2005)*. In line with these studies, in the present work, intraplantar CFA injection led to a significant increase in PKCε phosphorylation in the ipsilateral L4-L5 DRG neurons compared to contralateral DRG and to control rats, 72 h after injection. Acute treatment with morphine (5 mg/kg, sc) or CR4056 (6 mg/kg, os) was able to reduce PKCε phosphorylation in ipsilateral L4-L5 DRG neurons. In the same animals, CFA-induced inflammation was not associated with remarkable differences in TRPV1 expression *tout court*. Conversely, I found that colocalization ratio between pPKCε and TRPV1 expression, normalized for the total number of TRPV1 positive cells, was influenced by inflammatory insult and acute treatment: it was increased in CFA-treated animals after 72 hours. These findings are in line with other studies *(Zhou et al., 2003; Yu et al., 2008)*, which showed that phosphorylation of PKCε in DRG neurons was significantly increased, in the CFA model, predominantly in TRPV1 positive small diameter DRG neurons. Acute treatments with morphine (5 mg/kg, sc) or CR4056 (6 mg/kg, os) were able to reduce it, confirming a shared subcellular target as already suggested by the in vitro screening on PKCε translocation inhibition. Exploring TRPV1 expression in the IB4-positive neuronal subpopulation, I found no influence of CFA injection at 72h, nor of acute treatments with morphine (5 mg/kg, sc) or CR4056 (6 mg/kg, os). These data are not in agreement with the findings of Breese et al.: in fact, they showed that CFA-induced inflammation increased the percentage of IB4-positive neurons that was TRPV1-immunoreactive *(Breese et al., 2005)*. It can be speculated that this incongruity could be due to the use of different laboratory animals (mice in the above cited study versus rats in the present work).

Moreover, CFA-induced inflammation was associated with increased IBA-1 expression in microglial cells in the dorsal horn of the L4-L5 spinal cord trait ipsilateral to CFA injection. As known, chronic pain and inflammation lead to spinal microgliosis *(Ji et al., 2013; Chen et al.,*

2015; Milligan & Watkins, 2009). Acute treatment with CR4056 (6 mg/kg, os) but not with morphine (5 mg/kg, sc) was able to reduce ipsilateral expression of IBA-1, thus bringing back up one more time the hypothesis that CR4056 could directly act on microglia through anti-inflammatory actions.

Lastly, the injection of the retrograde fluorescent dye TB in the injured paw confirmed that the DRG neurons in which I found hyperphosphorylation of PKCε and upregulation of TRPV1 were exactly the subgroup of cells referring to the injured area in the periphery. Due to its low toxicity, TB is commonly used to label neurons in animals *(Yu et al., 2015; Taguchi et al., 2008)* and in particular in retrograde tracing of DRG somata *(Yi et al., 2011; Žele et al., 2010)*, while fluorescent dyes in general are often injected in the paw to retrograde label DRG neurons in animal models of pain, including the CFA model *(Lu & Gold, 2008; Kim et al., 2016)*. The present work, thus, provided as proof of concept of the results shown a direct evidence of the relationship between CFA-induced peripheral inflammation and the neurobiological changes observed at the DRG level.

In fact, as already inferred from in vitro screening of CR4056 and morphine in the bradykinin-induced model of inflammation, the two drugs seem to share a synergistic action on PKCε phosphorylation inhibition, which is not mediated by MORs, nor by idazoxan-sensitive I2R, nor by α2 receptors, but by other GPCRs. A consistent limit of this study is that the GPCR involved in the synergy is still unknown.

First issue to address in future studies will be to confirm in vivo that MORs, I2R and α2-adrenoceptors are not implied in the synergy, by administration of proper agonists and antagonists. Besides, idazoxan-sensitive I2Rs involvement is not so easy to exclude as for other receptors, being peculiar binding sites allosterically regulated, which require a not linear pharmacological modulation. Furthermore, some action at I2R-A (i.e., amiloride-sensitive) binding sites is still not excluded. In fact, as we know, it was shown that agmatine is able to increase β-endorphin secretion in the rat adrenal medulla and this effect is blocked by the I2R antagonists BU-224 and amiloride; I2R sites activation by agmatine also stimulates MORs *(Chang et al., 2010)*. As we saw, agmatine co-administered with morphine is able to reduce analgesic tolerance *(Regunathan, 2006)*, similarly to CR4056. The peripheral β-endorphin increase could possibly be additive to the central I2R agonists effect on the firing rate of locus coeruleus neurons, thus contributing to the antinociceptive action and the potentiation of morphine analgesia.

Moreover, further studies are needed in order to elucidate in vivo synergy: first of all, the effects of a combined acute treatment on PKCε should be investigated; second, a chronic administration protocol should be addressed, in order to verify synergy effects in the prevention of morphine tolerance establishment. For now, overviewing all these data, it is only possible to speculate about the synergy mechanism of action. One hypothesis is that CR4056 could act on an unknown (for now) GPCR, which in turn would contribute to PKCε phosphorylation inhibition exerted by morphine stimulation of MORs. Alternatively, the putative GPCR stimulated by CR4056 could directly potentiate MORs function. Further in vitro assays are needed to elucidate this aspect. Furthermore, PKCε phosphorylation as a potential therapeutic target should be carefully considered: in fact, pPKCε inhibition could have additional consequences other than TRPV1 desensitization. For example, a direct link was found between PKCε activation and P2X3R modulation *(Gu et al., 2016)* and GABA-A phosphorylation *(Newton and Messing, 2011).* Furthermore, the existence of negative feedback mechanisms on upstream GPCRs, such as TLR and MORs, has been taken into account *(Merighi et al., 2013)*; therefore, pPKCε inhibition outcomes should be deeply analyzed.

6.1. Conclusions

In summary, the present work has demonstrated that 1 mg/kg CR4056 significantly counteracts the development or the expression of morphine-induced analgesic tolerance, as assayed by mechanical hyperalgesia and spinal microgliosis evaluation, in the CFA-induced chronic inflammatory pain, without eliciting specific tolerance nor exacerbating opioid-induced constipation. Thus, this novel I2R ligand could represent a new highly effective treatment option for the recovery or the prevention of analgesic tolerance, induced by opioid drugs, nowadays widely used in the management of chronic pain. These findings enlarge CR4056's therapeutic window to the integration of opioid-based treatments, as it was already demonstrated to be an effective analgesic drug itself in several other kinds of pain.

Furthermore, CR4056's synergy with morphine was extensively investigated in vitro, from previous unpublished data, and in vivo, by assessing the effects of acute single drugs treatments at optimal doses (6 mg/kg for CR4056 and 5 mg/kg for morphine) on the phosphorylation of PKCε and the expression of TRPV1 in DRGs from CFA-injected rats, providing evidence for a shared downstream target of the two drugs, as well as a putative therapeutic tool for the prevention of peripheral sensitization in inflammatory pain.

7. References

Al-Hasani R, Bruchas MR, “Molecular mechanisms of opioid receptor-dependent signaling and behavior” (2011), *Anesthesiology*, 115(**6**): 1363-81.

Aricioglu F, Means A, Regunathan S, “Effect of agmatine on the development of morphine dependence in rats: potential role of cAMP system” (2004), *European Journal of Pharmacolog*y, 504(**3**): 191-7.

Arnold LM, Choy E, Clauw DJ, et al., “Fibromyalgia and chronic pain syndromes: a white paper detailing current challenges in the field” (2016), *Clinical Journal of Pain*, 32 (**9**): 737-746.

Beaudry H, Gendron L, Morón JA, “Implication of DOP2 but not DOP1 in development of morphine analgesic tolerance in a rat model of chronic inflammatory pain” (2015), *European Journal of Neuroscience*, 41(**7**): 901-7.

Billiau A, Matthys P, “Modes of action of Freund’s adjuvants in experimental models of autoimmune diseases” (2001), *Journal of Leukocyte Biology*, 70(**6**): 849-60.

Bohn LM, Gainetdinov RR, Lin FT, Lefkowitz RJ, Caron MG, “μ-opioid receptor desensitization by β-arrestin-2 determines morphine tolerance but not dependence” (2000), *Nature*, 408(**6813**): 720-3.

Breese NM, George AC, Pauers LE, Stucky CL, “Peripheral inflammation selectively increases TRPV1 function in IB4-positive sensory neurons from adult mouse” (2005), *Pain*, 115(**1-2**): 37-49.

Brennan TJ, Vandermeulen EP, Gebhart GF, “Characterization of a rat model of incisional pain” (1996), *Pain*, 64(**3**): 493-501.

Cahill CM, Walwyn W, Taylor AMW, Pradhan AAA, Evans CJ, “Allostatic mechanisms of opioid tolerance beyond desensitization and downregulation” (2016), *Trends in Pharmacological Sciences*, 37(**11**): 963-976.

Caprioli G, Mammoli V, Ricciutelli M, et al., “Biological profile and bioavailability of imidazoline compounds on morphine tolerance modulation” (2015), *European Journal of Pharmacology*, **769**: 219-24.

Chang CH, Wu HT, Cheng KC, Lin HJ, Cheng JT, "Increase of beta-endorphin secretion by agmatine is induced by activation of imidazoline I(2A) receptors in adrenal gland of rats" (2010), *Neuroscience Letters*, 468(**3**): 297-9.

Chen G, Park CK, Xie RG, Ji RR, "Intrathecal bone marrow stromal cells inhibit neuropathic pain via TGF-β secretion" (2015), *Journal of Clinical Investigation*, 125(**8**): 3226-40.

Chen Y, Willcockson HH, Valtschanoff JG, "Influence of the vanilloid receptor TRPV1 on the activation of spinal cord glia in mouse models of pain" (2009), *Experimental Neurology*, 220(**2**): 383-90.

Dubin AE, Patapoutian A, "Nociceptors: the sensors of the pain pathway" (2010), *Journal of Clinical Investigation*, 120(**11**): 3760-72.

Duquesnes N, Lezoualc'h F, Crozatier B, "PKC-delta and PKC-epsilon: Foes of the same family or strangers?" (2011), *Journal of Molecular and Cellular Cardiology*, 51(**5**): 665-73.

European Federation of IASP Chapters (EFIC), "EFIC's declaration on chronic pain as a major healthcare problem, a disease in its own right" (2001), available from: http://www.painreliefhumanright.com/pdf/06_declaration.pdf.

European Federation of IASP Chapters (EFIC), "Fact sheet: unrelieved pain is a major global healthcare problem" (2004), available from: http://www.painreliefhumanright.com/pdf/04a_global_day_fact_sheet.pdf.

Ferrari F, Fiorentino S, Mennuni L, et al., "Analgesic efficacy of CR4056, a novel imidazoline-2 receptor ligand, in rat models of inflammatory and neuropathic pain" (2011), *Journal of Pain Research*, **4**: 111-25.

Ferreira-Gomes J, Adães S, Mendonça M, Castro-Lopes JM, "Analgesic effects of lidocaine, morphine and diclofenac on movement-induced nociception, as assessed by the Knee-Bend and CatWalk tests in a rat model of osteoarthritis" (2012), *Pharmacology, Biochemistry and Behavior*, 101(**4**): 617-24.

Gao W, Zan Y, Wang ZJ, Hu XY, Huang F, "Quercetin ameliorates paclitaxel-induced neuropathic pain by stabilizing mast cells, and subsequently blocking PKCε-dependent activation of TRPV1" (2016), *Acta Pharmacologica Sinica*, 37(**9**): 1166-77.

Garland EL, "Treating chronic pain: the need for non-opioid options" (2014), *Expert Review of Clinical Pharmacology*, 7(**5**): 545-50.

Gentili F, Cardinaletti C, Carrieri A, et al., "Involvement of I2-imidazoline binding sites in positive and negative morphine analgesia modulatory effects" (2006), *European Journal of Pharmacology*, 553(**1-3**): 73-81.

Gold MS, Gebhart GF, "Nociceptor sensitization in pain pathogenesis" (2010), *Nature Medicine*, 16(**11**): 1248-57.

Goldberg DS, McGee SJ, "Pain as a global public health priority" (2011), *BMC Public Health*, **11**:770.

Gregersen LS, Røsland T, Arendt-Nielsen L, Whiteside G, Hummel M, "Unrestricted weight bearing as a method for assessment of nociceptive behavior in a model of tibiofemoral osteoarthritis in rats" (2013), *Journal of Behavioral and Brain Science*, 3(**3**): 306-314.

Gregory N, Harris AL, Robinson CR, Dougherty PM, Fuchs PN, Sluka KA, "An overview of animal models of pain: disease models and outcome measures" (2013), *Journal of Pain*, 14(**11**): 1255-69.

Griffioen MA, Dernetz VH, Yang GS, Griffith KA, Dorsey SG, Renn CL, "Evaluation of Dynamic Weight Bearing for Measuring Nonevoked Inflammatory Hyperalgesia in Mice" (2015), *Nursing research*, 64(**2**): 81-7.

Gu Y, Li G, Chen Y, Huang LY, "Epac–protein kinase C alpha signaling in purinergic P2X3R-mediated hyperalgesia after inflammation" (2016), *Pain*, 157(**7**): 1541-50.

Harada Y, Iizuka S, Saegusa Y, Mogami S, Fujitsuka N, Hattori T, "Mashiningan improves opioid-induced constipation in rats by activating cystic fibrosis transmembrane conductance regulator chloride channel" (2017), *Journal of Pharmacology and Experimental Therapeutics*, 362(**1**): 78-84.

He Y, Wang ZJ, “Nociceptor Beta II, Delta, and Epsilon isoforms of PKC differentially mediate paclitaxel-induced spontaneous and evoked pain” (2015), *Journal of Neuroscience*, 35(**11**): 4614-25.

Huang WY, Dai SP, Chang YC, Sun WH, “Acidosis mediates the switching of Gs-PKA and Gi-PKCε dependence in prolonged hyperalgesia induced by inflammation” (2015), *PLoS One*, 10(**5**): 1-17.

Jensen TS, Finnerup NB, “Allodynia and hyperalgesia in neuropathic pain: clinical manifestations and mechanisms” (2014), *Lancet Neurology*, 13(**9**): 924-35.

Ji RR, Berta T, Nedergaard M, “Glia and pain: is chronic pain a gliopathy?” (2013), *Pain*, 154(**0 1**): S10-28.

Jones TZ, Giurato L, Guccione S, Ramsay RR, “Interactions of imidazoline ligands with the active site of purified monoamine oxidase A” (2007), *FEBS Journal*, 274(**6**): 1567-75.

Joseph EK, Levine JD, “Multiple PKCε-dependent mechanisms mediating mechanical hyperalgesia” (2010), *Pain*, 150(**1**): 17-21.

Joseph EK, Reichling DB, Levine JD, “Shared mechanisms for opioid tolerance and a transition to chronic pain” (2010), *Journal of Neuroscience*, 30(**13**): 4660-6.

Keller B, García-Sevilla JA, “Immunodetection and subcellular distribution of imidazoline receptor proteins with three antibodies in mouse and human brains: Effects of treatments with I1- and I2-imidazoline drugs” (2015), *Journal of Psychopharmacology*, 29(**9**): 996-1012.

Kieffer BL, “Designing the ideal opioid” (2016), *Nature Reviews Drug Discovery*, 537(**7619**): 170-171.

Kim YS, Anderson M, Park K, et al., “Coupled activation of primary sensory neurons contributes to chronic pain” (2016), *Neuron*, 91(**5**): 1085-1096.

Kilkenny C, Browne WJ, Cuthill IC, Emerson M, Altman DG, “Improving bioscience research reporting: The ARRIVE guidelines for reporting animal research” (2010), *Journal of Pharmacology & Pharmacotherapeutics*, 1(**2**): 94-9.

Kolesnikov Y, Jain S, Pasternak GW, “Modulation of opioid analgesia by agmatine” (1996), *European Journal of Pharmacology*, 296(**1**): 17-22.

Kuner R, “Central mechanisms of pathological pain” (2010), *Nature Medicine*, 16(**11**): 1258-66.

Lanza M, Ferrari F, Menghetti I, Tremolada D, Caselli G, “Modulation of imidazoline I2 binding sites by CR4056 relieves postoperative hyperalgesia in male and female rats” (2014), *British Journal of Pharmacology*, 171(**15**): 3693-701.

Latremoliere A, Woolf CJ, “Central sensitization: a generator of pain hypersensitivity by central neural plasticity” (2010), *Journal of Pain*, 10(**9**): 895-926.

Li JX, “Imidazoline I2 receptors: an update” (2017), *Pharmacology & Therapeutics*, **178**: 48-56.

Li JX, Thorn DA, Qiu Y, Peng BW, Zhang Y, “Antihyperalgesic effects of imidazoline I2 receptor ligands in rat models of inflammatory and neuropathic pain” (2014), *British Journal of Pharmacology*, 171(**6**): 1580-90.

Li JX, Zhang Y, “Imidazoline I2 receptors: target for new analgesics?” (2011), *European Journal of Pharmacology*, 658(**2-3**): 49-56.

Lu SG, Gold MS, “Inflammation-induced increase in evoked calcium transients in subpopulations of rat DRG neurons” (2008), *Neuroscience*, 153(**1**): 279-88.

Manchikanti L, Kaye AM, Knezevic NN, et al., “Responsible, safe, and effective prescription of opioids for chronic non-cancer pain: American Society of Interventional Pain Physicians (ASIPP) Guidelines” (2017), *Pain Physician*, 20(**2S**): S3-S92.

Manglik A, Lin H, Aryal DK, et al., “Structure-based discovery of opioid analgesics with reduced side effects” (2016), *Nature*, 537(**7619**): 185-190.

McGrath JC, Drummond GB, McLachlan EM, Kilkenny C, Wainwright CL, “Guidelines for reporting experiments involving animals: the ARRIVE guidelines” (2010), *British Journal of Pharmacology*, 160(**7**): 1573-6.

Melzack R, Wall PD, “Pain mechanisms: a new theory” (1965), *Science*, 150(**3699**): 971-9.

Meregalli C, Ceresa C, Canta A, et al., “CR4056, a new analgesic I2 ligand, is highly effective against bortezomib-induced painful neuropathy in rats” (2012), *Journal of Pain Research*, **5**: 151-67.

Merighi S, Gessi S, Varani K, Fazzi D, Stefanelli A, Borea PA, “Morphine mediates a proinflammatory phenotype via μ-opioid receptor–PKCε–Akt–ERK1/2 signaling pathway in activated microglial cells” (2013), *Biochemical Pharmacology*, 86(**4**): 487-96.

Milligan ED, Watkins LR, “Pathological and protective roles of glia in chronic pain” (2009), *Nature Reviews Neuroscience*, 10(**1**): 23-36.

Mogil JS, Crager SE, “What should we be measuring in behavioral studies of chronic pain in animals?” (2004), *Pain*, 112(**1-2**): 12-5.

Newton PM, Kim JA, McGeehan AJ, et al., “Increased response to morphine in mice lacking protein kinase C epsilon” (2007), *Genes, Brain and Behavior*, 6(**4**): 329-38.

Newton PM, Messing RO, “The substrates and binding partners of protein kinase Cε” (2011), *The Biochemical Journal*; 427(**2**): 189-96.

Okun A, DeFelice M, Eyde N, et al., “Transient inflammation-induced ongoing pain is driven by TRPV1 sensitive afferents” (2011), *Molecular pain*, **10**; 7:4.

Paxinos G, Watson C, “The rat brain in stereotaxic coordinates” (1982), *Academic Press*.

Pertovaara A, “The noradrenergic pain regulation system: a potential target for pain therapy” (2013), *European Journal of Pharmacology*, 716(**1-3**): 2-7.

Price TJ, Inyang KE, “Commonalities between pain and memory mechanisms and their meaning for understanding chronic pain” (2015), *Progress in Molecular Biology and Translational Science*, **131**: 409-34.

Priest TD, Hoggart B, “Chronic pain: mechanisms and treatment” (2002), *Current Opinion in Pharmacology*, 2(**3**): 310-315.

Qiu Y, Zhang Y, Li JX, “Discriminative stimulus effects of the imidazoline I2 receptor ligands BU224 and phenyzoline in rats” (2015), *European Journal of Pharmacology*, **749**: 133-41.

Qiu Y, Zhao W, Wang Y, et al., “FK506-binding protein 12 modulates μ-opioid receptor phosphorylation and protein kinase Cε-dependent signaling by its direct interaction with the receptor” (2014), *Molecular Pharmacology*, 85(**1**): 37-49.

Quartu M, Carozzi VA, Dorsey SG, et al., “Bortezomib treatment produces nocifensive behavior and changes in the expression of TRPV1, CGRP, and substance P in the rat DRG, spinal cord, and sciatic nerve” (2014), *BioMed Research International*, **2014**: 1-19.

Regunathan S, “Agmatine: biological role and therapeutic potentials in morphine analgesia and dependence” (2006), *AAPS Journal*, 8(**3**): E479-84.

Sachs D, Villarreal C, Cunha F, Parada C, Ferreira SH, ”The role of PKA and PKCε pathways in prostaglandin E2-mediated hypernociception” (2009), *British Journal of Pharmacology*, 156(**5**): 826-34.

Shangguan Y, Hall KE, Neubig RR, Wiley JW, “Diabetic neuropathy: inhibitory G protein dysfunction involves PKC-dependent phosphorylation of Gα” (2003), *Journal of Neurochemistry*, 86(**4**): 1006-14.

Snekhalatha U, Anburajan M, Venkatraman B, Menaka M., “Evaluation of complete Freund’s adjuvant-induced arthritis in a Wistar rat model. Comparison of thermography and histopathology” (2013), *Zeitschrift für Rheumatologie*, 72(**4**): 375-82.

Szallasi A, Cortright DN, Blum CA, Eid SR, “The vanilloid receptor TRPV1: 10 years from channel cloning to antagonist proof-of-concept” (2007), *Nature Reviews Drug Discovery*, 6(**5**): 357-72.

Taguchi T, Hoheisel U, Mense S, “Dorsal horn neurons having input from low back structures in rats” (2008), *Pain*, 138(**1**): 119-29.

Tétreault P, Dansereau MA, Doré-Savard L, Beaudet N, Sarret P, “Weight bearing evaluation in inflammatory, neuropathic and cancer chronic pain in freely moving rats” (2010), *Physiology & Behavior*, 104(**3**): 495-502.

Thorn DA, Qiu Y, Jia S, Zhang Y, Li JX, “Antinociceptive effects of imidazoline I2 receptor agonists in the formalin test in rats” (2016), *Behavioral Pharmacology*, 27(**4**): 377-83.

Thorn DA, Zhang Y, Li JX, “Effects of the imidazoline I2 receptor agonist 2-BFI on the development of tolerance to and behavioural/physical dependence on morphine in rats” (2016), *British Journal of Pharmacology*, 173(**8**): 1363-72.

Thorn DA, Zhang Y, Li JX “Tolerance and cross-tolerance to the antinociceptive effects of oxycodone and the imidazoline I2 receptor agonist phenyzoline in adult male rats” (2017), *Psychopharmacology (Berl)*, 234(**12**): 1871-1880.

Trang T, Al-Hasani R, Salvemini D, Salter MW, Gutstein H, Cahill CM, “Pain and poppies: the good, the bad, and the ugly of opioid analgesics” (2015), *Journal of Neuroscienc*e, 35(**41**): 13879-88.

Treede R-D, Rief W, Barke A, et al., “A classification of chronic pain for ICD-11” (2015), *Pain*, 156(**6**): 1003-1007.

van Hecke O, Torrance N, Smith BH, “Chronic pain epidemiology and its clinical relevance” (2013), *British Journal of Anaesthesia*, 111(**1**): 13-18.

Velázquez KT, Mohammad H, Sweitzer SM, “Protein kinase C in pain: Involvement of multiple isoforms” (2007), *Pharmacological research*, 55(**6**): 578-89.

Vellani V, Franchi S, Prandini M, et al., “Effects of NSAIDs and paracetamol (acetaminophen) on protein kinase C epsilon translocation and on substance P synthesis and release in cultured sensory neurons” (2013), *Journal of Pain Research*, **6**: 111-20.

Vellani V, Franchi S, Prandini M, et al., “Nimesulide inhibits protein kinase C epsilon and substance P in sensory neurons – comparison with paracetamol” (2011), *Journal of Pain Research*, **4**: 177-87.

Vellani V, Giacomoni C, “Gabapentin inhibits Protein Kinase C Epsilon translocation in cultured sensory neurons with additive effects when coapplied with paracetamol (acetaminophen)” (2016), *The Scientific World Journal*, **2017**: 3595903.

Vellani V, Mapplebeck S, Moriondo A, Davis JB, McNaughton PA, “Protein kinase C activation potentiates gating of the vanilloid receptor VR1 by capsaicin, protons, heat and anandamide” (2001), *The Journal of Physiology*, 534(**Pt 3**): 813-25.

Volkow ND, McLellan AT, “Opioid abuse in chronic pain - misconceptions and mitigation strategies” (2016), *New England Journal of Medicine*, 374(**13**): 1253-63.

Watkins LR, Hutchinson MR, Rice KC, Maier SF, “The “toll” of opioid-induced glial activation: improving the clinical efficacy of opioids by targeting glia” (2009), *Trends in Pharmacological Sciences*, 30(**11**): 581-91.

Yekkirala AS, Roberson DP, Bean BP, Woolf CJ, “Breaking barriers to novel analgesic drug development” (2017), *Nature Reviews Drug Discovery*, 16(**8**): 545-564.

Yi H, Kim MA, Back SK, Eun JS, Na HS, “A novel rat forelimb model of neuropathic pain produced by partial injury of the median and ulnar nerves” (2011), *European Journal of Pain*, 15(**5**): 459-66.

Yoshimura M, Furue H, “Mechanisms for the anti-nociceptive actions of the descending noradrenergic and serotonergic systems in the spinal cord” (2006), *Journal of Pharmacological Sciences*, 101(**2**): 107-17.

Yu L, Yang F, Luo H, et al., “The role of TRPV1 in different subtypes of dorsal root ganglion neurons in rat chronic inflammatory nociception induced by complete Freund's adjuvant” (2008), *Molecular Pain*, **4**: 61.

Yu Y, Zhang P, Yin X, Han N, Kou Y, Jiang B, “Specificity of motor axon regeneration: a comparison of recovery following biodegradable conduit small gap tubulization and epineurial neurorrhaphy” (2015), *American Journal of Translational Research*, 7(**1**): 53-65.

Žele T, Sketelj J, Bajrović FF, “Efficacy of fluorescent tracers in retrograde labeling of cutaneous afferent neurons in the rat” (2010), *Journal of Neuroscience Methods*, 191(**2**): 208-14.

Zhang R-X, Ren K, “Animal models of pain” (2011), Chao Ma and Jun-Ming Zhang (eds.), *Neuromethod*s, vol. 49.

Zhou Y, Li GD, Zhao ZQ, ”State-dependent phosphorylation of ε-isozyme of protein kinase C in adult rat dorsal root ganglia after inflammation and nerve injury” (2003), *Journal of Neurochemistry*, 85(**3**): 571-80.